TOPEX/POSEIDON GDR-F Products Handbook

CNES Reference: SALP-MU-MAO-OP-17607-CN

JPL Reference: JPL D-73899

Issue: 1 rev 0

Date: June 16, 2023

National Aeronautics and Space Administration
Jet Propulsion Laboratory
California Institute of Technology

cnes

Chronology Issues:

Issue:	Date:	Reason for change:
1rev0	June 16, 2023	First version

People involved in this issue:

Written by (*):		Date
V. Rosmorduc	CLS	Approval not required
H. Roinard	CLS	Approval not required
Shailen Desai	NASA/JPL	07-26-2023 Electronic signature on file
Jean-Damien Desjonqueres	NASA/JPL	07-26-2023 Electronic signature on file
Philip S. Callahan	NASA/JPL	07-26-2023 Electronic signature on file
F. Bignalet-Cazalet	CNES	

Index Sheet:

Context:	
Keywords:	
Hyperlink:	

Electronic signatures in EPDM

User-Group/Role	...	Decision	Comments	Date
Desjonqueres, Jean-Damien M (jdesjonq)-JPL Consumer/Project Consumer	...	Approve		26-Jul-2023 14:15
Callahan, Philip S (pscallah)-JPL Consumer/Project Consumer	...	Approve		26-Jul-2023 15:08
Desai, Shailen D (sdesai)-JPL Author/JPL Author	...	Approve		26-Jul-2023 14:15

Contents

List of tables and figures

1. Quick reference guide

This is a combination of a guide to using the TOPEX/POSEIDON version F Geophysical Data Record (GDR-F) products and a reference handbook, so not all sections will be needed by all readers.

➢ A description of the background and motivation for this reprocessed product is provided in Section 2, including a description of the TOPEX/POSEIDON mission and missions events that may impact the quality of the reprocessed product. All users are advised to read this section.

➢ Details on the TOPEX altimeter data retracking are provided in Section 4.4.1.

➢ Details on the POSEIDON altimeter data retracking are provided in Section 4.4.2.

➢ Bibliographic references and acronyms are given in the appendices.

The document is organized as follows:

Section 2. Overview of the reprocessing of TOPEX/POSEIDON data products, with an overview of the mission, and summary of mission events affecting data quality.

Section 3. Using altimetry data, including classical formulas to use altimetry data.

Section 4. Product fields and processing, with explanations on the different parameters provided within the data, their content, rationale and how they are computed.

Section 5. Data content and format.

Section 6. How to read the data (software & languages).

Section 7. Data Distribution, identifying where to find the data.

Appendix A: References to articles, manuals and reports cited in this document.

Appendix B: POSEIDON Active Periods provides periods when POSEIDON altimeter was active.

Appendix C: Equator Crossing Longitudes with the longitudes at which each pass (half orbit) crosses the equator.

Appendix D: Leap seconds

Appendix E: Acronyms. List of acronyms used in this document

Appendix F: Contacts

- **How to cite this document?**

When referencing this document, please use the following citation:

"TOPEX/POSEIDON GDR-F Products Handbook", May 25, 2023, JPL D-73899,
SALP-MU-MAO-OP-17607-CN

2. Introduction

2.1. Purpose and Scope

This document provides the background and how to use the reprocessed version F TOPEX/POSEIDON Geophysical Data Record (GDR) product, designated GDR-F. It also includes some historical information on the TOPEX/POSEIDON project and the path that led to this version.

Many people have contributed to this product over nearly 35 years. In many ways it encapsulates what has been learned about high accuracy ocean altimetry during that time. This product attempts to tie the TOPEX/POSEIDON data into the 30-year history of global sea level climate record.

Users of this reprocessed product are strongly advised to refer to Section 2.4.3 on TOPEX/POSEIDON events that impact the quality of the data.

2.2. Overview

Data from the TOPEX/POSEIDON mission was previously reprocessed in 1996-98. Those products were based upon the on-board estimates for the altimeter range, significant wave height (SWH) and backscatter coefficient (sigma0). For TOPEX, these on-board estimates were particularly impacted by the instrument degradation of the side A altimeter. The reprocessed data in this release are based upon the processing of the TOPEX and POSEIDON altimeter echoes on-ground using more advanced retracking algorithms. In addition, this product adopts additional advances in data processing and geophysical models as summarized below. This product is based on the GDR-F standard applied to other altimeter missions and provides improved product quality and consistency with the current altimetry missions.

Compared to this previous dataset, the GDR-F version of the product benefits from:

- Ground reprocessing of the TOPEX altimeter data based on a numerical retracking of the echoes, with MLE-4 and MLE-3 solutions for Ku band and an MLE-3 solution for C band. This approach has been developed to apply modern ground retracking to the altimeter data and to mitigate the impact of degradation in the altimeter instrument, especially for the TOPEX Side A altimeter, on the science data.
- Ground reprocessing of the POSEIDON altimeter data based on retracking of the echoes, with MLE-4 and MLE-3 solutions for Ku band.
- Two new computations of the satellite orbit ephemeris based on recent processing standards from the NASA Goddard Space Flight Center (GSFC) and the Centre National d'Etudes Spatiales (CNES), and in the 2014 International Terrestrial Reference Frame (ITRF).
- Reprocessing of the TOPEX Microwave Radiometer (TMR) data using the best available end-of-mission calibration.
- Non-parametric Sea State Bias models for the TOPEX altimeter that are self-consistent with the reprocessed data products. These include a 2-D model from the University of Colorado, Boulder, and a 3-D model from the University of New Hampshire.
- Updated models for the geophysical and environmental corrections consistent with the GDR-F standards of other altimeter missions.

2.3. TOPEX/POSEIDON Legacy: from Jason-1 to Sentinel-6

The TOPEX/POSEIDON mission [1] was launched on August 10, 1992 on a 9.9156-day repeat orbit, and operated until October 9, 2005. The mission was jointly developed by the United States National Aeronautics and Space Administration (NASA) and the French Space Agency, Centre National d'Etudes Spatiales (CNES). This collaboration has extended into this release of the reprocessed science data products.

The success of the TOPEX/POSEIDON mission is especially evident in the series of successor missions over the past three decades. These include the Jason-1 (2001-2013) [2], Ocean Surface Topography Mission/Jason-2 (2008-2019) [3], Jason-3 (2016-), and Sentinel-6 Michael Freilich (2020-) [4] missions. The next successor, Sentinel-6B is already built and planned for launch in 2025. Each of the successor missions were placed in a tandem orbit with their predecessor for at least 6 months, whereby the two missions followed each other on the same ground track less than a few minutes apart. The objective of each tandem phase is to facilitate a continuous climate data record by cross-calibrating their respective sea surface height measurement systems. All of these successor missions have flown on the exact same ground track established by the TOPEX/POSEIDON mission, thereby providing a continuous sea surface height data record on the same ground track from 1992. After the tandem phase between TOPEX/POSEIDON and Jason-1, the TOPEX/POSEIDON satellite was moved into an interleaved ground track on August 15, 2002 that also repeated to within +/-1 km every 9.9156 days. The finer spatial sampling from two active missions in an interleaved orbit allowed for studies of the ocean mesoscale as well as the large-scale circulation from the overall sea surface height. The legacy of the TOPEX/POSEIDON mission also extends to the onboard sensors. Improved versions of the POSEIDON altimeter, the microwave radiometer, and the DORIS and GPS tracking systems have been used on the successor missions.

2.4. TOPEX/POSEIDON Mission Overview

Users are advised to refer to [1] for an extensive discussion of the TOPEX/POSEIDON mission and its science objectives. As noted in [1], TOPEX/POSEIDON was the "first space mission specifically designed and conducted for studying the circulation of the world's oceans". Numerous articles on the calibration and validation of the TOPEX/POSEIDON measurement system are provided in a special issue of the Journal of Geophysical Research, volume 99 (C12) published in 1994. This was followed by another special issue in the Journal of Geophysical Research, volume 100 (C12) published in 1995 dedicated to science results from TOPEX/POSEIDON.

The original requirements for TOPEX/POSEIDON were to provide single pass sea level measurements with a root-sum-square accuracy of 13.7 cm. However, results soon after launch indicated accuracies of 4.7 cm for TOPEX and 5.1 cm for POSEIDON. The significantly better performance was primarily due to advances in precise orbit determination that resulted in early orbit altitude accuracies of 3.5 cm [5] [6] versus the pre-launch allocation of 12.8 cm. Two other significant requirements on TOPEX/POSEIDON were that the orbit (Section 2.4.4) not alias the tides in important ways and errors not be "geographically correlated". While the original concern for the latter was orbit error, it now largely hinges on environmental corrections.

This reprocessed TOPEX/POSEIDON data product provides sea surface height measurements with an accuracy of 3.54 cm for TOPEX and 3.99 cm for POSEIDON, with performance similar to its Jason-series successors [7]. This reprocessed GDR-F product significantly improves many components of the data, as summarized in Section 2.2.

2.4.1. TOPEX/POSEIDON Sensors

Figure 1 provides an overview of the TOPEX/POSEIDON satellite and its payload. The figure shows the main components of the satellite itself as well as the sensors and tracking systems. Note the large one-sided solar array and the large size of the overall system. The satellite weighed nearly 2500 kg, and the solar array generated over 1 kW of power for the system. The design of the solar array caused an unusual effect because its thermal distortion (hotter front side expanded more than the cooler back side causing a bend or arch) resulted with changes in the spacecraft's center of mass of about 1 cm per orbit revolution as the array rotated to track the sun.

The satellite bus contained the flight computer and three magnetic tape recorders to store the data between data transmissions. The high gain antenna was articulated to point to and track NASA's Transfer and Data Relay Satellite Systems for data playback. Motion of the high gain antenna did not significantly affect the spacecraft's center of mass.

The TOPEX/POSEIDON satellite carried the following sensors which are each briefly described below. The TOPEX and POSEIDON altimeters shared the same antenna, which means that only one of the two was active at any time. Appendix B provides the time periods when the POSEIDON altimeter was active, with the TOPEX altimeter active for all other periods.

1. Dual frequency (Ku and C band) redundant TOPEX radar altimeter, with two separate sides designated as Side A and Side B.
2. Ku band solid state POSEIDON altimeter.
3. Three-frequency TOPEX Microwave Radiometer (TMR).
4. Laser Retroreflector Array (LRA).
5. Doppler Orbitography and Radiopositioning Integrated by Satellite (DORIS) tracking system receiver.
6. Global Position System (GPS) Demonstration Receiver.
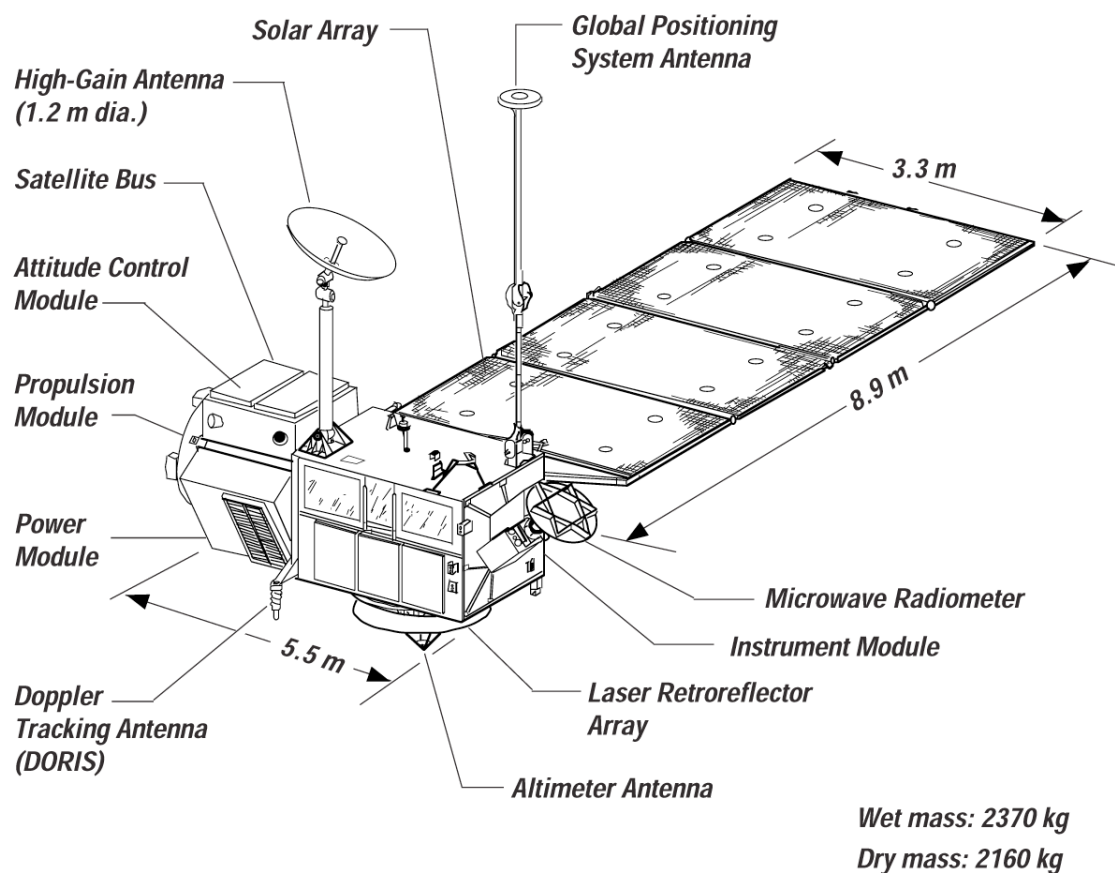
Figure 1. The TOPEX/POSEIDON spacecraft.

2.4.1.1. TOPEX Altimeter

The TOPEX altimeter, also referred to as the NASA Radar Altimeter (NRA), simultaneously operated at 13.6 GHz (Ku band) and 5.3 GHz (C band). It was the primary sensor for the TOPEX/POSEIDON mission. It was redundant except for the microwave transmission unit and the antenna, with the two sides designated Side A and Side B. The TOPEX Side A altimeter was activated soon after launch and turned off on February 10, 1999. The TOPEX Side B altimeter was turned on for the first time on February 10, 1999 and became the primary operational altimeter until it was turned off on October 9, 2005.

After TOPEX Side A first turn-on in space, small signal leakages were observed in the leading edge of the waveforms. There was no evidence of these leakages in any ground test data, and Side B did not have these leakages. In retrospect, Side A began to show signs of change/degradation in early 1997 (in addition to a calibration jump discussed later). The effects of these leakages on Side A data are described in [8]. Changes in the Side A point target response were observed as an apparent drift in the measured significant wave heights and instrument range RMS, and as a result Side A was turned off on February 10, 1999 and Side B turned on. After detection of the point target response problem, a software patch was implemented to provide a better measure of the degraded shape. This patch, known as the Sweep Calibrations, was first executed on September 8, 1998, and subsequently performed regularly on Side A and the full period of Side B. Side B never showed a degradation in its point target response. In addition, analysis of the original data revealed that there was a sub-centimeter bias in the data near the equator that was associated with a change in sign of the range rate. This characteristic was in both the Side A and Side B data but had slightly different values.

The numerical retracking applied to the reprocessed Side A and Side B data in this GDR-F product significantly mitigates the impact of the Side A waveform leakages, the changes in the Side A point target response, and the hemispheric effect observed in both Side A and Side B. Nevertheless, the quality of the reprocessed Side A data is impacted by the following:

1. Sweep Calibration measurements to monitor the behavior of the point target response were only available from September 8, 1998.

2. Improved quality of reprocessed data has exposed a jump in the TOPEX altimeter calibration data on April 1, 1996. **Users, especially for climate studies, are strongly advised to treat the TOPEX Side A time series as discontinuous with a potential jump in altimeter geophysical measurements on April 1, 1996.**

2.4.1.2. POSEIDON Altimeter

The POSEIDON or Single frequency Ku band Solid State ALTimeter (SSALT), operated at a single frequency of 13.65 GHz (Ku band) (see Table 1). The POSEIDON altimeter measurements give the same geophysical information as the TOPEX altimeter. However, a model is required to provide a correction for the ionosphere delay of the POSEIDON range measurements because it used a single frequency (see section 4.5.4). POSEIDON was used to validate the new technology of a low-power (49 W), lightweight (23 kg) altimeter for future Earth-observing missions. The POSEIDON altimeter proved to have excellent stability through the life of the TOPEX/POSEIDON mission. The outcome was that improved versions of this instrument were used for all the Jason, Sentinel-6 and Sentinel-3 series in a dual-frequency version; moreover, the instruments onboard SARAL, CRYOSAT and SWOT are also modified versions of this first solid state altimeter.

This GDR-F product includes reprocessing of the internal calibration sequences and retracking of the waveforms when they were available [9]. The POSEIDON waveforms were only downlinked from 1995 (cycle 090) onward and archived in MegaFiles from cycle 137 (1996/06) to cycle 307 (2001/01). Retracked POSEIDON data are only available for this period. Prior to cycle 137 and after cycle 307, this product provides the onboard geophysical estimates. Refer to Appendix B for the periods when the POSEIDON altimeter was active.

Parameter	Value
Center Frequency	13.65 GHz
Pulse Duration	105 μs
Bandwidth	320 MHz
Peak Transmitted Power	5 W
Pulse Compression Ratio	32000
Pulse Repetition Frequency	1718 MHz
Number of Integrated Pulses	86
Number of Waveform Samples	64
Time Delay Resolution	3.125 ns
Distance Resolution	46.875 cm
Antenna Beamwidth	1.1 degrees
Antenna Diameter and Gain	1.5 m and 43.9 dBi

Table 1. POSEIDON-1 main features.

2.4.1.3. TOPEX Microwave Radiometer

As described in [10] and [11], the TOPEX Microwave Radiometer (TMR) was a three-frequency radiometer that operated at 18, 21, and 37 GHz. It had a nadir-only viewing direction which was co-aligned with the TOPEX and POSEIDON altimeters. The primary objective of the TMR was to correct for the propagation path delay of the altimeter radar signal due to water vapor and nonprecipitating liquid water in the atmosphere. The main antenna of the TMR was a partially offset parabolic reflector with a projected aperture of 79 cm. This resulted in a footprint diameter on the ground of 43.4, 36.4, and 22.9 km at 18, 21, and 37 GHz, respectively. In comparison the altimeter pulse-limited footprint is approximately 3 km in diameter. The 21 GHz channel was the primary channel for water vapor measurements. The 18 and 37 GHz channels were used to remove the effects of wind speed and cloud cover, respectively, on the water vapor measurements.

A drift in the TMR measurements of wet troposphere delay of ~2 mm/year was identified and attributed to a drift in the brightness temperature measurements in the 18 GHz channel [12]. In addition, the tandem phase between the TOPEX/POSEIDON and Jason-1 missions revealed a time-variable path delay bias between the radiometers on each mission that was correlated with the TMR instrument temperature. This bias of 5 mm peak-to-peak error was related to the physical temperature variation of the instrument that repeated on 60-day intervals as the TOPEX/POSEIDON satellite transitioned through different relative sun angles and yaw steering modes.

This GDR-F product uses a dedicated end-of-mission recalibration of the TMR [13] that eliminates drifts in all three channels and mitigates the error related to instrument temperature variations. It also applies the near land path delay algorithm that was first developed for the Jason-2 Advanced Microwave Radiometer [14].

2.4.1.4. Laser Retroreflector Array (LRA)

The Laser Retroreflector Array (LRA) reflects signals from a ground network of satellite laser ranging (SLR) tracking stations to provide tracking data for the precise orbit determination of the satellite [5]. The LRA is a passive instrument. The LRA on the TOPEX/POSEIDON mission consisted of 192 corner cube reflectors arranged in a toroidal ring around the altimeter antenna. In comparison, the LRA on the Jason-series consists of 9 corner cubes and is not on the altimeter antenna.

2.4.1.5. Doppler Orbitography and Radiopositioning Integrated by Satellite (DORIS)

The Doppler Orbitography and Radiopositioning Integrated by Satellite (DORIS) receiver uses two channels (1401.25 MHz and 2036.25 MHz) to observe Doppler signals from a ground network of transmitter stations. It provides all-weather tracking of the satellite for precise orbit determination of the satellite [6]. The dual frequency DORIS measurements from multiple satellites are also used to generate a model of the global total electron content, which can also be used to provide a correction for the ionosphere delay of the altimeter range measurements. Given its excellent performances on TOPEX/POSEIDON, a DORIS instrument has been onboard nearly all altimeter missions ever since (except for GFO and HY-2B).

This GDR-F product provides recent precise orbit determination solutions from the NASA GSFC and CNES that both use SLR and DORIS tracking data, together with modern processing standards and background force models.

2.4.1.6. Global Positioning System (GPS) Demonstration Receiver

The Global Positioning System (GPS) Demonstration Receiver tracked the dual L band radio signals (1.57542 GHz (L1) and 1.2276 GHz (L2)) from a constellation of 24 GPS satellites, collecting navigation data from up to six satellites at once. When the orbit positions and clock offsets of the GPS satellites are known, the GPS tracking data can be used to determine the position and time of the satellite from only four satellites. The GPS receiver was intended to be an experiment to evaluate the accuracy and operational potential of GPS for tracking Earth-orbiting satellites. The TOPEX/POSEIDON GPS receiver could not receive both frequencies when the GPS security feature known as antispoofing (AS) was active. Arrangements were made with the U. S. Department of Defense to turn AS off for nine 10-day periods in the first year of the TOPEX/POSEIDON mission. Initial precise orbit determination results with the GPS tracking data yielded radial orbit accuracies of better than 3 cm [15]. The experiment was so successful that all of the TOPEX/POSEIDON successors carry GPS receivers.

2.4.2. TOPEX and POSEIDON Antenna Sharing Plan

An antenna sharing plan for the TOPEX and POSEIDON altimeters was developed for the TOPEX/POSEIDON mission because they shared the same antenna. In general, this sharing plan had the TOPEX altimeter active for 90% of the time and POSEIDON active for 10% of the time. From launch through repeat cycle 16, the two altimeters shared each cycle with the approximate 90/10 split indicated above. Thereafter, the POSEIDON altimeter was active for approximately one out of every 10 complete repeat cycles (~9.9156 days), with TOPEX active for the remaining cycles. Table 16 in Appendix B provides more details on when the POSEIDON altimeter was active.

2.4.3. Important TOPEX/POSEIDON Timelines and Impact on Reprocessed Data Quality

Table 2 below provides a timeline of the most significant events during the life of the TOPEX/POSEIDON mission. The most notable events impacting data quality and availability are the following:

1. From launch through repeat cycle 16, various changes to the sensors were performed. Data up to repeat cycle 16 have varying quality and should not be used for climate studies.
2. TOPEX Side A was active from September 22, 1992 to February 10, 1999, and Side B was active from February 10, 1999 to end of mission. **Users are advised to treat the data from Side A and Side B as two independent time series. No effort has been made to enforce continuity between Side A and Side B in this reprocessed data.**
3. TOPEX Side A calibration data have a jump on April 1, 1996. This very likely causes a jump in all TOPEX altimeter geophysical measurements at this time. **Users are advised to treat data from Side A1 (Launch – April 1, 1996) and Side A2 (April 1, 1996 – February 10, 1999) as two independent time series. No effort has been made to enforce continuity between Sides A1 and A2.**

4. Sweep Calibration measurements to monitor the TOPEX point target response only started from September 8, 1998 onward for both Side A and Side B. **Users are cautioned that this may cause larger errors in the reprocessed Side A data.** The Sweep Calibration data available for Side A from September 8, 1998 to February 10, 1999 are not used by themselves to process the Side A data in this product. Instead, for Side A, the available Sweep Calibrations have been used to generate a model for oversampled calibrations. The nominal Cal-1 data are used with this model to process all of Side A data to generate a consistent Side A time series. Refer to Section 4.4.1.2.2 for more details.

5. Three 8-track tape recorders (TR A, B, C) were utilized to continuously record the 16K data stream, acquiring over 99.9% of all spacecraft and science data. However, after 5 years of excellent performance the recorders, starting with TRB, slowly started to degrade. Work arounds involving recording and playback speed restored some performance for periods. TRB was deactivated in September 2001 and TRA in October 2002. Real time acquisition through TDRSS filled much of the loss allowing approximately 90% data coverage. Finally, in October 2004 TRC failed. Real time data acquisition provided approximately 82% data coverage until the end of the mission.

Date	Description
August 10, 1992	Launch
September 23, 1992 – February 22, 1993	Calibration and Validation Phase. On reference ground track. Beginning of cycle 001: 19920923T033815.5 Various changes to attitude, sensors, with data quality varying. Data should not be used for climate studies.
February 22, 1993 – August 15, 2002	Observation Phase on reference ground track with nominal sensor operation
September 23, 1992 – February 10, 1999	TOPEX Side A active, except when POSEIDON active (See Appendix B).
April 1, 1996	Jump in TOPEX calibration data with root cause unknown.
From cycle 137 (1996/06/02) to cycle 307 (2001/01)	Initiated download of POSEIDON waveform data archived in MegaFiles. (Retracked POSEIDON data only available for cycles 137-307.)
September 8, 1998	Initiated regular "Cal Sweep" measurements to monitor point target response.
February 10, 1999 – October 9, 2005	TOPEX Side B active, except when POSEIDON active (see Appendix B).
December 7, 2001 – August 15, 2002	Tandem Phase with Jason-1
August 15, 2002 – September 20, 2002	Moved to interleaved ground track (not in repeating orbit)
September 20, 2002 – October 9, 2005	Interleaved ground track
August 27-29, 1992	Satellite Safehold. No data available.
September 24-25, 1992	Satellite Safehold. No data available.
August 6-7, 1993	Satellite Safehold. No data available.
November 26-December 5, 1995	Satellite Safehold. No data available.
January 20-22, 1996	Satellite Safehold. No data available.
August 31-September 3, 1999	Satellite Safehold. No data available.
November 24, 2000	Satellite Safehold. No data available.
May 26-June 11, 2004	Satellite Safehold. No data available.
December 17-18, 2004	Satellite Safehold. No data available.
October 9, 2005	End of mission

Table 2. Important TOPEX/POSEIDON events.

2.4.4. TOPEX/POSEIDON Orbit

The orbit chosen for the TOPEX/POSEIDON mission is a compromise among conflicting requirements. It provides broad coverage of the ice-free oceans as frequently as possible without aliasing tides to unacceptable frequencies (annual, semi-annual, diurnal). It is also high enough to optimize the accuracy of precise orbit determination of the satellite by minimizing the effects of atmospheric drag and the Earth's gravity field. The orbital characteristics of the nominal ground track are provided in Table 3 below. Figure 2 shows a map of the nominal TOPEX/POSEIDON ground track that repeats every 9.9156 days. Figure 3 shows a map of the overlay between the interleaved and nominal TOPEX/POSEIDON ground track, which shows how the spatial resolution of the measurements improved by a factor of two when Jason-1 assumed the nominal ground track and TOPEX/POSEIDON was moved to the interleaved ground track.

Parameter	Value
Semi-major axis	7714.43 km
Eccentricity	0.000095
Inclination	66.04 degrees
Argument of periapsis	90.0 degrees
Inertial longitude of the ascending node	116.56 degrees
Mean Anomaly	253.13 degrees
Inertial nodal rate	-2.08 degrees/day
Orbital speed	7.2 km/s
Ground track speed	5.8 km/s
Reference altitude	1336 km
Nodal period	6745.72 seconds
Repeat period	9.9156 days
Number of orbit revolutions per cycle	127
Equatorial cross track separation	315 km
Ground track control band	+/- 1 km

Table 3. Orbit characteristics of the TOPEX/POSEIDON mission.

**TOPEX/POSEIDON and follow-on missions
altimetry reference mission nominal ground track**
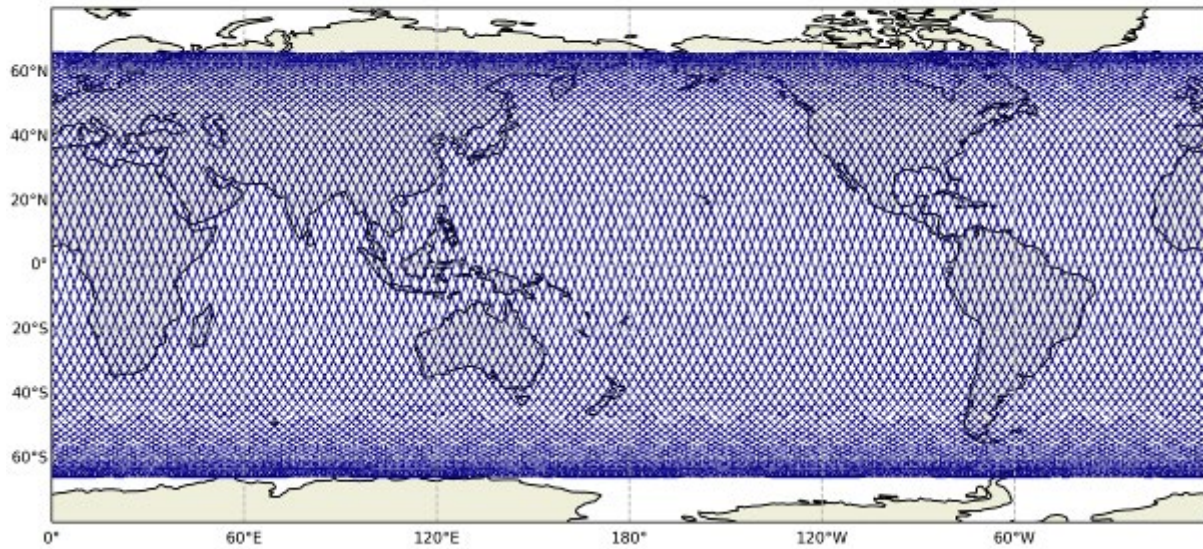
Figure 2. Nominal ground track of the TOPEX/POSEIDON (and successor) missions.

**TOPEX/POSEIDON and follow-on missions
altimetry reference mission nominal (blue) and interleaved (red) ground track**
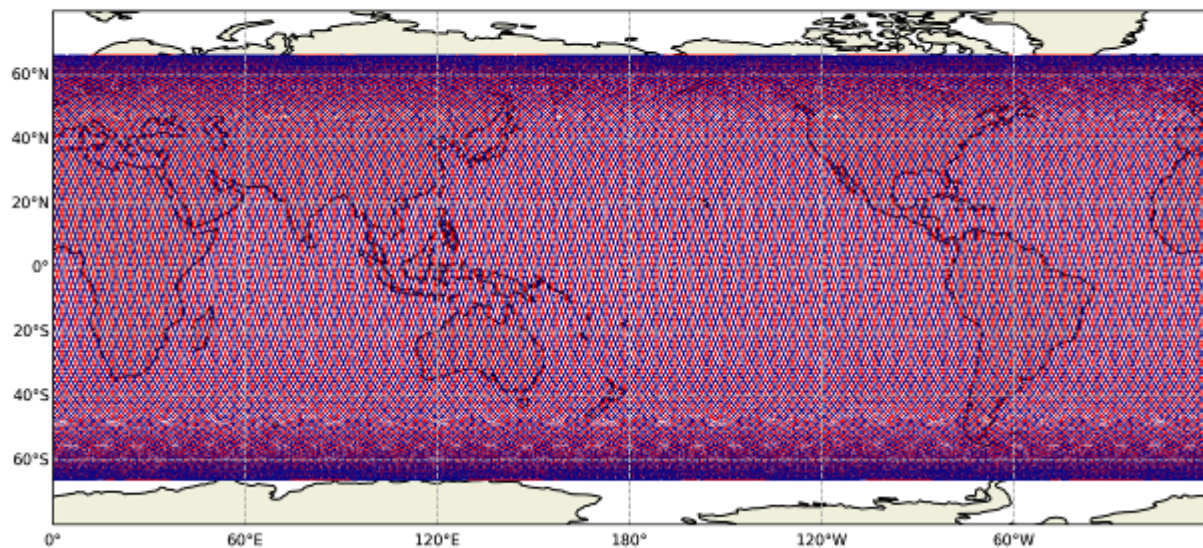
Figure 3. Overlay of nominal and interleaved TOPEX/POSEIDON (and successor) ground tracks.

----

3. Using Altimeter Data

This section provides some basic descriptions and terminology related to satellite altimeter data and how to use altimetry data. Users already familiar with these contents may choose to skip this section.

3.1. Conventions

3.1.1. Filename conventions

The product names are based on the following convention:

TP_<G>P<N>_2P<v><P><ccc>_<ppp>_<yyyymmdd_hhnnss>_<yyyymmdd_hhnnss>

With:

<G>: product family (always set to "G" = GDR for this product release.)
<N >: product type (always set to "N" = native for this product release.)
<v>: product version (always set to 'f' for this product release.)
<P>: product duration (always set to "P" for this product release, to indicate each file spans one "pass")
<ccc>: cycle number of 1st measurement in product record
<ppp>: pass number of 1st measurement in product record (1-254)
<yyyymmdd_hhnnss>: UTC date of 1st measurement in product record
<yyyymmdd_hhnnss>: UTC date of last measurement in product record

Note: The same file naming convention is used for products including either TOPEX or POSEIDON measurements.

3.1.2. Vocabulary

3.1.2.1. Altimetric standards

Altimetry "standards" refer to the version of corrections (models or processing algorithms) that are applied to the data products. They result from recommendations from the Ocean Surface Topography Science Team and responsible agencies. These standards are continuously evolving as new processing approaches and models become available. This release of the TOPEX/POSEIDON reprocessed data products applies the version "F" altimetry standards.

3.1.2.2. Altimetric distances

The following terminology is used in this document and illustrated in Figure 4:

Distance and **Length** are general terms with no special meaning in this document.

Range is the distance from the satellite to the surface of the Earth, as measured by the altimeter. Thus, the altimeter measurement is referred to as "range" or "altimeter range", not height.

Altitude is the distance of the satellite or altimeter above a reference point. The reference point used is the reference ellipsoid. This distance is computed from the satellite ephemeris data.

Height is the distance of the sea surface above the reference ellipsoid. The sea surface height is the difference of the altimeter range from the satellite altitude above the reference ellipsoid.
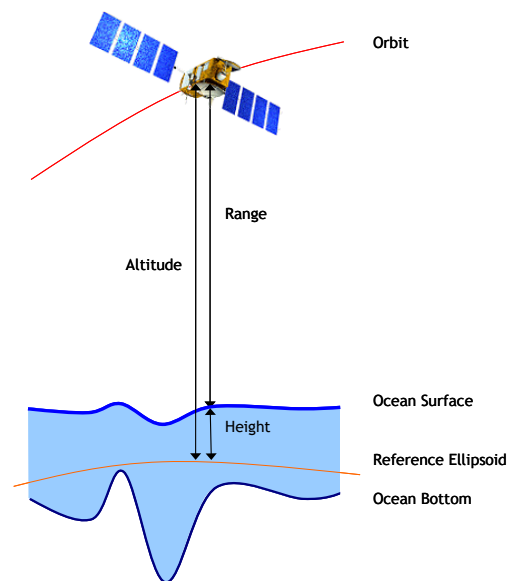
Figure 4. Altimetric distances – Altitude, Range and Height.

3.1.2.3. Orbits, Revolutions, Passes, and Repeat Cycles

An **Orbit** is one circuit of the earth by the satellite as measured from one ascending node crossing to the next. An ascending node occurs when the sub satellite point crosses the earth's equator going from south to north. A **Revolution** (REV) is synonymous with orbit.

The GDR data product is organized into pass files in order to avoid having data boundaries in the middle of the oceans, as would happen if the data were organized by orbit. A **Pass** is half a revolution of the earth by the satellite from extreme north or south latitude to the opposite extreme latitude.

For TOPEX/POSEIDON, an **Ascending Pass** begins at the latitude -66.15 degrees and ends at +66.15 degrees. A **Descending Pass** is the opposite (+66.15 degrees to -66.15 degrees). The passes are numbered from 1 to 254, representing a full repeat cycle of the TOPEX/POSEIDON ground track. Ascending passes are odd numbered and descending passes are even numbered.

After one **repeat cycle** of 254 passes, TOPEX/POSEIDON revisits the same ground-track within ±1 km. This means that locations along the TOPEX/POSEIDON ground-track are measured every approximately 9.9156 days. Lists of passes in numerical and equator longitude order can be found in Appendix C. The pass list is the same for Jason-series and Sentinel-6 missions.

3.1.2.4. Reference Ellipsoid

The **Reference Ellipsoid** is a first-order representation of the non-spherical shape of the Earth. The GDR-F Standard adopts the WGS84 Reference Ellipsoid with an equatorial radius of 6378.1370 kilometers and a flattening coefficient of 1/298.257223563. The values of the radius and flattening of the adopted reference ellipsoid are also provided as global attributes in the product named *ellipsoid_axis* and *ellipsoid_flattening*.

The original TOPEX/POSEIDON products adopted a reference ellipsoid defined with a radius of 6378.1363 km and a flattening coefficient of 1/298.257. For user convenience, the GDR-F products provide the height difference between the original and currently used ellipsoid in a variable named *delta_ellipsoid_tp_wgs84*. Subtract this value from the provided orbit altitude or model of the mean sea surface to reference them to the ellipsoid on the original Topex products. There is no impact to

the provided sea surface height anomaly as the provided orbit altitude and mean surface adopt the same reference ellipsoid.

3.1.3. Correction Conventions

All environmental and instrument corrections are computed so that they should be added to the quantity which they correct. That is, a correction is applied to a measured value by

Corrected Quantity = Measured Value + Correction

This means that a correction to the altimeter range for an effect that lengthens the apparent signal path (e.g., wet troposphere correction) is provided as a negative value. Adding this negative value to the uncorrected (measured) range results with a smaller corrected range. For example: Corrected Range = Measured Range + Range Correction.

3.1.4. Time Convention

Time tags for each measurement data record are provided in the UTC and TAI time scales using the variables *time* and *time_tai*, respectively.

- *time*: Time in UTC time scale (seconds since January 1, 2000 00:00:00 UTC which is equivalent to January 1, 2000 00:00:32 TAI)

- *time_tai*: Time in TAI time scale (seconds since January 1, 2000 00:00:00 TAI, which is equivalent to December 31, 1999 23:59:28 UTC)

The variable *time* has an attribute named *tai_utc_difference*, which represents the difference between TAI and UTC (i.e., total number of leap seconds) at the time of the first measurement record in the product. A UTC leap second can occur on June 30 or December 31 of any year. The leap second is a sixty-first second introduced in the last minute of the day. Thus the UTC values (minutes:seconds) appear as: 59:58 ; 59:59 ; 59:60 ; 00:00 ; 00:01.

- *time_tai[0] = time[0] + tai_utc_difference*

The above relationship holds true for all measurement records unless an additional leap second occurs within the time span of the product. To account for this, the variable *time* also has an attribute named *leap_second* which provides the date at which a leap second occurred within the time span of the product granule. The variable *time* will exhibit a jump when a leap second occurs. If no additional leap second occurs within the time span of the product granule *time: leap_second* is set to "0000-00-00 00:00:00". Appendix D provides a list of the leap seconds that occurred throughout the life of the TOPEX/POSEIDON mission.

3.1.5. Unit Convention

All distances and distance corrections are reported in units of meters after applying the scaling factor associated with each variable. In general, most distances are provided with a precision of 0.1 millimeters.

3.1.6. Flagging and Editing

In general, flagging consists of three parts: instrument flags (on/off), geophysical flags (preliminary flagging and editing) and data quality flags. In most cases, an editing flag is set to 0 for good data.

Instrument flags provide information about the state of the instruments on the satellite. For the altimeters, a global attribute, *altimeter_sensor_name*, and a variable flag, *alt_state_flag_oper*, indicate the operating altimeter from which the measurements are provided (TOPEX Side A, TOPEX Side B or the POSEIDON altimeter).

Geophysical flags are set based on ground conditions such as surface type (land/water-type), bathymetry, possible coastal corruption, ice or rain in the altimeter footprint as determined from data values/characteristics, and tide model availability/reliability.

Quality flags are determined from various statistical checks on the residuals after smoothing or fitting through the data themselves. These flags are set if gaps in the data are detected, or residuals have exceeded predetermined thresholds, or if the first derivative (i.e., slope) of the data exceed predetermined thresholds.

3.2. Typical computation from altimetry data

In this section references are made to specific product variables by name as described in the netCDF datasets. More detailed discussion of most of these data items is given in Section 4.

Ku band altimeter parameters have been computed with both MLE-4 and MLE-3 retracking, with both provided in the products. For TOPEX data, most users are advised to use the Ku band MLE-4 altimeter parameters for typical scientific applications. The Ku band MLE-3 parameters are provided for the convenience of specialized studies on the calibration and validation of the mission and impact of altimeter retracking. As such, Ku band altimeter parameters and related geophysical parameters computed from MLE-3 retracking are named with the "*_mle3*" extension, while those from MLE-4 retracking are named without an extension. C band altimeter parameters and related geophysical parameters have only been computed with MLE-3 retracking and are also named without an extension. For POSEIDON-1 data, additional parameters, with the extension "*_mgdr*" are included in the data. See section 3.2.1.2 for more details.

Default values are assigned to data when computed values are not available. Users are advised to screen variables for default values, as provided in variable attributes named *_FillValue*. Users are also advised to screen data based upon provided flags. The relevant flags are provided in the description of each variable. Some discussion of flags is also provided in this document.

3.2.1. Corrected Altimeter Range

3.2.1.1. TOPEX

The product reports MLE-4 and MLE-3 Ku band ranges and MLE-3 C band ranges in variables named *range_ku*, *range_ku_mle3*, and *range_c*, respectively. The Ku band range is used for most applications. The reported ranges have already been corrected for instrument effects. The applied instrument corrections are reported for each of the Ku and C band ranges in variables named *net_instr_cor_range_ku*, *net_instr_cor_range_ku_mle3*, and *net_instr_cor_range_c*.

The reported ranges must be corrected for path delay in the atmosphere through which the radar pulse passes and the nature of the reflecting sea surface. All range corrections should be added to the reported ranges. The corrected range is given by:

Corrected Range =	Range	+ Wet Troposphere Correction
		+ Dry Troposphere Correction
		+ Ionosphere Correction
		+ Sea State Bias Correction

NOTE: The ionosphere and sea state bias corrections are both frequency dependent. Therefore, Ku band corrections should only be applied to Ku band ranges, and C band corrections should only be applied to C band ranges.

Wet Troposphere Correction:

Most applications should use the wet troposphere correction measured by the onboard microwave radiometer, *rad_wet_tropo_cor*. However, alternative wet troposphere corrections are also provided from a meteorological model in a variable named *model_wet_tropo_cor_zero_altitude*, and from a combination of radiometer and ground GNSS data in a variable named *composite_wet_tropo_gpd*. A wet troposphere correction at measurement altitude, for inland surfaces, is not provided.

Dry Troposphere Correction:

Most applications should use the dry troposphere correction computed from a meteorological model in a variable named *model_dry_tropo_cor_zero_altitude*. This correction is computed for the altitude of the mean sea level and most appropriate for ocean surfaces. For the benefit of potential inland water applications, a variable named *model_dry_tropo_cor_measurement_altitude* is also provided, to account for the altitude of the inland surfaces.

Ionosphere Correction:

The Ku band ionosphere correction that should be used to correct the reported MLE-4 ranges (*range_ku*) is reported in a variable named *iono_cor_alt_ku*. Similarly, the correction that should be used to correct the MLE-3 ranges (*range_ku_mle3*) is in a variable named *iono_cor_alt_ku_mle3*. They are computed from the dual-frequency altimeter range measurements. An alternative Ku band ionosphere correction from a global ionosphere model based on global terrestrial GPS data [16] is also provided in a variable named *iono_cor_gim_ku*. Section 3.2.3 explains how the C band ionosphere correction can be derived from the Ku band ionosphere corrections.

Sea State Bias Correction:

The sea state bias corrections for the TOPEX data are computed using 2-D non-parametric models that are functions of significant wave height and wind speed. The models have been developed specifically for the TOPEX data on this product. Most users are advised to use the sea state bias corrections. These corrections are provided in variables named, *sea_state_bias_ku*, *sea_state_bias_ku_mle3*, and *sea_state_bias_c* for the Ku band MLE-4 and MLE-3 ranges and the C band range, respectively. Alternative sea state bias corrections computed from 3-D non-parametric models that are functions of significant wave height, wind speed, and wave period obtained from a model (in a variable named *mean_wave_period_t02*) are also provided in variables named *sea_state_bias_ku_3d* and *sea_state_bias_c_3d*. The 3-D model may be more suitable for fine regional scales.

3.2.1.2. POSEIDON-1

The GDR provides ranges measured at Ku band (*range_ku* for MLE-4 and *range_ku_mle3* for MLE-3 for recently retracked data, plus *range_ku_mgdr* for historical data). The reported ranges have already been corrected for instrument effects. The applied instrument corrections are reported for each of the Ku ranges in variables named *net_instr_cor_range_ku*, *net_instr_cor_range_ku_mle3*, and *net_instr_cor_range_ku_mgdr*.

The given ranges must be corrected for path delay in the atmosphere through which the radar pulse passes and the nature of the reflecting sea surface. All range corrections should be added to the reported ranges. The corrected Ku range is given by:

Corrected Range =	Range	+ Wet Troposphere Correction
		+ Dry Troposphere Correction
		+ Ionosphere Correction
		+ Sea State Bias Correction

Wet Troposphere Correction:

· Use TMR correction (*rad_wet_tropo_cor*).

Dry Troposphere Correction:

· Use model correction (*model_dry_tropo_cor_zero_altitude*).

Ionosphere Correction:

· Use DORIS-derived correction (*iono_cor_doris*) to correct POSEIDON-1 Ku band range from all retrackings.

Sea State Bias Correction:

The sea state bias corrections for the POSEIDON data are computed from an empirical model derived from analyses of altimeter data itself (see part 4.5.5.3). Most users are advised to use the sea state bias corrections. Based on the results of [48] and [49], the so-called BM4 model is used to estimate the SSB of POSEIDON. This model takes the form:

$$SSB_{Ku} = SWH_{Ku} [a1 + a2 * U + a3 * U^2 + a4 * SWH_{Ku}]$$

where

SSB is the sea state bias, in meters (Ku band),

U is the wind intensity, in m/s (Ku band)

SWH is the Significant Wave Height, in meters (Ku band)

These corrections are provided in POSEIDON-1 products in variables named *sea_state_bias_ku*, *sea_state_bias_ku_mle3* and *sea_state_bias_ku_mgdr*, for the Ku band MLE-4 and MLE-3 retracked ranges and the MGDR deduced range, respectively. As previously explained, *sea_state_bias_ku* and *sea_state_bias_ku_mle3* are set to default values out of the retracked period. Users are advised to :

· Use MLE-4 sea state bias correction (*sea_state_bias_ku*) to correct Ku band range issued from MLE-4 retracking (*range_ku*).

· Use MLE-3 sea state bias correction (*sea_state_bias_ku_mle3*) to correct Ku band range issued from MLE-3 retracking (*range_ku_mle3*).

· Use MGDR sea state bias correction (*sea_state_bias_ku_mgdr*) to correct Ku band range issued from legacy MGDR retracking (*range_ku_mgdr*).

3.2.2. Sea Surface Height and Sea Surface Height Anomaly

Sea surface height (SSH) is the height of the sea surface above the reference ellipsoid. It is calculated by subtracting the corrected range from the satellite altitude:

Sea Surface Height = Altitude - Corrected Range

The sea surface height anomaly (SSHA) (or Sea Surface Height with respect to a mean sea surface, often also called Sea Level Anomaly) is reported in the product with variables named *ssha* and *ssha_mle3*, as computed from MLE-4 and MLE-3 Ku band parameters, respectively. SSHA is defined here as the sea surface height after subtracting for known geophysical effects. Models are used for these known geophysical effects and primarily include the mean sea surface, solid Earth and ocean tides, the pole tide, and the high-frequency (periods of less than 20 days) dynamic response to the atmospheric pressure and winds. The SSHA is computed as follows:

> Sea surface height Anomaly =   Sea Surface Height - Mean Sea Surface
>
> - Solid Earth Tide Height
>
> - Geocentric Ocean Tide Height
>
> - Non-Equilibrium Long Period
>
> - Internal Tide Height
>
> - Pole Tide Height
>
> - Dynamic Atmospheric Correction

The SSHA contains information about:

· Real changes in ocean topography related to ocean currents.

· Long-period dynamic response to atmospheric pressure and winds.

· Errors in all of the applied geophysical models.

· Errors in the altimeter measurements and range corrections.

· Errors in the orbit altitude.

Details on the geophysical effects and models provided on the product are provided in Section 4.6

3.2.3. Total Electron Content from Ionosphere Correction

The ionospheric Total Electron Content (TEC) along the line-of-sight of the TOPEX range measurements can be computed from the Ku and C band range measurements, as follows:

$$\text{Ionospheric Total Electron Content} = \frac{-\partial R \times f^2}{40.3}$$

where:

Ionospheric Total Electron Content is in electrons/m^2

∂R = reported Ku band ionospheric range correction in meters (e.g., *iono_cor_alt_ku* or *iono_cor_alt_ku_mle3*)

f = frequency in Hz (13.6 GHz for Ku band)

The C band ionosphere range correction can be derived from the Ku band ionosphere range correction by correcting if from the corresponding frequencies as follows:

$$\partial R(c) = \frac{\partial R(ku) \times f(ku)^2}{f(c)^2}$$

where:

$\partial R(c)$ = computed C band ionospheric range correction in meters (e.g., *iono_cor_alt_ku* or *iono_cor_alt_ku_mle3*)

$\partial R(ku)$ = reported Ku band ionospheric range correction in meters (e.g., *iono_cor_alt_ku* or *iono_cor_alt_ku_mle3*)

$f(ku)$ = Ku band frequency in Hz (13.6 GHz)

$f(c)$ = C band frequency in Hz (5.3 GHz)

3.2.4. Data 1-Hz Compression

3.2.4.1. TOPEX

Individual measurements (from on-board tracking intervals) are compressed into 1 Hz measurements using 20 consecutive tracking interval measurements.

The actual duration of the TOPEX tracking intervals varies between 53.6 and 54.3 ms depending on the satellite altitude. As a consequence, the actual duration of the so-called 1 Hz measurements varies nominally between 1.07 and 1.09 s. For simplicity, here these data are simply referred to as 20 Hz and 1 Hz, respectively.

3.2.4.1.1. Waveform resampling to 20 Hz

The TOPEX altimeter on-board tracking loop parameters and waveforms were generated at a 20 Hz data rate. However, due to telemetry limitations at the time, the downlinked telemetry contains the original 20 Hz tracking loop range and Automatic Gain Control (AGC) data but only averages of the 20 Hz waveforms. Specifically, the downlinked Ku and C band waveforms were averaged to 10 and 5 Hz samples, respectively. The on-ground numerical retracking has been performed on the available 10 and 5 Hz waveforms and the corresponding outputs have then been simply replicated to 20 Hz samples (2x for Ku band and 4x for C band). The resulting 20 Hz values from the retracking have then been combined with the corresponding 20 Hz tracking loop data (ranges and AGC) in order to derive the 20 Hz ranges and backscatter coefficients reported on this product. The significant wave heights are determined exclusively from the waveform retracking.

Note that a shift in the index for the relationship between the 20 Hz tracking loop data and the averaged waveforms was identified during TOPEX reprocessing. This shift has been taken into account in this product when combining the 20 Hz tracking loop data with the retracking outputs of the averaged 10 Hz Ku band and 5 Hz C band waveforms, as illustrated in Figure 5 and Figure 6 below. The tandem mission with Jason-1 has been used to verify this shift. In particular, differences between TOPEX and Jason-1 uncorrected sea surface height (altitude – range – mean sea surface) have lower standard deviation when the shift is applied than when it is not applied, as illustrated in Figure 7 below [17].
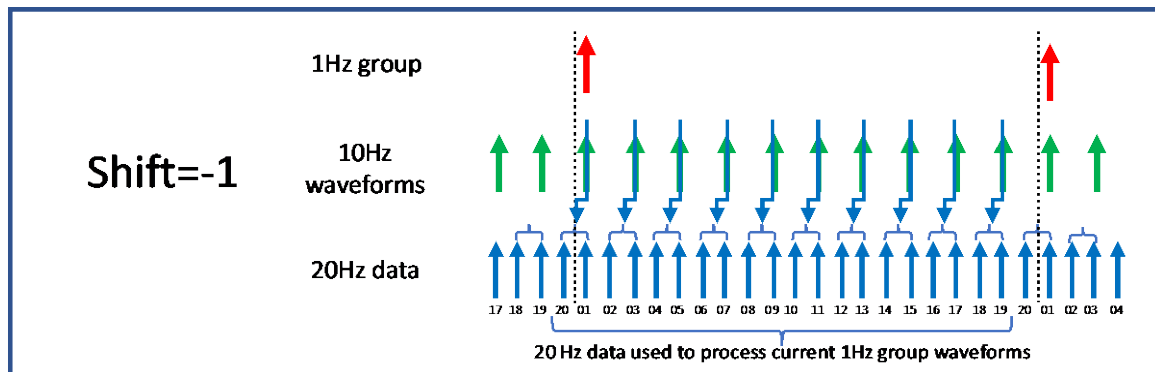
Figure 5. 20 Hz tracking data shift for combination with 10 Hz Ku Band waveforms.
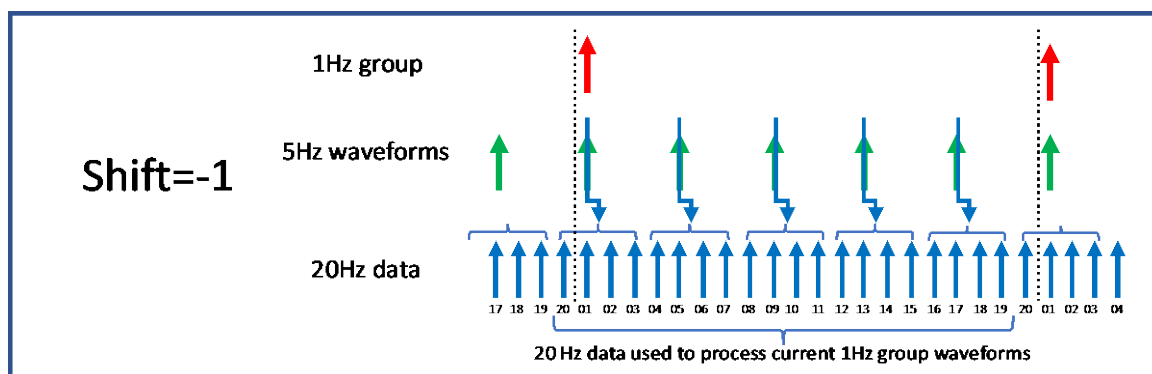
Figure 6. 20 Hz tracking data shift for combination with 5 Hz C Band waveforms.
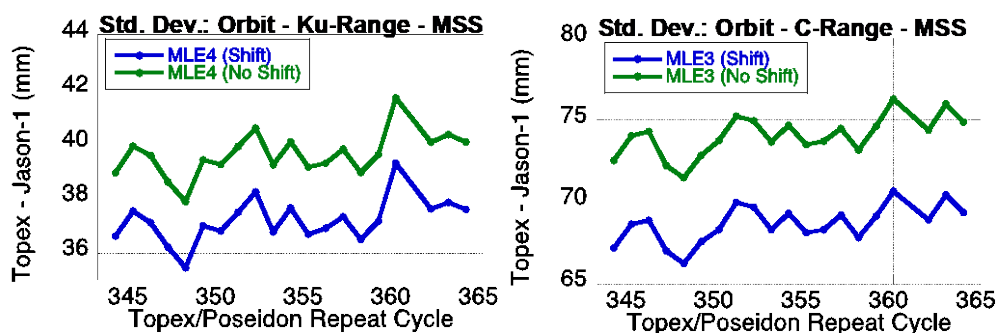
Figure 7. Standard deviation of uncorrected sea surface height (orbit altitude - range – mean sea surface) differences between TOPEX and Jason-1 during their tandem mission for Ku band (left panel) and C band (right panel), with and without applying shift in relationship between averaged waveforms and onboard tracking loop parameters.

3.2.4.1.2. Range compression

Each 1 Hz frame of the TOPEX Ku and C band range measurements (*range_ku, range_ku_mle3* and *range_c*) is derived from the linear regression of the respective valid 20 Hz range measurements (*range_20hz_ku, range_20hz_ku_mle3* and *range_20hz_c*). Valid 20 Hz ranges are first determined by verifying the convergence of the waveform retracking and a threshold on the Mean Quadratic Error (MQE). The MQE represents the root-mean-square of the difference between the corresponding measured echoes and the echoes as modeled at the end of the retracking process, and is provided in variables named *mqe_20hz_ku, mqe_20hz_ku_mle3*, and *mqe_20hz_c*. An iterative outlier detection scheme is then adopted in the linear regression when computing the 1 Hz ranges. The resulting valid 20 Hz measurements that are used to determine the 1 Hz measurements are provided in flags named *range_used_20hz_ku, range_used_20hz_ku_mle3, range_used_20hz_c*. Valid 20 Hz measurements have this parameter set to a value of 0. Note that the linear regression is actually performed on altitude-range values instead of range values. The number of valid 20 Hz measurements that are used to derive each of the 1 Hz measurements is provided in variables named *range_numval_ku, range_numval_ku_mle3*, and *range_numval_c*. The root-mean-square (RMS) of the differences between the valid 20 Hz measurements with respect to the linear fit are also provided in variables named *range_rms_ku, range_rms_ku_mle3*, and *range_rms_c*. The validity of the 1 Hz compressed value is based on a minimum threshold on the number of corresponding 20 Hz valid measurements and on a maximum threshold on the value of the RMS of the differences. Flags named *range_ku_qual, range_ku_mle3_qual*, and *range_c_qual* reflect the validity of the 1 Hz measurements, where valid measurements have a value of 0. Specialized applications, such as over land, ice, lakes or rivers, may benefit from using the 20 Hz measurements or alternative compression algorithms.

3.2.4.1.3. SWH compression

Each 1 Hz frame of the TOPEX significant wave height measurements (*swh_ku*, *swh_ku_mle3*, *swh_c*) are derived from the averages of the respective valid 20 Hz measurements (*swh_20hz_ku*, *swh_20hz_ku_mle3* and *swh _20hz_c*). As with the ranges, valid 20 Hz data are first determined by verifying the convergence of the waveform retracking and a threshold on the MQE. The number of valid 20 Hz measurements that are used to derive each of the 1 Hz measurements is provided in variables named *swh_numval_ku*, *swh_numval_ku_mle3*, and *swh_numval_c*. The RMS of the differences between the individual valid 20 Hz measurements with respect to the 1 Hz averaged value are provided in variables named *swh_rms_ku*, *swh_rms_ku_mle3*, and *swh_rms_c*. The validity of the 1 Hz compressed value is based on a minimum threshold on the number of corresponding 20 Hz valid measurements. Flags named *swh _ku_qual*, *swh _ku_mle3_qual* and *swh _c_qual* reflect the validity of the 1 Hz measurements, where valid measurements have a value of 0. Specialized applications, such as over land, ice, lakes or rivers, may benefit from using the 20 Hz measurements or alternative compression algorithms.

3.2.4.1.4. Sigma0 compression

Each 1 Hz frame of the TOPEX sigma0 measurements (*sig0_ku*, *sig0_ku_mle3* and *sig0_c*) are derived from the averages of the respective valid 20 Hz measurements (*sig0 _20hz_ku*, *sig0_20hz_ku_mle3* and *sig0_20hz_c*). As with the ranges, valid 20 Hz data are first determined by verifying the convergence of the waveform retracking and a threshold on the MQE. The 20 Hz sigma0 data are also tested for the validity (i.e., not defaulted) of the atmospheric attenuation correction (*rad_atm_cor_sig0_ku* and *rad_atm_cor_sig0_c*). The number of valid 20 Hz measurements that are used to derive each of the 1 Hz measurements is provided in variables named *sig0_numval_ku*, *sig0_numval_ku_mle3*, and *sig0_numval_c*. The RMS of the differences between the individual valid 20 Hz measurements with respect to the 1 Hz averaged value are provided in variables named *sig0_rms_ku*, *sig0_rms_ku_mle3*, and *sig0_rms_c*. The validity of the 1 Hz compressed value is based on detection of default values only (i.e., if compression fails). Flags named *sig0_ku_qual*, *sig0_ku_mle3_qual* and *sig0_c_qual* reflect the validity of the 1 Hz measurements, where valid measurements have a value of 0. Specialized applications, such as over land, ice, lakes or rivers, may benefit from using the 20 Hz measurements or alternative compression algorithms.

3.2.4.1.5. AGC compression

Each 1 Hz frame of the TOPEX AGC measurements (*agc_ku* and *agc_c*) are derived from averages of the respective valid 20 Hz measurements (*agc_20hz_ku* and *agc_20hz_c*). The number of valid 20 Hz measurements that are used to derive each of the 1 Hz measurements is provided variables named *agc_numval_ku* and *agc_numval_c*. The RMS of the differences between the individual valid 20 Hz measurements with respect to the 1 Hz averaged value are provided in variables named *agc_rms_ku* and *agc _rms_c*.

3.2.4.1.6. Mispointing compression

Each 1 Hz frame of the TOPEX Ku band off-nadir angle (or mispointing) measurements (*off_nadir_angle_wf _ku*) are derived from the average of the respective valid 20 Hz measurements (*off_nadir_angle_wf_20hz_ku*). As with the ranges, valid 20 Hz data are first determined by verifying the convergence of the waveform retracking and a threshold on the MQE. The number of valid 20 Hz measurements that are used to derive each of the 1 Hz measurements is provided in a variable named *off_nadir_angle_wf_numval_ku*. The RMS of the differences between the individual valid 20 Hz measurements with respect to the 1 Hz averaged value are provided in a variable named *off_nadir_angle_wf _rms_ku*. The validity of the 1 Hz compressed value is based on a maximum threshold on the absolute value of the 1 Hz mispointing estimate. A flag named *off_nadir_angle_wf_ku_qual* reflects the validity of the 1 Hz measurements, where valid measurements have a value of 0.

3.2.4.2. POSEIDON-1

Over the retracked period (cycles 137 to 307), 20 Hz data are available for POSEIDON-1, so that no waveform resampling is necessary (see 3.2.4.1.1 for waveform resampling process applied to TOPEX data only). The same compression method as used for TOPEX data has been applied to POSEIDON Ku band range and SWH compression from MLE-4 and MLE-3 outputs (no secondary band on POSEIDON-1). Using the corresponding retracking quality flag from retracker output, the range and SWH parameters are compressed to the provided 1 Hz measurements. Note that the parameters to be compressed must not be corrected for instrumental effects. Range estimation is described in section 4.4.2.3 and SWH estimation in section 4.4.2.4 (see part 4.4.2.7 for more details on instrumental corrections). Note that as there is no archive to recompute new sigma0 values at 20 Hz, there is no compression of sigma0 during the POSEIDON-1 GDR-F reprocessing.

In addition to the retracking quality flag, and in order to achieve a correct compression, the measurements for which the MQE is too high are not taken into account during the compression. It is then necessary to define a threshold on the MQE from which the output estimates are considered to have poor quality. Currently on Jason-3, this threshold is defined at 0.0171 (-17.67 dB), so that over ocean, about 2.2 % of the measurements have an MQE higher than this threshold. In order to obtain a similar compression on POSEIDON-1, thresholds are estimated to obtain about the same rejection rate (this rejection rate is set at 2.5 %). For the compression of the estimates from MLE-3 / MLE-4 retracking, the threshold was therefore respectively set at -20.55 dB and -16.65 dB (see Figure 8).
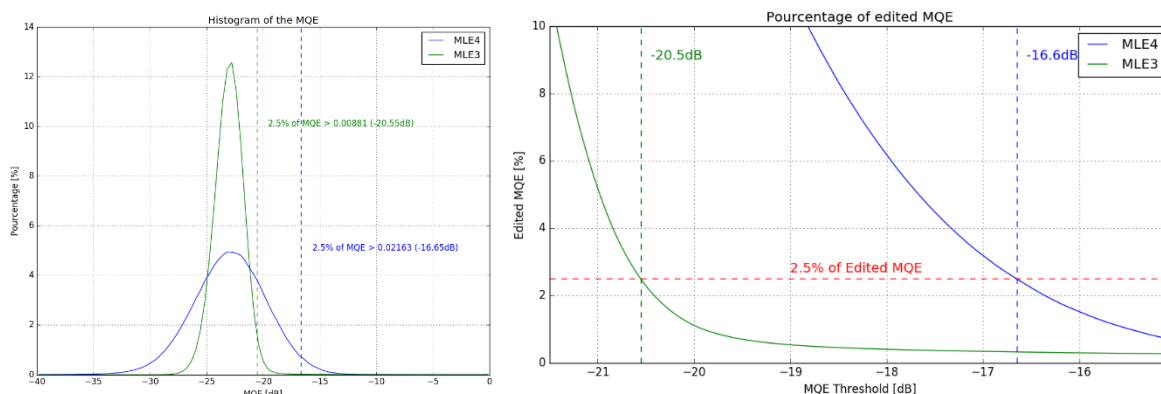
Figure 8. POSEIDON-1. Histogram and threshold position (left), and percentage of rejected data during compression (right) according to the chosen threshold on the MQE for MLE-3 and MLE-4.

3.2.5. Data Editing

The following editing criteria are a suggested guideline for finding good sea surface height anomaly measurements. The user should review these criteria before using them and may wish to modify them.

3.2.5.1. TOPEX

First, check for open ocean data not covered by ice using the following conditions:

surface_classification_flag = 0   (i.e., Open oceans)
ice_flag = 0   (i.e., No ice)

Then, filter the data as shown in Table 4 to retain only valid data, and exclude data where any of the parameters below are set to FillValue. The additional filtering criteria in Table 5 can then be used to

retain only highly reliable data. Note that the parameter *alt_echo_type* is generated while performing the 1 Hz altimeter range compression. The value of *alt_echo_type* is set to 0 if *range_rms_ku* < 150 mm and if *range_numval_ku* $\geq$ 15 (see section 3.2.4.1.2). To restrict studies to deep water, apply a threshold, e.g., water depth of 1000 m or greater, using the bathymetry parameter, *depth_or_elevation*.

Parameter	Validity conditions
model_dry_tropo_cor_zero_altitude	-2 500 $\leq$ x (mm) $\leq$ - 1 900
rad_wet_tropo_cor	-500 $\leq$ x (mm) $\leq$ - 1
iono_cor_alt_ku	-500 $\leq$ x (mm) $\leq$ 100
swh_ku	50 $\leq$ x (mm) $\leq$ 16 000
sig0_ku	5 $\leq$ x (dB) $\leq$ 28
off_nadir_angle_wf_ku	-0.2 $\leq$ x (deg^2) $\leq$ 0.5
SSHA	-2 000 $\leq$ x (mm) $\leq$ 2 000

Table 4. Recommended TOPEX functional filtering criteria for sea surface height anomaly.

Parameter	Validity conditions
alt_echo_type	x = 0
sig0_rms_ku	x (dB) $\leq$ 1
swh_rms_ku	x (dB) $\leq$ 2
off_nadir_angle_wf _rms_ku	x (deg^2) $\leq$ 0.1

Table 5. Recommended TOPEX performance filtering criteria for sea surface height anomaly.

3.2.5.2. POSEIDON-1

The same approach as used for TOPEX is recommended for POSEIDON-1 data:

✓ First, the removal of land and ice data, using the following conditions:

surface_classification_flag = 0   (i.e., Open oceans)
ice_flag = 0   (i.e., No ice)

✓ Then, the filtering of the remaining ocean data using thresholds detailed in Table 6.

Note that to restrict studies to deep waters, users can apply a threshold, e.g., water depth of 1000 m or greater, using the bathymetry parameter, *depth_or_elevation*.

Parameter	Validity conditions
range_numval (or with ext _mle3 or _mgdr)	$10 \leq x$ (count) ≤ 20
range_rms_ku (or with ext _mle3 or _mgdr)	$0 \leq x$ (mm) ≤ 200
sea_state_bias (or with ext _mle3 or _mgdr)	$-500 \leq x$ (mm) ≤ 0
sig0_ku (or with ext _mle3 or _mgdr)	$7 \leq x$ (dB) ≤ 30
off_nadir_angle_wf_ku	$-0.2 \leq x$ (deg^2) ≤ 0.64
swh_ku (or with ext _mle3 or _mgdr)	$0 \leq x$ (mm) $\leq 11\,000$
wind_speed (or with ext _mle3 or _mgdr)	$0 \leq x$ (m/s) ≤ 30
iono_cor_doris	$-400 \leq x$ (mm) ≤ 40
rad_wet_tropo_cor	$-500 \leq x$ (mm) ≤ -1
model_dry_tropo_cor_zero_altitude	$-2\,500 \leq x$ (mm) $\leq -1\,900$
dac	$-2\,000 \leq x$ (mm) $\leq 2\,000$
ssha (or with ext _mle3 or _mgdr)	$-2\,000 \leq x$ (mm) $\leq 2\,000$

Table 6: Recommended POSEIDON-1 filtering criteria for sea surface height anomaly.

----

4. Product fields and processing

4.1. Models and Editing on Version "f" Products

Table 7 below summarizes the processing approaches and models used to generate the TOPEX/POSEIDON data product, and specifically identifies where there are differences between the TOPEX and POSEIDON data. Additional information is provided in the sections that follow.

Model	TOPEX	POSEIDON
Orbit Solutions	Two orbit solutions from NASA GSFC and CNES in ITRF2014 reference frame. • NASA GSFC solution computed using SLR and DORIS tracking data for cycles 1 – 446, and SLR with sea surface height crossover data for cycles 447-480. • CNES solution is following POE-F computation standards (see more details in part 4.3.2).	
Altimeter Retracking	Numerical retracking with: • Ku band MLE-4 and MLE-3 • C band MLE-3 MLE-4 fits a 2nd order Brown analytical model to retrieve epoch (=> range), significant wave height, amplitude (=> sigma0), and square of mispointing angle. MLE-3 fits a 2nd order Brown analytical model to retrieve epoch (=> range), significant wave height, and amplitude (=> sigma0).	• Ku band MLE-4 and MLE-3 retracked (available over cycles 137 to 307 only) MLE-4 fits a 2nd order Brown analytical model to retrieve epoch (=> range), significant wave height, amplitude (=> sigma0), and square of mispointing angle. MLE-3 fits a 2nd order Brown analytical model to retrieve epoch (=> range), significant wave height, and amplitude (=> sigma0). • Ku band historical MLE-3 (available over the whole period)
Altimeter Instrument Corrections	Provided for each of Ku band MLE-4 and MLE-3, and C band MLE-3.	Provided for each of Ku band MLE-4 and MLE-3
TOPEX Microwave Radiometer	Computed using algorithms from [18], a near-land path delay algorithm from [14], and an end-of-mission calibration from [13].	
Dry Troposphere Range Correction	Computed from spatial and temporal interpolation of the ERA-Interim numerical weather model [19]. Provided at mean sea level and measurement altitude.	
Wet Troposphere Range Correction from Model	Computed from spatial and temporal interpolation of the ERA-Interim numerical weather model [19]. Provided at mean sea level only. Value from University of Porto GPD+ also provided.	
Ionosphere Range Correction	Computed using dual-frequency altimeter measurements.	Using DORIS correction
Ionosphere Range Correction from Model	Computed using Global Ionosphere Maps for cycles 48 onward.	
Sea State Bias Correction	Computed from two non-parametric models: • 2-D model from [20]. • 3-D model from [21].	3 BM4 solutions computed from MLE-4 / MLE-3 / MGDR SSH
Reference Ellipsoid	WGS84	
Geoid Model	EGM2008 from [22].	

Mean Sea Surface Model	Computed using two models: • MSS_CNES_CLS15 from [23]. • DTU10 from [24].	
Mean Dynamic Topography Model	MDT_CNES-CLS2018 model from [25].	
Ocean and Load Tide Models	Computed using two models: • FES2014b from [26]. • GOT4.10c from [27].	
Equilibrium Long-Period Ocean Tide Model	Computed using tide-generating potential from [28] [29].	
Non-equilibrium Long-Period Ocean Tide Model	Computed using FES2014b [26] with 6 frequencies (Mf, Mm, MSqm, Mtm, Sa, and Ssa)	
Solid Earth Tide Model	Computed using tide-generating potential from [28] [29] using frequency-independent Love numbers except at K1 frequency.	
Pole Tide Model	Computed using model from [30] with linear mean pole model from [31].	
Internal Tide Model	Computed using model from [32] for M2, S1, K1, and O1 frequencies.	
Dynamic Atmosphere Correction Model	Computed using MOG2D model from [33] forced by ERA-Interim numerical weather model [19] pressure and wind.	
Inverse Barometer Correction	Computed from ERA-Interim numerical weather model [19].	
Wind Speed from Altimeter	Computed using Ku band altimeter wind speed and significant wave height from [34] and [35]. Provided for MLE-3 and MLE-4.	Computed using Ku band altimeter wind speed and significant wave height. Provided for MLE-3 and MLE-4 and MGDR.
Wind Speed from Radiometer	Computed using TMR brightness temperatures and algorithm from [18].	
Wind Speed from Model	Wind speed vector computed from spatial and temporal interpolation fo ERA-Interim numerical weather model [19].	
Wave Model	Provides model of significant wave height and mean wave period from [36].	
Rain Flag	Altimeter rain flag computed using sigma0 and TMR cloud liquid content. TMR rain flag computed using 18 GHz TMR brightness temperatures and cloud liquid content.	/
Ice Flag	Altimeter ice flag computed using climatological sea ice extent and altimeter wind speed. Radiometer sea ice flag computed using TMR brightness temperatures.	
Surface Classification Flag	Computed with 7 states from map derived from GMT, GLOBCOVER, and MODIS.	

Table 7. Summary of TOPEX/POSEIDON Product Processing and Models.

4.2. Fields Specific to TOPEX and POSEIDON data

All the variables and their respective availability for TOPEX and POSEIDON data are listed in Table 8 below:

	TOPEX	POSEIDON CYCLES 137 - 307	POSEIDON CYCLES 003 - 126 + 361
time	X	X	X
time_20hz	X	X	
time_tai	X	X	X
meas_ind	X	X	
l2_record_counter	X		
altitude	X	X	X
altitude_20hz	X	X	
altitude_cnes	X	X	X
altitude_rate_mean_sea_surface	X	X	X
delta_ellipsoid_tp_wgs84	X	X	X
latitude	X	X	X
latitude_20hz	X	X	
longitude	X	X	X
longitude_20hz	X	X	
alt_state_flag_oper	X	X	X
alt_state_flag_c_band	X		
alt_state_flag_ku_band_status	X		
alt_state_flag_c_band_status	X		
alt_echo_type	X		
num_iterations_ku	X		
num_iterations_ku_mle3	X		
num_iterations_c	X		
mqe_20hz_ku	X	X	
mqe_20hz_ku_mle3	X	X	
mqe_20hz_c	X		
range_ku	X	X	X
range_20hz_ku	X	X	
range_ku_mle3	X	X	X
range_20hz_ku_mle3	X	X	
range_ku_mgdr		X	X
range_c	X		
range_20hz_c	X		
range_used_20hz_ku	X	X	
range_used_20hz_ku_mle3	X	X	
range_used_20hz_c	X		
range_rms_ku	X	X	X
range_rms_ku_mle3	X	X	X
range_rms_ku_mgdr		X	X
range_rms_c	X		
range_numval_ku	X	X	X

	TOPEX	POSEIDON CYCLES 137 - 307	POSEIDON CYCLES 003 - 126 + 361
range_numval_ku_mle3	X	X	X
range_numval_ku_mgdr		X	X
range_numval_c	X		
range_ku_qual	X	X	X
range_ku_mle3_qual	X	X	X
range_c_qual	X		
osc_drift_cor	X		
range_cor_doppler_ku	X		
range_cor_doppler_c	X		
cg_to_altimeter_timevarying_offset	X		
net_instr_cor_range_ku	X	X	X
net_instr_cor_range_ku_mle3	X	X	X
net_instr_cor_range_ku_mgdr		X	X
net_instr_cor_range_c	X		
swh_ku	X	X	X
swh_20hz_ku	X	X	
swh_ku_mle3	X	X	X
swh_20hz_ku_mle3	X	X	
swh_ku_mgdr		X	X
swh_c	X		
swh_20hz_c	X		
swh_used_20hz_ku	X	X	
swh_used_20hz_ku_mle3	X	X	
swh_used_20hz_c	X		
swh_rms_ku	X	X	X
swh_rms_ku_mle3	X	X	X
swh_rms_c	X		
swh_numval_ku	X	X	X
swh_numval_ku_mle3	X	X	X
swh_numval_c	X		
swh_ku_qual	X	X	X
swh_ku_mle3_qual	X	X	X
swh_c_qual	X		
net_instr_cor_swh_ku		X	X
net_instr_cor_swh_ku_mle3		X	X
swh_model	X	X	X
mean_wave_period_t02	X	X	X
sig0_ku	X	X	X
sig0_20hz_ku	X		
sig0_ku_mle3	X		
sig0_20hz_ku_mle3	X		
sig0_c	X		
sig0_20hz_c	X		

	TOPEX	POSEIDON CYCLES 137 - 307	POSEIDON CYCLES 003 - 126 + 361
sig0_ku_mgdr		X	X
sig0_used_20hz_ku	X		
sig0_used_20hz_ku_mle3	X		
sig0_used_20hz_c	X		
sig0_rms_ku	X		
sig0_rms_ku_mle3	X		
sig0_rms_c	X		
sig0_rms_ku_mgdr		X	X
sig0_numval_ku	X		
sig0_numval_ku_mle3	X		
sig0_numval_c	X		
sig0_ku_qual	X		
sig0_ku_mle3_qual	X		
sig0_c_qual	X		
agc_ku	X	X	X
agc_20hz_ku	X	X	
agc_c	X		
agc_20hz_c	X		
agc_rms_ku	X		
agc_rms_c	X		
agc_numval_ku	X		
agc_numval_c	X		
net_instr_cor_sig0_ku	X		
net_instr_cor_sig0_ku_mle3	X		
net_instr_cor_sig0_c	X		
net_instr_cor_sig0_ku_mgdr		X	X
off_nadir_angle_wf_ku	X	X	X
off_nadir_angle_wf_20hz_ku	X	X	
off_nadir_angle_wf_used_20hz_ku	X	X	
off_nadir_angle_wf_rms_ku	X	X	X
off_nadir_angle_wf_numval_ku	X	X	X
off_nadir_angle_wf_ku_qual	X	X	X
off_nadir_angle_wf_ku_smoothed	X		
off_nadir_angle_wf_ku_mgdr		X	X
rain_flag	X		
ice_flag	X	X	X
iono_cor_alt_ku	X		
iono_cor_alt_ku_mle3	X		
iono_cor_doris		X	X
iono_cor_gim_ku	X	X	X
wind_speed_alt	X	X	X
wind_speed_alt_mle3	X	X	X
wind_speed_alt_mgdr		X	X

	TOPEX	POSEIDON CYCLES 137 - 307	POSEIDON CYCLES 003 - 126 + 361
sea_state_bias_ku	X	X	X
sea_state_bias_ku_mle3	X	X	X
sea_state_bias_c	X		
sea_state_bias_ku_mgdr		X	X
sea_state_bias_ku_3d	X		
sea_state_bias_c_3d	X		
rad_wet_tropo_cor	X	X	X
rad_water_vapor	X	X	X
rad_cloud_liquid_water	X	X	X
rad_wind_speed	X	X	X
rad_atm_cor_sig0_ku	X	X	X
rad_atm_cor_sig0_c	X		
rad_wet_tropo_cor_qual	X	X	X
rad_water_vapor_qual	X	X	X
rad_cloud_liquid_water_qual	X	X	X
rad_wind_speed_qual	X	X	X
rad_atm_cor_sig0_ku_qual	X	X	X
rad_atm_cor_sig0_c_qual	X		
rad_surface_type_flag	X	X	X
rad_distance_to_land	X	X	X
rad_land_frac_18	X	X	X
rad_land_frac_21	X	X	X
rad_land_frac_37	X	X	X
rad_rain_flag	X	X	X
rad_sea_ice_flag	X	X	X
rad_tb_18	X	X	X
rad_tb_21	X	X	X
rad_tb_37	X	X	X
rad_ta_18	X	X	X
rad_ta_21	X	X	X
rad_ta_37	X	X	X
rad_tmb_18	X	X	X
rad_tmb_21	X	X	X
rad_tmb_37	X	X	X
rad_tb_18_qual	X	X	X
rad_tb_21_qual	X	X	X
rad_tb_37_qual	X	X	X
rad_ta_18_qual	X	X	X
rad_ta_21_qual	X	X	X
rad_ta_37_qual	X	X	X
rad_tmb_18_qual	X	X	X
rad_tmb_21_qual	X	X	X
rad_tmb_37_qual	X	X	X

	TOPEX	POSEIDON CYCLES 137 - 307	POSEIDON CYCLES 003 - 126 + 361
surface_classification_flag	X	X	X
distance_to_coast	X	X	X
model_dry_tropo_cor_zero_altitude	X	X	X
model_dry_tropo_cor_measurement_altitude	X	X	X
model_wet_tropo_cor_zero_altitude	X	X	X
composite_wet_tropo_gpd	X	X	X
mean_sea_surface_cnescls	X	X	X
mean_sea_surface_cnescls_acc	X	X	X
mean_sea_surface_cnescls_qual	X	X	X
mean_sea_surface_dtu	X	X	X
mean_sea_surface_dtu_acc	X	X	X
mean_sea_surface_dtu_qual	X	X	X
mean_dynamic_topography	X	X	X
mean_dynamic_topography_acc	X	X	X
mean_dynamic_topography_qual	X	X	X
geoid	X	X	X
depth_or_elevation	X	X	X
inv_bar_cor	X	X	X
dac	X	X	X
ocean_tide_fes	X	X	X
ocean_tide_fes_qual	X	X	X
ocean_tide_got	X	X	X
ocean_tide_got_qual	X	X	X
ocean_tide_eq	X	X	X
ocean_tide_non_eq	X	X	X
internal_tide_hret	X	X	X
load_tide_fes	X	X	X
load_tide_got	X	X	X
solid_earth_tide	X	X	X
pole_tide	X	X	X
wind_speed_mod_u	X	X	X
wind_speed_mod_v	X	X	X
ssha	X	X	
ssha_mle3	X	X	
ssha_mgdr		X	X

Table 8. List of all possible fields and their presence in the TOPEX/POSEIDON data files. Geophysical models are in green and common for TOPEX and POSEIDON; radiometer parameters are in orange and common for TOPEX and POSEIDON; variables not in a particular dataset in yellow.

Compared to data files containing TOPEX data, POSEIDON-1 data files do not provide variables related to C band data as there this altimeter is Ku band only. In addition, there is no altimeter-derived rain_flag on these POSEIDON-1 products.

The POSEIDON-1 ionospheric correction variable is provided using information derived from the DORIS instrument in these products (see section 4.5.4)

Users are advised that there is no recent retracking outputs out of cycles 137 to 307 period, so that variables with no extension (related to MLE-4), or variables with extension "_mle3" related to new MLE-3 retracking outputs are set to default value for cycles 3 to 126 and over cycle 361 (see parts 2.4.1.2 and 4.4.2).

POSEIDON-1 data files contain specific fields with _mgdr suffix. These fields represent specific outputs fields that are not reprocessed with recent retracker algorithms (see section 4.4.2) but copied from previous versions of data (with some updates depending on the variable). Variables with this suffix are only available over ocean and at the 1 Hz resolution.

4.3. Precise Orbits

Two precise orbit determination solutions are provided in the TOPEX/POSEIDON products, as described below.

4.3.1. GSFC

The NASA GSFC precise orbit ephemeris version std1808 for the TOPEX/POSEIDON satellite computed in the 2014 International Terrestrial Reference Frame (ITRF14) is provided in variables named, *latitude*, *longitude*, *altitude*, *latitude_20hz*, *longitude_20hz*, *altitude_20hz*. This orbit ephemeris has been computed using a combination of SLR and DORIS tracking data for repeat cycles 1-446, and SLR tracking data and sea surface height crossover measurements for repeat cycles 447-480.

4.3.2. CNES

The CNES precise orbit ephemeris version POE-F for the TOPEX/POSEIDON satellite computed in the 2014 International Terrestrial Reference Frame (ITRF14) is provided in a variable named *altitude_cnes*. Note that separate latitude and longitude coordinates from this orbit ephemeris are not provided as they are almost identical (to within 1 microdegree) to those already provided in the corresponding variables.

	POE-F
Gravity model	EIGEN-GRGS.RL04-v1.MEAN-FIELD
	Non-tidal TVG: one annual, one semi-annual, one bias and one drift terms for each year up to deg/ord 90; C21/S21 non modified
	Solid Earth tides: from IERS2003 conventions
	Ocean tides: FES2014
	Oceanic/atmospheric gravity: 3hr dealiasing products from GFZ AOD1B RL06
	Pole tide: solid Earth and ocean from IERS2010 conventions
	Third bodies: Sun, Moon, Venus, Mars and Jupiter
Surface forces	Radiation pressure model: calibrated semi-empirical solar radiation pressure model
	Earth radiation: Knocke-Ries albedo and IR satellite model
	Atmospheric density model: **DTM-13**

Estimated dynamical parameters	Dynamic solutions
Satellite reference	Mass and center of gravity: post-launch values + variations generated by Control Center Attitude model: nominal attitude law
Displacement of reference points	Earth tides: IERS2003 conventions Ocean loading: **FES2014** Pole tide: solid earth pole tides and ocean pole tides (Desai, 2002), **new linear mean pole model** S1-S2 atmospheric pressure loading, implementation of Ray & Ponte (2003) by van Dam
Geocenter variations	Tidal: ocean loading and S1-S2 atmospheric pressure loading Non-tidal: **full non-tidal model (semi-annual, annual, inter-annual) derived from DORIS data and the OSTM/Jason-2 satellite, applied to DORIS/SLR stations**
Terrestrial Reference Frame	**Extended ITRF2014 (SLRF/ITRF2014, DPOD2014)**
Earth orientation	Consistent with IERS2010 conventions and **ITRF2014**
Propagations delays	SLR troposphere correction: Mendes-Pavlis SLR range correction: **geometrical models for all satellites** DORIS troposphere correction: **GPT2/VMF1 model** DORIS beacons phase center correction
Estimated measurement parameters	DORIS: one frequency bias per pass, one troposphere zenith bias per pass SLR: one range bias per pass

Table 9: CNES POE-F orbit computation parameters

4.3.3. Solar array center of mass correction

As shown in the satellite description, the TOPEX/POSEIDON satellite had a one-sided solar array. The array deformed by differential thermal expansion as the front side was heated by the sun while the back faced cold space. An experimental correction that is intended to reflect the time varying center of mass correction (sometimes also referred to as the center of gravity correction, cg) due to fuel consumption and motion of the solar array is provided in a variable named *cg_to_altimeter_timevarying_offset* (available for TOPEX data only). This correction is not included in the reported net instrument range corrections and not applied to the reported ranges. To use this correction its value should be added to the reported ranges.

4.4. Altimeter retracked data

Retracking is the process of estimating the altimetry parameters from the actual waveform obtained by the altimeter. Several kinds of retracking are used today. Over ocean, these estimations are best performed by adjusting the parameters of an echo model (e.g., Brown model for an analytical solution [37]) to fit with the measured echoes waveforms. It allows estimation of all altimetry parameters as outputs, including the echo epoch (for range), the significant wave height, the echo amplitude (for sigma0 and winds), the altimeter antenna mispointing (from the echo trailing edge slope). A Maximum Likelihood Estimation (MLE) algorithm is used for this reprocessing. It allows estimation of 3 parameters, namely the echo epoch, significant wave height and amplitude for the MLE-3 approach, and 4 parameters which then includes the altimeter antenna mispointing for the MLE-4 approach.

4.4.1. TOPEX

4.4.1.1. Numerical Retracking Basics

The TOPEX altimeter data processing used for this product is based upon a numerical retracking approach, as shown in Figure 9. This retracking technique introduces the instrument Point Target Response (PTR) to obtain an echo model that better reflects the characteristics of the altimeter. The PTR waveforms must be oversampled to be processed by the numerical retracker. Because of this constraint, as described later in section 4.4.1.2, a workaround was necessary to process Side A.

Unlike the classical analytical MLE solution, in principle no instrument corrections are needed with the numerical retracking approach for range, SWH and sigma0 as a function of SWH and off nadir angle (i.e., Look Up Tables are not required or applied). In addition, the use of the measured PTR compensates for the impact of the altimeter evolution on the range, SWH and sigma0 measurements without having to introduce external corrections. In particular, this approach allows for much more stable SWH measurements when compared to the original TOPEX dataset. However, note that for TOPEX Side A range only, due to limitations in the quality and availability of the calibrations, the contribution of the Cal-1 range correction is removed from the range estimates (see Section 4.4.1.4.5). Note that the TOPEX retracking is performed using a skewness value of 0. While GDR-F products for Jason missions are using a value of 0.1 for the skewness, the impact of this choice will be absorbed by the dedicated sea state bias correction.

Retracking Process Basic Schematic
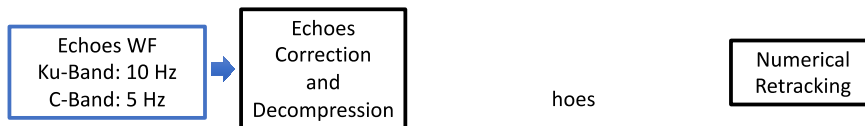
Figure 9. Numerical Retracking Processing Flow.

4.4.1.2. Point Target Response data and processing

4.4.1.2.1. Side B

For TOPEX Side B, two types of Point Target Response (PTR) calibrations have been routinely performed in-flight. First, the Cal-1 non-oversampled PTR calibrations were performed daily. Second, Sweep Calibrations to measure the on-board oversampled PTR waveforms have been scheduled regularly but with a lower frequency (every 30 days until August 11, 2002 and every 10 days thereafter).

A dedicated processing of the Sweep Calibrations allows measurement of the oversampled PTR as illustrated in Figure 10. These oversampled PTR waveforms are simply normalized and centered in amplitude and range prior to being introduced in the numerical retracker. The values for the amplitude normalization coefficient and range shifting are stored and applied when computing sigma0 and range, respectively, through the instrument corrections (*net_instr_cor_sig0*, *net_instr_cor_range*).

Ku-Band Oversampled PTR Waveforms for Side-B
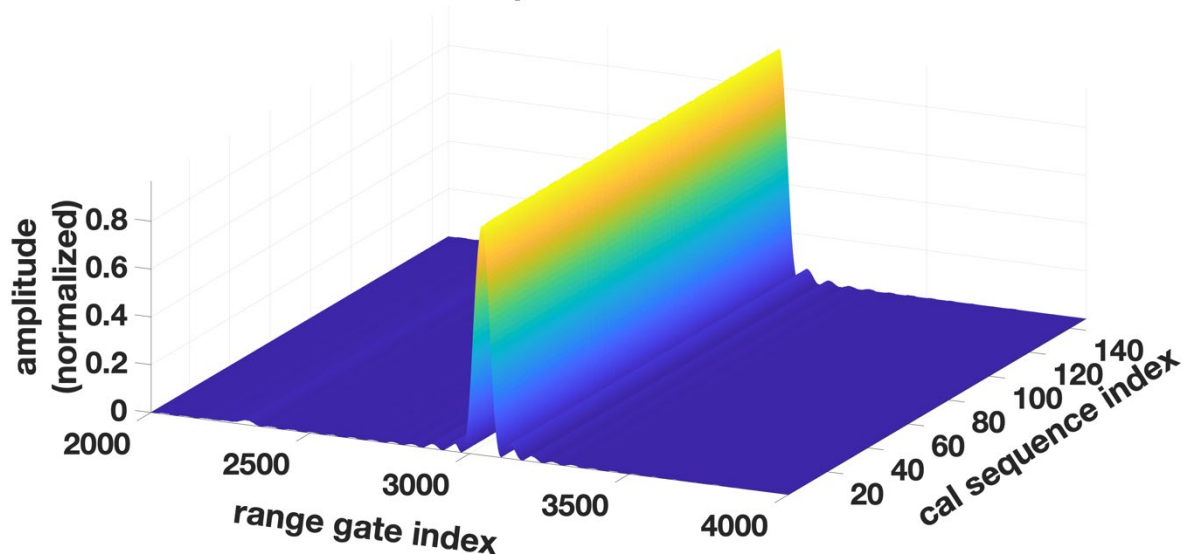
Figure 10. TOPEX Side B Sweep Calibration oversampled PTR waveforms.

4.4.1.2.2. Side A

For TOPEX Side A, the capability to perform Sweep Calibrations in-flight was only implemented at the end of the Side A altimeter lifetime and just a few Sweep Calibrations were scheduled from September 8, 1998 to February 10, 1999. As a result, no regular Sweep Calibrations were available through the lifetime of Side A and oversampled waveform timeseries cannot be directly used with the numerical retracker. Instead, for consistency only the Cal-1 sequences are used to process all of the Side A data.

The Cal-1 mode provides the on-board non-oversampled Point Target Response waveforms. A dedicated processing was developed to derive oversampled Point Target Response waveforms suitable for the numerical retracking. This processing uses a model derived from the few available oversampled PTR waveforms (from the Sweep Calibrations) in combination with the PTR non-oversampled waveform time series from the Cal-1 calibrations. As a result, a time series of synthetic oversampled PTR waveforms is generated for Side A, as shown in Figure 11.

The PTR waveforms in Cal-1 mode are tracked and the corresponding amplitude and range tracker information must be processed and stored for post retracking correction. The Cal-1 range tracker evolution corresponds to the so-called "Wallops (or WFF) range correction" [38] [39] computed during the life of the mission.

As for Side B processing, the oversampled PTR waveforms time series are normalized and centered in amplitude and range prior to be introduced in the numerical retracker. The values for the amplitude normalization coefficient and range shifting are stored and added to the amplitude and range tracker information. The resulting corrections are then applied when computing the sigma0 and range, respectively, through the instrument corrections (*net_instr_cor_sig0*, *net_instr_cor_range*).

Ku-Band routine PTR Waveforms for Attenuator step5 over Side-A

Reconstructed Sweep PTR Time Series

Non Oversampled Cal-1 PTR waveform time series   Modeled Oversampled PTR waveform time series
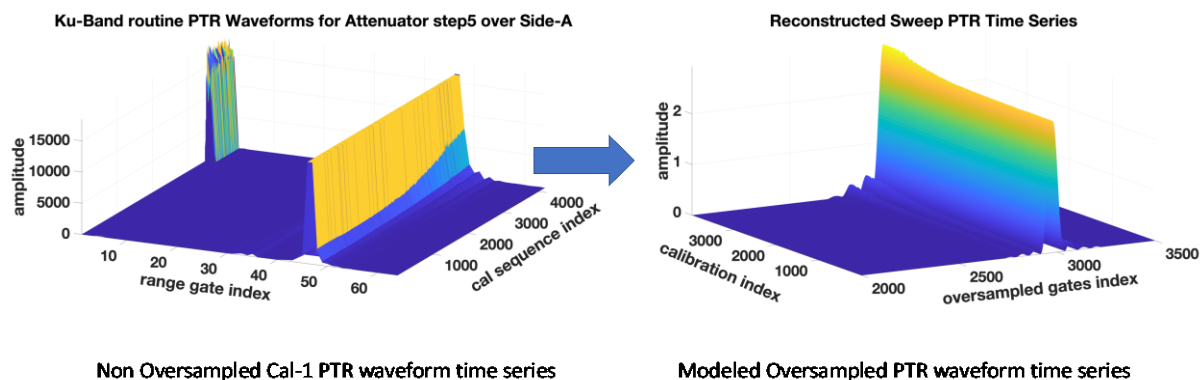
Figure 11. TOPEX Side A generation of oversampled PTR waveforms.

4.4.1.3. Cal-2 correction of waveforms

Prior to processing through the numerical retracker, the echoes have to be corrected from instrument distortions. The Cal-2 mode waveforms correspond to the output signal measured when the altimeter input is a white noise signal. In this way, the Cal-2 mode provides the equivalent altimeter distortion signature (called filter). The echo waveforms are therefore simply corrected using the Cal-2 mode waveforms (filters).

Over a Cal-2 sequence, waveforms are acquired over the whole fine height command (FHC) range of the altimeter. However, depending on the satellite vertical velocity, echo waveforms are measured from a limited range of these fine height commands. Instead of deriving one Cal-2 filter by averaging all data from a Cal-2 sequence, different filters are generated here as shown in Figure 12 (one corresponding to the lower values of the FHC, one corresponding to the upper values of the FHC and one averaged over all FHCs). Depending on the vertical velocity of the satellite at the time of the ocean measurement, the echo waveforms are corrected using the appropriate Cal-2 filter.

The selection of the Cal-2 derived filters based upon the vertical velocity allowed significant reduction of the so-called hemispheric bias affecting all of the altimeter measurements of TOPEX Side A and Side B, as shown in Figure 13. This is particularly noticeable for Side B which benefits from better instrument calibrations and echo measurement quality.
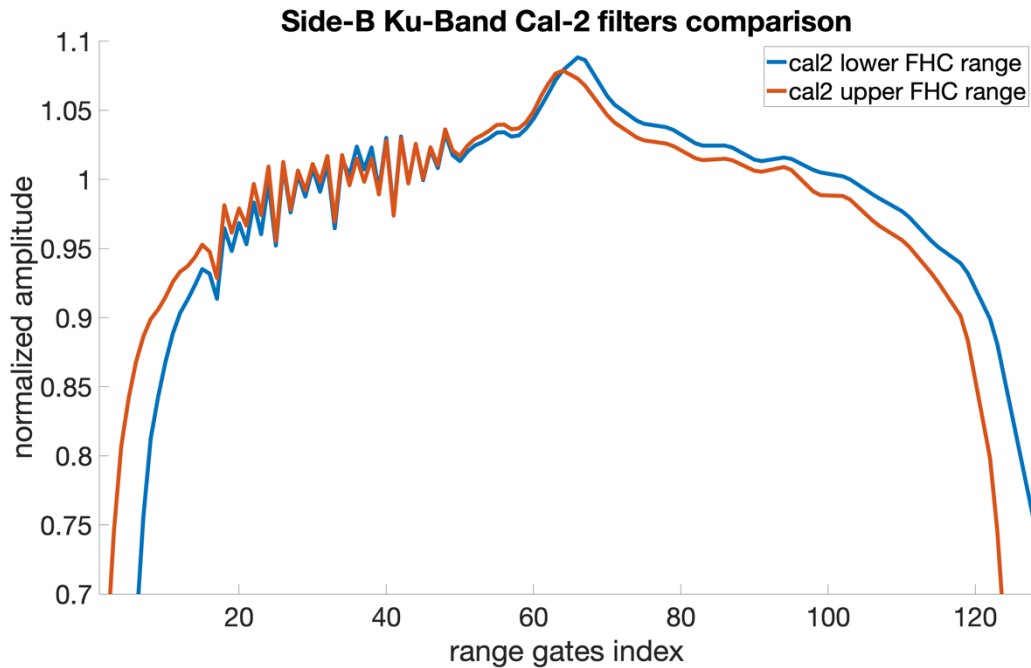
Figure 12. Cal-2 filters comparison for lower and upper Fine Height Command (FHC) ranges.
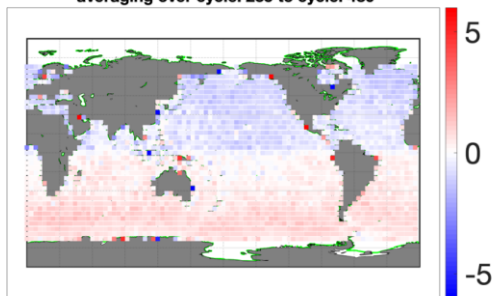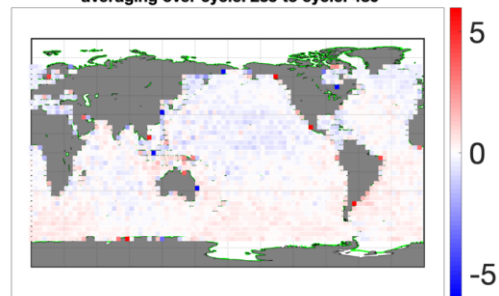
Figure 13. Improvement of hemispheric bias by selecting Cal-2 Fine Height Commands based upon vertical velocity.

4.4.1.4. Range estimation

The altimeter range is derived from the position in range of the echo waveforms in the altimeter measurement window estimated with the numerical retracker. The computation of the range takes into account additional delays that affect the radar signal in the different altimeter sub-systems. The range computation includes several steps described below.

Note: For this product dataset, users should **not** apply the so-called "Wallops correction" [38] [39](also referred as "WFF correction").

While the numerical retracking itself is the same for Side A and Side B, because Side A processing uses Cal-1 data and Side B uses Sweep Calibration data, there are some differences in the overall processing.

4.4.1.4.1. Epoch estimation

Using the numerical retracker and the oversampled PTR waveforms timeseries (derived from the Cal-1 mode for Side A and available with the Sweep Calibration mode for Side B), the epoch (i.e., the position in range of the echo in the measurement window) for each echo is estimated.

With the numerical retracking approach, no post retracking instrument corrections are needed as a function of the SWH and off nadir angle (i.e., Look Up Tables are not required or applied).

4.4.1.4.2. Tracker correction

The range is derived by adding the estimated echo's epoch information and the corresponding onboard range tracker information provided in the 20 Hz telemetry (from the Sensor Data Records (SDR)).

4.4.1.4.3. PTR waveforms centering correction

Prior to its use with the numerical retracker, for purely numerical computation purpose, the PTR waveform has been centered. The range is corrected from the shift applied to the PTR.

For Side A only, the range is, in addition, corrected from the Cal-1 PTR range tracker (see Cal-1 processing 4.4.1.2.2).

4.4.1.4.4. Calibration for alignment with the Sensor Data Records (SDR)

For this reprocessing all the necessary information to derive an absolute range based on the output of the echo processing were not available. This information corresponds to measurements performed on-ground prior to the satellite launch and provides a bias to apply to the altimeter internal echo path delay. In the absence of this information, a bias was computed to align the range for this reprocessed product with the range as originally provided in the SDR at the start of each of Side A and Side B (i.e., prior to instrument evolution). The repeat cycles used to compute this alignment bias are:

- Cycle 17 for Side A which corresponds to the first full cycle for TOPEX
- Cycle 280 for Side B.

4.4.1.4.5. Side A specific corrections for impact of Cal-1 on range

This step concerns Side A only and not Side B which uses Sweep Calibrations. Some anomalies in the effect of the tracker range command on the waveforms were observed for Side A. Because of this observation, to our understanding, the Cal-1 cannot be used reliably to calibrate the drift in range over the mission duration. Actually, this could explain why the "Wallops" range correction [38] [39] shows a non-typical "V-shape" evolution and why applying it would make the derived sea level rise evolution more different when compared to other systems. Therefore, it has been decided to remove the contribution of the Cal-1 range correction from the retracking estimates of range values for Side A. There are actually two different effects from the Cal-1 which impact the range. The first corresponds to the correction derived from the tracker range information (equivalent to the "Wallops correction" [38] [39]). The second corresponds to the impact of the PTR waveforms in the numerical retracking itself. Both effects have been removed for this product. We recommend using the ranges as provided in the product, namely where we have removed the contribution of the Cal-1 range correction to the retracking estimates. Nevertheless, for a full transparency, the corresponding corrections applied for each pass are provided in the global attributes of the product (*range_long_term_evolution_ptr_tracking_correction_ku_mm* and *range_long_term_evolution_retracking_correction_ku_mm* respectively for MLE-3 and MLE-4 Ku band, *range_long_term_evolution_ptr_tracking_correction_c_mm* and *range_long_term_evolution_retracking_correction_c_mm* respectively for C band). For both

corrections and both bands, the time series have been arbitrarily levelled to 0 at the very beginning of the calibration time series (which corresponds to cycle 1) which is slightly different from the levelling strategy with respect to the SDR described above.

For Side B, for product consistency, these attributes are provided and have a value of zero.

Note: This actually means that the TOPEX Side A Ku and C band ranges, are not calibrated over the mission (cycle 1 to 236). As such, the range estimates can be affected by a potential drift of the instrument internal path delay.

4.4.1.5. SWH estimation

The significant wave height (SWH) is derived by the retracker from the slope of the leading edge of the echo waveforms. The values of SWH on this product are provided exactly as computed from the numerical retracker. They take into account the evolution of the altimeter PTR. No post retracking corrections are needed as a function of SWH and off nadir angle (i.e., Look Up Tables are not required or applied), or to correct for the altimeter evolution.

4.4.1.6. Sigma0 estimation

4.4.1.6.1. Echoes amplitude estimation

The backscatter coefficient (sigma0), is derived by the retracker from the amplitude of the echo waveforms estimated with the numerical retracking and the on-board AGC gain tracker information provided in the 20 Hz telemetry (from the SDRs).

This amplitude is corrected for the PTR amplitude normalization coefficient. For Side A it is in addition corrected for the amplitude tracking of the Cal-1 PTR waveforms (see 4.4.1.2).

The computation of sigma0 takes into account the altitude of the satellite with respect to the measured surface as well as the gain and losses that affect the signal in the altimeter sub-systems.

With the numerical retracking approach, no post retracking corrections are needed as a function of the SWH and off nadir angle, (i.e., Look Up Tables are not required or applied) or to correct for the altimeter evolution.

4.4.1.6.2. Calibration of Sigma0

For this reprocessing all of the necessary information to compute an absolute sigma0 based on the output of the echoes processing (echoes amplitude) were not available. This information corresponds to measurements performed on-ground prior to launch and provides a bias to apply in the altimeter internal gain chain. In the absence of this information, a bias has been applied to the time series as described below.

4.4.1.6.2.1. Side B

For Side B the calibration bias has been computed to align the sigma0 values with the original GDR data after removing the atmospheric corrections (for both products) and not applying the Wallops corrections on the original GDR [38] [39].

The bias has been computed as a mean difference over cycles 280 to 355 for Side B. The first Side B cycles have been avoided because a change in the altimeter configuration during cycle 255 led to a discontinuity in the sigma0 measurement at the beginning of the timeseries.

4.4.1.6.2.2. Side A

For Side A the calibration bias has been computed to align the sigma0 values with the Side B values (for this processing) after removing the atmospheric corrections (for both sides).

The bias has been computed as a mean difference over cycles 21 to 235 for Side A and again cycles 280 to 355 for Side B. The first cycles for Side A have been avoided as the mission configuration was not stable.

4.4.1.7. Mispointing estimation

Two retracking solutions (MLE-3 and MLE-4) for Ku band echoes processing are provided in the product while only an MLE-3 solution is provided for C band. The MLE-3 solution provides estimates of epoch (for range), SWH and amplitude (for sigma0) of the measured echoes. The MLE-4 solution also provides an estimate of the altimeter antenna mispointing with respect to the geodetic nadir, derived from the echo's waveforms (*off_nadir_angle_wf_ku* and *off_nadir_angle_wf_20hz_ku*, for 1 Hz and 20 Hz data, respectively). This information is derived by the retracker from the slope of the trailing edge of the echo waveforms. It is provided in the product as the square of the estimated total mispointing angle combining roll and pitch (in degrees^2).

Mispointing estimates from MLE-4 are filtered, smoothed and used as input for the MLE-3 retracking in Ku band. The corresponding information is reported in the product (*off_nadir_angle_wf_ku_smoothed*). For C band, the mispointing used as input is forced to a constant value. Due to the larger antenna aperture in C band compared to Ku band, the C band is much less sensitive to mispointing. For Ku band however, introducing estimates of the antenna mispointing in MLE-3 was necessary as the satellite suffered numerous events of platform mispointing.

4.4.1.8. Instrument Corrections

The TOPEX altimeter data are based upon numerical retracking of the waveforms that takes into account instrument calibration in the processing model. Therefore, no instrument corrections as a function of significant wave height are necessary. However, additional instrument corrections are required to account for various effects as described below.

4.4.1.8.1. Range

The reported value of range has various instrument corrections already applied. These instrument corrections are provided in variables named *net_instr_cor_range_ku*, *net_instr_cor_range_ku_mle3*, and *net_instr_cor_range_c*. They include the following:

- Correction from the numerical retracking to take into account changes in the point target response position (4.4.1.2) and bias, which are not provided separately.
- A correction to remove the overall impact of the point target response calibration on the range (see Section 4.4.1.4.5). These are provided in global attributes named *range_long_term_evolution_retracking_correction_ku_mm*, *range_long_term_evolution_ptr_tracking_correction_ku_mm*, *range_long_term_evolution_retracking_correction_c_mm*, and *range_long_term_evolution_ptr_tracking_correction_c_mm*.
- The static offset for the position of the altimeter antenna with respect to the center of mass of the satellite, provided in a variable named *cg_to_altimeter_static_offset_mm*. A separate correction for the time varying offset of the center of mass is provided in a separate variable name *cg_to_altimeter_timevarying_offset*, and not included in the reported ranges or respective net instrument corrections (see Section 4.3.3).
- The correction for the oscillator shift and drift in frequency provided in a variable named *osc_drift_cor*.
- The correction for the doppler effect, provided in variables named *range_cor_doppler_ku* and *range_cor_doppler_c*.
- A correction depending on the altimeter tracking mode, which always has a value of 0 so not provided explicitly.

4.4.1.8.2. Sigma0

The reported values of sigma0 have various instrument corrections already applied. These instrument corrections are provided in variables named *net_instr_cor_sig0_ku*, *net_instr_cor_sig0_ku_mle3*, and

net_instr_cor_sig0_c. They correspond to corrections from the numerical retracking to take into account changes in the point target response amplitude (4.4.1.2) and bias. Note that they do not include any biases that are applied before computing the rain flag (*rain_flag*, see Section 4.8.2) or altimeter wind speed (*wind_speed_alt* and *wind_speed_alt_mle3, see Section 4.8.6.1*).

4.4.1.8.3. Significant Wave Height

Use of the numerical retracking approach means that no instrument corrections are required for the reported values of TOPEX significant wave height.

4.4.2. POSEIDON-1

Three solutions are available in POSEIDON product for variables linked to the retracking outputs.
Due to a lack of available data, waveforms have been retracked for POSEIDON data only for cycles between 137 and 307 inclusive. In this document, we will mention cycles 137 to 307 as the POSEIDON retracked period. For all the other periods (i.e., until cycle 126 and for cycle 361), a database derived from the last M-GDR version, available over ocean and at a 1 Hz resolution only, has been used as the unique information available. In order to provide a homogeneous series for POSEIDON-1 data, this solution is available in the product over the whole POSEIDON-1 series. Retracker output derived or copied from this M-GDR version of data are variables with _mgdr suffix.

In this section references are made to specific GDR parameters by name using the name of the variable as described in the netCDF data sets. In addition to the historical M-GDR parameters (from an MLE-3 retracking), new MLE-4 and MLE-3 retracker outputs are also included in the POSEIDON-1 GDR-F products. Altimeter parameters (e.g. Range, swh, sigma0, etc) and related geophysical parameters (e.g. Ionosphere correction, sea state bias correction, wind speed, etc) named with a "_mgdr" extension are derived from the last official M-GDR distributed version of retracking, while those with the "_mle3" or without extension are derived from MLE-3 or MLE-4 recent retracking, respectively.

These two retracking algorithms are based on the same least square principle (MLE is the acronym of Maximum Likelihood Estimator but in our case, the MLE has been degraded in a LSE solution): the MLE-3 algorithm provides the estimations of three parameters (range, significant wave height, and power from which the backscatter coefficient is derived) whereas MLE-4 provides the estimations of four parameters (the three previous ones and the slope of the waveform trailing edge). Details of the differences between MLE-3 and MLE-4 processing are provided in [40].

Parameters derived from basic waveform shape are represented in Figure 14:
- o epoch at mid-height: this gives the time delay of the expected return of the radar pulse (estimated by the tracker algorithm) and thus the two-way travel time between satellite and surface.
- o P: the amplitude of the useful signal. This amplitude derives into the sigma0 estimation.
- o P_0: thermal noise
- o leading edge slope: this can be related to the significant wave height (SWH)
- o skewness: the leading edge curvature (POSEIDON-1 retracking assumed a fixed value of skewness set to 0.1 for both MLE-3 and MLE-4 retrackings)
- o trailing edge slope: this is linked to any mispointing of the radar antenna (i.e. any deviation from nadir of the radar pointing).
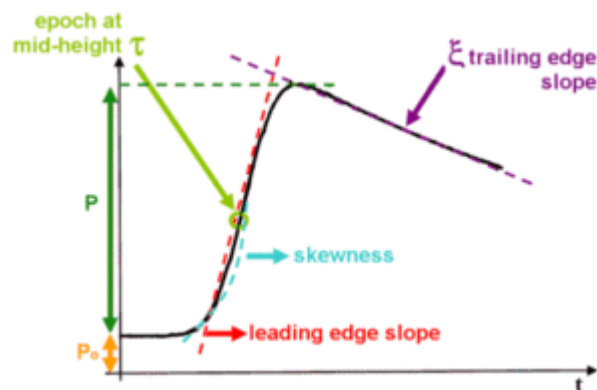
Figure 14. Parameters determined from basic waveform shape.

Please note that, the list of available variables in the POSEIDON data files is not the same in all cycles:
- 20 Hz variables (and meas_ind dimension) are available only over the POSEIDON retracked period (i.e., cycles 137 to 307)
- out of POSEIDON retracked period (i.e. until cycle 126, + cycle 361), retracking variables related to MLE-4 or MLE-3 are then set to default value at 1 Hz and no 20 Hz variable has been included.

The list of retracker output variables available in POSEIDON-1 products (at 1 Hz) are:

- ☐ range_ku_mgdr
- ☐ range_ku
- ☐ range_ku_mle3
- ☐ range_rms_ku_mgdr
- ☐ range_rms_ku
- ☐ range_rms_ku_mle3
- ☐ range_numval_ku_mgdr
- ☐ range_numval_ku
- ☐ range_numval_ku_mle3
- ☐ range_ku_qual
- ☐ range_ku_mle3_qual
- ☐ net_instr_cor_range_ku_mgdr
- ☐ net_instr_cor_range_ku
- ☐ net_instr_cor_range_ku_mle3
- ☐ swh_ku_mgdr
- ☐ swh_ku
- ☐ swh_ku_mle3
- ☐ swh_rms_ku
- ☐ swh_rms_ku_mle3
- ☐ swh_numval_ku
- ☐ swh_numval_ku_mle3
- ☐ swh_ku_qual
- ☐ swh_ku_mle3_qual
- ☐ net_instr_cor_swh_ku

- ☐ net_instr_cor_swh_ku_mle3
- ☐ sig0_ku_mgdr
- ☐ sig0_ku
- ☐ sig0_rms_ku_mgdr
- ☐ agc_ku
- ☐ net_instr_cor_sig0_ku_mgdr
- ☐ off_nadir_angle_wf_ku_mgdr
- ☐ off_nadir_angle_wf_ku
- ☐ off_nadir_angle_wf_rms_ku
- ☐ off_nadir_angle_wf_numval_ku
- ☐ off_nadir_angle_wf_ku_qual

At a second order, the following range corrections are computed from the retracker outputs:
- ☐ wind_speed_alt_mgdr
- ☐ wind_speed_alt
- ☐ wind_speed_alt_mle3
- ☐ sea_state_bias_ku_mgdr
- ☐ sea_state_bias_ku
- ☐ sea_state_bias_ku_mle3

A choice was made to implement two retrackings (MLE-3 and MLE-4) as it is the case on Jason-2 and Jason-3. Both give relevant results with the differences that we know, especially on small sea states (see chapter 7 in [41]). Note that in case of POSEIDON-1, the waveform provided on 60 points is a limiting factor for MLE-4 for waves over 8 m (see more results on part 4.4.2.7).

> **Concerning POSEIDON-1, most users are advised to use the MLE-3 altimeter parameters for typical scientific applications. Use the variables with _mle3 extension in variable name over the retracked period, and with the _mgdr extension in variable name out of this period. Users should use these data with caution on global biases between retrackings (see part 4.4.2.8).**

4.4.2.1. Input files

4.4.2.1.1. MegaFiles

In order to ease expertise and archiving, all tracking altimetry data related to a half-orbit were gathered in a single file called MegaFile. These files are archived at CTDP (Centre de Traitement DORIS/POSEIDON) [42].

These MegaFiles are used as an input for the latest retracking computation. Variables with no extension in their name are from MLE-4 retracking, and variables with the _mle3 suffix are from MLE-3 retracking.

Waveforms are read from the echo_ccd variable. Concerning POSEIDON-1, the waveform is built with 60 points, with a tracker reference gate numbered 30. Waveforms are retracked with the following outputs:

- o For MLE-3: epoch, sigmaC, amplitude, thermal noise, quality flag, mean quadratic error and iteration number.
- o For MLE-4, an additional output is computed: the square off nadir angle.

4.4.2.1.2. M-GDR

In order to ensure the continuity of the POSEIDON-1 dataset over the whole mission period, and as MegaFiles production began in June 1996, M-GDR datasets [43] are used for POSEIDON cycles 3 to 361 (copy of retracker outputs at 1 Hz, reported in fields with suffix _mgdr).

4.4.2.2. Calibrations analysis

Cal-1 (PTR) and Cal-2 (filter) historical files are reused, using the following POSEIDON-1 characteristics:

- o   Bandwidth : 320 MHz
- o   Antenna beamwidth : 1.1°
- o   Center frequency: 13.65 GHz
- o   Number of integrated pulses : 86
- o   Mean altitude : 1336 km
- o   Tracker reference index: 29
- o   0hz PTR index: 432
- o   0hz filter index: 29
- o   Pulse duration :105 µs

Their interpretation is compared to archive data in order to evaluate the impact of new retracking with regard to historical results.

4.4.2.2.1. Cal-2 filter

In order to check the stability of the filter, all filters (Cal-2) of the POSEIDON-1 mission were analyzed previous to the reprocessing (throughout the mission, 1 filter per cycle of operation of POSEIDON-1). The non-normalized filters on 60 points corresponding to the frequencies starting from -290 kHz to 300 kHz by step of 10 kHz are considered. As the filter is deemed sufficiently stable, we can consider that the same average filter can be used for all the measurements of the mission. We have therefore averaged all the filters of the mission and generated a text file containing the average filter that is used for processing. The stored filter is not normalized.

4.4.2.2.2. Cal-1 (PTR)

From the raw impulse responses (PTR) corresponding to the operating cycles of POSEIDON-1, the corrections, and associated parameters (Internal Path Delay, Total Power, etc. ...), have been recomputed. All the parameters of the PTR that we have recalculated are consistent with those measured in the past. Despite some small deviations, the trends of the curves are preserved (which allow good confidence of consistency with historical outputs). The new MLE-3 and MLE-4 results are obtained using the recomputed values.

The PTR values are stored on 896 points ranging from -270 kHz to 289.375 kHz in steps of 625 Hz. 625 Hz is an approximation obtained by rounding the pulse duration to 100 µs with a 16th gate sampling (1/100 µs)/16 = 625 Hz.

PTR selection

Since some PTRs were heavily interfered with and therefore unusable (they were all listed in the instrumental monitoring reports), a quality flag associated with the PTR is filled in "by eye", since the erroneous PTRs appear very clearly (Figure 15).
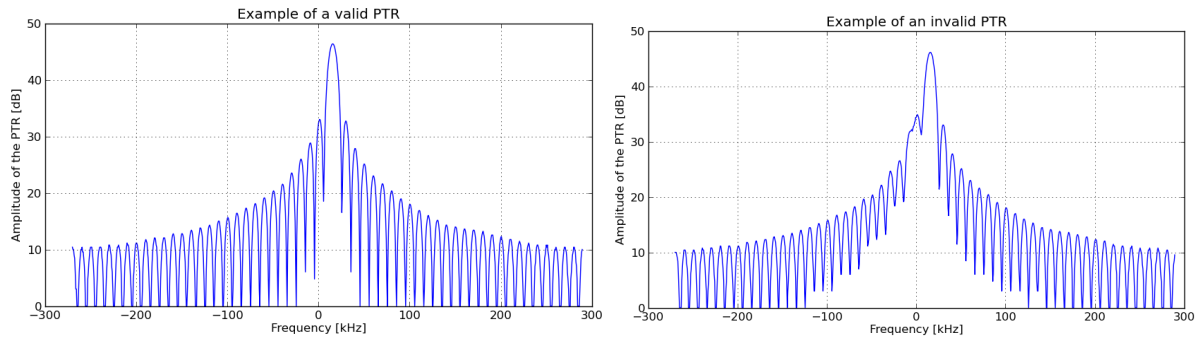
Figure 15. POSEIDON-1 PTR examples, valid (left) or invalid (right).

In addition, due to the waiting time between each POSEIDON 1 operating cycle, the instruments have a warm-up time that affects the calibration results. This is clearly seen in the total power of the PTR (Figure 16). The first calibrations of each calibration series were therefore not taken into account for the calculation of the PTR parameters.
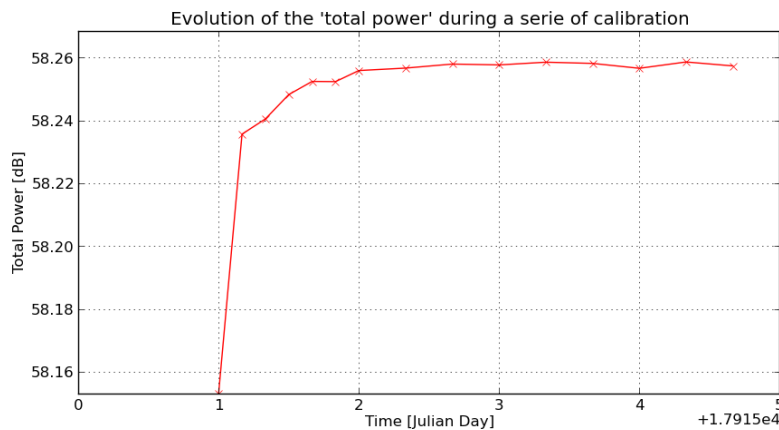
Figure 16. POSEIDON-1 PTR. Evolution of the total power during a series of calibrations.

The cycles for which we have valid PTRs and the number of valid PTRs in each cycle are listed in Table 10:

Cycle number	40	102	103	162	180	185	186	197	209	216	224	233	234	242	243	266	278	289	299	306	307
PTR number	6	4	3	10	14	3	5	9	11	6	4	2	31	4	28	8	2	4	32	2	28

Table 10. Number of valid calibrations per cycle (for cycle with Cal-1 only).

Parameters derived from PTR

Once valid PTR are identified, the following parameters (Figure 17) are computed and monitored over time:

- o   Internal Path Delay
- o   Total Power of the PTR
- o   Attenuation of the secondary lobes
- o   Frequency of the secondary lobes
- o   Maximum power
- o   Maximum distance
- o   Width of the main lobe
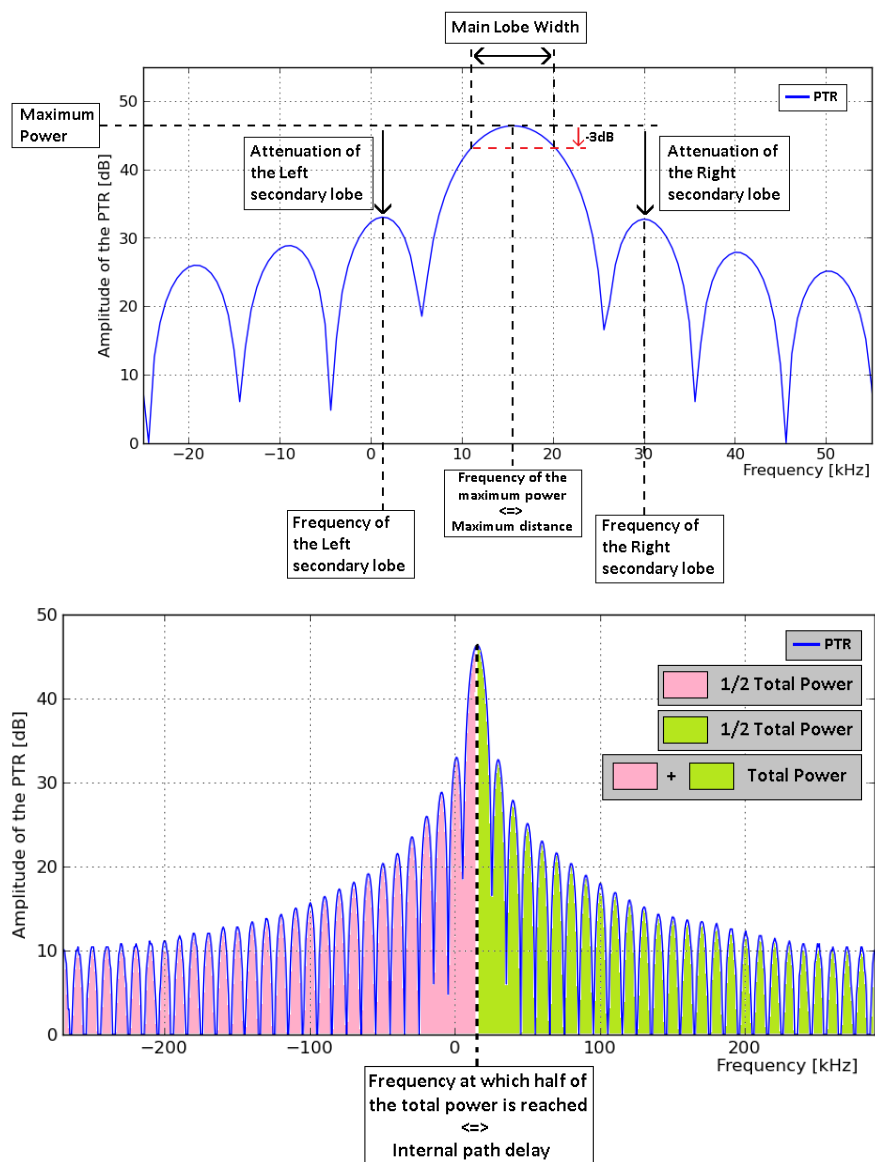
Figure 17. POSEIDON-1: Parameters derived from PTR.

The average filter calculated in section 4.4.2.2.1 have been normalized and then oversampled by a factor of 16 by a linear interpolation. Indeed, as a reminder, the filter is sampled by steps of 10 kHz and the PTR by steps of 625 Hz (10 kHz/16). The PTR are corrected by this normalized and oversampled filter.

The two parameters "Maximum distance" and "Internal path delay" are parameters derived from frequency measurements on the PTR but are usually expressed in meters. To achieve this, the following relationships are used:

$$\Delta f = \frac{B}{T} * \Delta t \ (1) \quad \text{and} \quad Distance = \frac{c}{2} * \Delta t \ (2)$$

with

Δf = measured in PTR frequency   [Hz]

Δt = time stamp of the measured frequency   [seconds]

$Distance$ = distance related to the measured frequency [meters]

T = Impulsion duration (105µs)   [seconds]

B = Bandwidth (320 MHz)   [Hz]

c = light velocity (299792458 m/s)   [m/s]

By combining (1) and (2), we find the measurements in distances by the following relationship:

$$Distance = \frac{c}{2} * \frac{T}{B} * \Delta f \ (3)$$

Now, we know that the frequencies measured on the PTR are themselves dependent on the pulse duration, in fact, the frequency step with an oversampling factor of 16 is as follows:

$$Step_{freq} = \frac{1}{T} * \frac{1}{16} \ (4)$$

The frequencies measured on the PTR can therefore be written:

$$\Delta f = Index * Step_{freq} \ (5) \quad \text{è} \quad \Delta f = index * \frac{1}{T*16} \ (6)$$

Combining (3) and (6) we obtain the following relationship:

$$Distance = \frac{c}{2} * \frac{1}{B} * \frac{index}{16} \ (7)$$

The distance measurements do not depend on the pulse duration. Approximating the pulse duration to 100 µs as it has probably been done in the past should not affect the value of the "internal path delay" or the "maximum distance".

Nevertheless, the impact of pulse duration on certain parameters such as the side lobe frequency measurements is evaluated from the results for two pulse duration values: the approximate one at 100 µs and the exact one at 105 µs.

In the same way, displaying the results with and without the filter correction on the PTR allows to evaluate its real impact on the parameters.

Internal path delay and total power

The **internal path delay** is the most important parameter of the PTR because it is a correction that will be applied to all distance measurements. This parameter will be even more important as one seeks to carry out studies on large time scales.

There is a difference of about 1 mm at the beginning of the mission between the internal path delay recalculated with the filter and the one measured before. This difference is reduced to 0.5 mm at the end of the mission.

The application of the filter correction on the PTR leads to a constant increase of the internal path delay over the whole mission of about 0.139 mm.

The **total power** is also one of the parameters of the PTR which is important because it allows the correction of the sigma0 measurement (allowing later to provide products such as wind speed etc.).

The filter correction applied to the PTR induces a constant difference of about 0.05 dB with the old values. When the PTR is not corrected by the filter, the total power calculation loses 0.032 dB.

Correcting the PTR of the filter is equivalent to dividing the PTR by the normalized filter (≤ 1), so this correction can only increase the total power calculation. The total power calculated without filter correction is surprisingly larger than the total power from the archive that was normally already corrected by the filter (Figure 18). However, the orders of magnitude are extremely small.
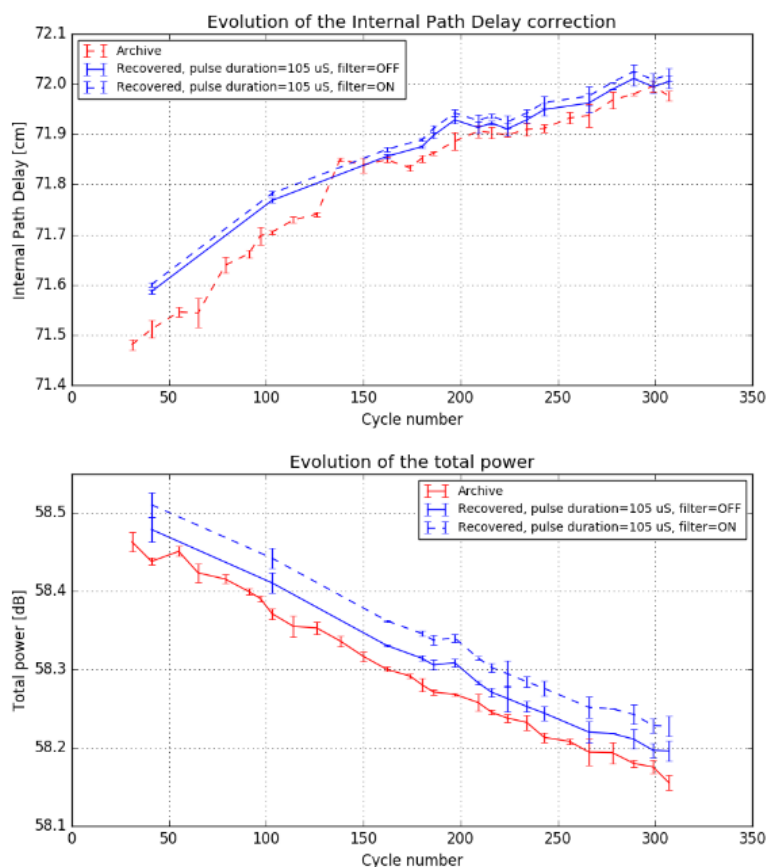
Figure 18. POSEIDON-1: Evolution of the internal path delay and total power of the PTR.

Secondary lobes: attenuation and frequency

The right secondary lobe is on average 0.3 dB lower than the left secondary lobe (Figure 19). Despite some small deviations, the results appear consistent and similar to those in the archive.
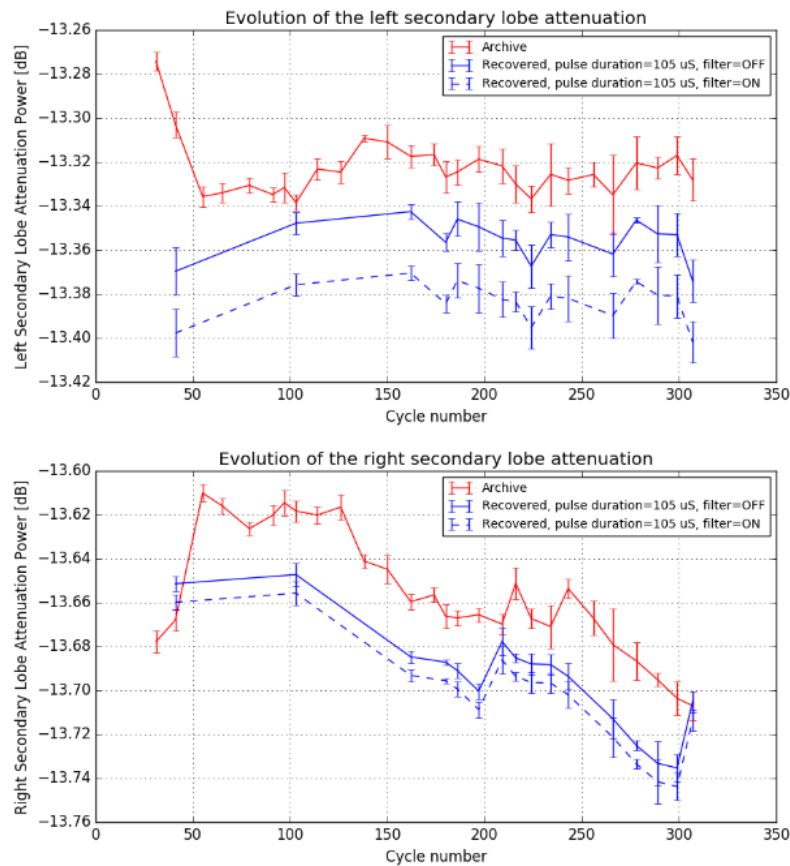
Figure 19. POSEIDON-1 left and right secondary lobes attenuation.

The secondary lobe frequencies recalculated for this reprocessing and those calculated in the archives show slight differences (Figure 19). For example, a difference of about 1400 Hz on the calculation of the frequency of the right secondary lobe.

In the files we recovered, the frequency abscissa of the PTR was sampled by steps of 625 Hz, equivalent to the approximation of a pulse duration of 100 µs with an oversampling factor of 16. However, we know that this value of pulse duration is only an approximation. The true pulse duration of the altimeter is 105 µs, i.e. a step of 595.24 Hz (used to produce the most recent results).

This difference in pulse duration explains such differences in the evolution: generating the results using a pulse duration of 100 µs leads back to the same values of the archives (see green and red curves on Figure 20).
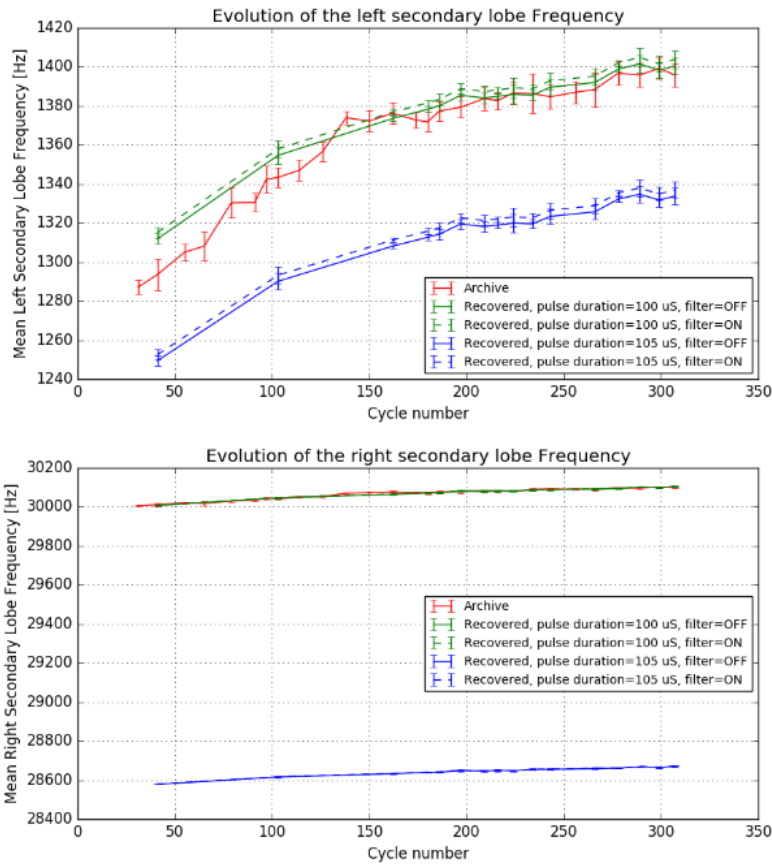
Figure 20. POSEIDON-1 left and right secondary lobes frequency.

Max power and distance

The application of the filter makes a difference of about 350 FFT pu in the maximum power estimation. Between the beginning and the end of the mission, the maximum power has lost about 3000 FFT pu or 0.3 dB (Figure 21). As for the internal path delay, the curves for maximum power and distance have the same trends, which confirms consistency of previous and new retracking results.
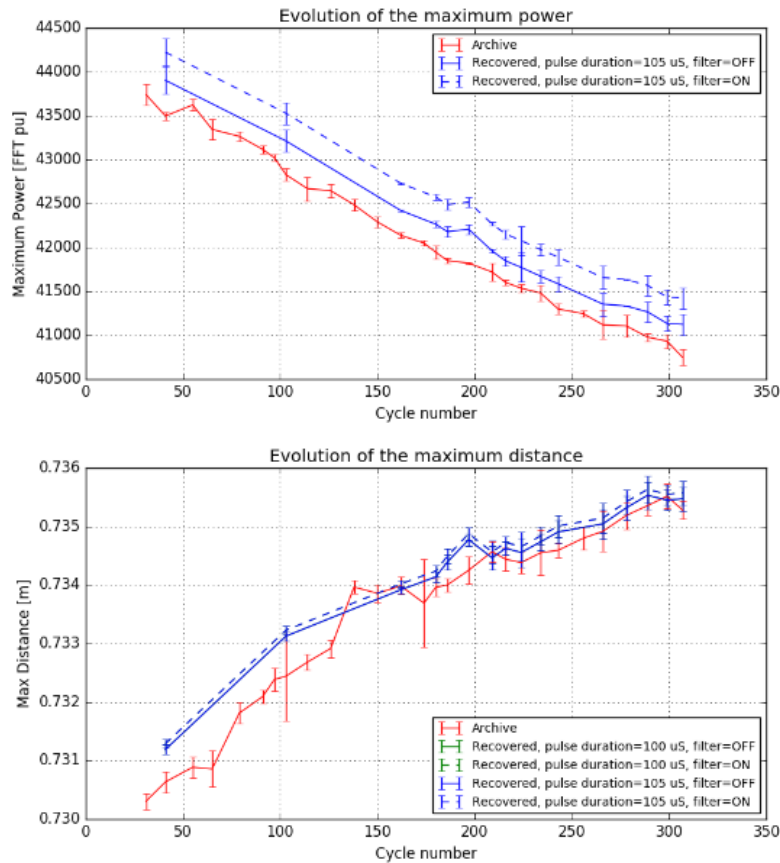
Figure 21. POSEIDON-1 maximum power and distance.

Main lobe width

The width of the main lobe differs of only 6 Hz between the beginning and the end of the mission (relative variation of about 0.07 %) (see Figure 22). No valid archive is available to be compared with this monitoring.
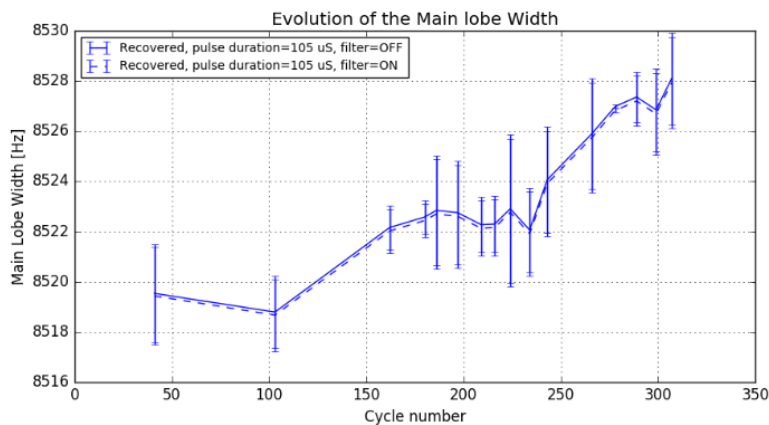
Figure 22. POSEIDON-1 evolution of the main lobe width.

4.4.2.3. Range estimation

4.4.2.3.1. MLE-4 and MLE-3 retracked data (cycles 137 to 307)

At 20 Hz, range without instrumental corrections is derived from the value of the relative tracker that have been extracted from the MegaFiles *htr_dis_sdr* variable, and the epoch output of respectively MLE-3 or MLE-4 retracking (see part 3.2.4.2 data compression at 1 Hz).

$$RANGE_{NO_{CORR}} = relative\_tracker + epoch$$

Then 1 Hz and 20 Hz range estimations are computed adding instrumental corrections (see part 4.4.2.7 for instrumental corrections details), and set into *range_20hz_ku, range_ku, range_20hz_ku_mle3, range_ku_mle3*.

$$RANGE = RANGE_{NO_{CORR}} + range\_instrumental\_corrections$$

4.4.2.3.2. M-GDR historical data (cycle 003 to 361)

Range estimation from M-GDR archive is only available at 1 Hz, all instrumental corrections included. These values are copied from historical database without any additional correction and set into *range_ku_mgdr*.

4.4.2.4. SWH estimation

4.4.2.4.1. MLE-4 and MLE-3 retracked data (cycles 137 to 307)

At 20 Hz, SWH without instrumental corrections is derived from the σ_C output of the different retrackings (see section 3.2.4.2 or data compression at 1 Hz).

$$SWH_{NO_{CORR}} = 2 * V_{light} * \sqrt{(\sigma_C)^2 - (0.513 * 3.125e^{-9})^2}$$

Then 1 Hz and 20 Hz SWH estimations are computed adding instrumental corrections (see part 4.4.2.7 for instrumental corrections details), and set into *swh_20hz_ku, swh_ku, swh_20hz_ku_mle3, swh_ku_mle3*.

$$SWH = SWH_{NO_{CORR}} + swh\_instrumental\_corrections$$

4.4.2.4.2. M-GDR historical data (cycle 003 to 361)

SWH estimation from M-GDR archive is only available at 1 Hz, all instrumental corrections included. These values are copied from historical database without any additional correction and set into *swh_ku_mgdr*.

4.4.2.5. Sigma naught (Sigma0)

It has not been possible to recompute new sigma naught values from new retrackings, due to a lack of information (no KCAL factor, which allows to convert the waveform amplitude information to

sigma0). As a consequence, there is no new backscatter coefficient related to MLE-3 or MLE-4 retracking provided in the GDR-F products.

In addition, sigma0 values from MegaFiles (*sig_moy_sfr*) are only averaged values at 1 Hz.

Users are advised that over both periods (1) and (2), sigma0 is only available at 1 Hz in GDR-F POSEIDON-1 products.

Over the whole period, M-GDR archive values of corrected sigma0 are uncorrected from M-GDR version of atmospheric attenuation, then the GDR-F values from the radiometer data reprocessing (*rad_atm_cor_sig0_ku*) are added (see 4.5.3), leading to the *sig0_ku_mgdr* variable. *sig0_rms_ku_mgdr* and *net_instr_cor_sig0_ku_mgdr* variables are copied from M-GDR database.

Over the retracked period, sigma0 values from MegaFiles (*sig_moy_sfr*) are reused. SFR megafiles data are at level 1.5, so that no atmospheric attenuation had been applied (this step is only included at level 2). These values are thus corrected using the GDR-F values from the radiometer data reprocessing (*rad_atm_cor_sig0_ku,* see 4.5.3) at 1 Hz, leading to the availability of the *sig0_ku* variable between cycles 137 and 307.

Users are advised that there is a bias between *sig0_ku_mgdr and sig0_ku*, mainly due to the difference in radiometer atmospheric attenuation applied to sigma0 output.

4.4.2.6. Mispointing

Over the retracked period, the MLE-4 solution also provides an estimate of the altimeter antenna mispointing with respect to the geodetic nadir, derived from the echo's waveforms (*off_nadir_angle_wf_ku* and *off_nadir_angle_wf_20hz_ku*, for 1 Hz and 20 Hz data, respectively). This information is derived by the retracker from the slope of the trailing edge of the echo waveforms. It is provided in the product as the square of the estimated total mispointing angle combining roll and pitch (in degrees[2]).

Out of this period, only *off_nadir_angle_wf_ku_mgdr* is available. It is directly computed as the square of the M-GDR variable *att_wvf* (see [43])

4.4.2.7. Instrumental corrections

After compression (see 3.2.4), the corrections due to the model bias are calculated for the fields of the low resolution database.

Then, using the corrections calculated from the LUTs (section 5.5.1) and the additional instrumental corrections already provided in the MEGA files (see part 4), we calculate the sum of the instrumental corrections to be applied on each parameter (Range, SWH and Sigma0) for each retracking (MLE-3 and MLE-4).

The range and swh of the low resolution table can be updated with the corrections due to the model's bais calculated in the previous section 5.5.1.

For each retracking, we therefore perform:

Range = Range + Range_CorrInstru

SWH = SWH + SWH_CorrInstru

4.4.2.7.1. Instrumental corrections applied to the range

The reported values of range have various instrument corrections already applied. These instrument corrections are provided in variables named *net_instr_cor_range_ku*, *net_instr_cor_range_ku_mle3*, and *net_instr_cor_range_mgdr*. If *net_instr_cor_range_mgdr* values are copied from M-GDR ocean database, the related to retracked data are recomputed and they include the following:

     o   <u>The correction due to the variations of the center of gravity</u>

Because the altimeter reference point is not along the line to nadir from the satellite center of mass (CM), there is a change in the range when the satellite attitude changes. This algorithm is supplied with satellite roll and pitch error angles and satellite geometry in order to compute the change in range. It assumes that the nominal satellite pointing is to nadir (normal to the Earth's ellipsoid). Due to a difference in the antenna reference point, please note that the global attribute referring this distance between the center of mass and the antenna (*cg_to_altimeter_static_offset_mm*) is not the same for TOPEX (1525 mm) or POSEIDON (918.6 mm) data. POSEIDON antenna reference point is the parabola center whereas TOPEX data are computed using the feedhorn as the antenna reference point [44].

     o   <u>The Doppler correction</u>

Copied from megafiles *dop_htr_sfr* variable, and applied to both GDR-F *net_instr_cor_range_ku* and *net_instr_cor_range_ku_mle3*

     o   <u>The correction for internal path delay</u>

Copied from megafiles *dipc_htr_sfr* variable and applied to both GDR-F *net_instr_cor_range_ku* and *net_instr_cor_range_ku_mle3*

     o   <u>The correction due to POSEIDON tracker bias</u>

Copied from megafiles *bias_track_sfr* variable and applied to both GDR-F *net_instr_cor_range_ku* and *net_instr_cor_range_ku_mle3*

     o   <u>The correction of the system bias</u>

Copied from megafiles *sys_htr_sfr* variable and applied to both GDR-F *net_instr_cor_range_ku* and *net_instr_cor_range_ku_mle3*

     o   <u>The correction from the LUT (recalculated)</u>

The correction tables (LUT) are specific to each retracking. There will therefore be a correction term from the LUTs for each retracking performed (MLE-3 and MLE-4). Megafiles input data contains bad values (*bia_htr_sfr* variable) for this correction. New LUT are computed and applied in GDR-F variables: *net_instr_cor_range_ku* and *net_instr_cor_range_ku_mle3*.

As this correction is dependent on SWH, the point-to-point correction values from the correction tables (LUT) are determined once the SWH is calculated for each retracking (MLE-3 and MLE-4) (see Figure 23). Note that we chose to truncate the MLE-4 table at 9 m to avoid the erroneous values observed below:
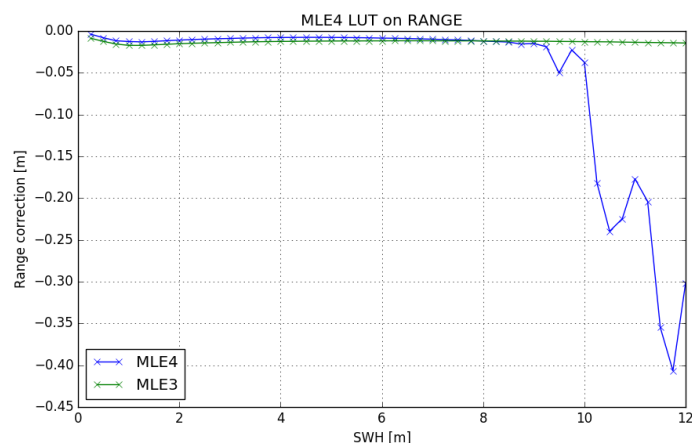
Figure 23. Look Up Tables correction for MLE-3 or MLE-4 range estimations.

At the time the POSEIDON-1 data were archived, an additional correction was added to the sum of the instrumental corrections on the range: the correction due to mispointing (MegaFile variable *dep_htr_sfr*). In the current standards, the sum of the instrumental corrections does not take into

account a correction due to antenna mispointing. Following today's convention, this correction has not been considered in GDR-F *net_instr_cor_range_ku* and *net_instr_cor_range_ku_mle3* (applied respectively in *range_ku* and *range_ku_mle3*).

4.4.2.7.2. Instrumental corrections applied to SWH

The reported values of SWH have various instrument corrections already applied. These instrument corrections are provided in variables named *net_instr_cor_swh_ku*, *net_instr_cor_swh_ku_mle3*, and *net_instr_cor_swh_mgdr*. If *net_instr_cor_ swh _mgdr* values are copied from M-GDR ocean database, the related to retracked data are recomputed and they include the following:

 o <u>The correction of the system bias</u>
Copied from megafiles *sys_hva_sfr* variable and applied to both GDR-F *net_instr_cor_swh_ku* and *net_instr_cor_swh_ku_mle3*

 o <u>The correction from the LUT (recalculated)</u>
The correction tables (LUT) are specific to each retracking. There will therefore be a correction term from the LUTs for each retracking performed (MLE-3 and MLE-4). New LUT are computed and applied in GDR-F variables: *net_instr_cor_swh_ku* and *net_instr_cor_swh_ku_mle3*.

As this correction is SWH-dependent, the point-to-point correction values from the correction tables (LUT) are determined once the SWH is calculated for each retracking (MLE-3 and MLE-4) (see Figure 24). Note that we chose to truncate the MLE-4 table at 9 m to avoid the erroneous values observed below:
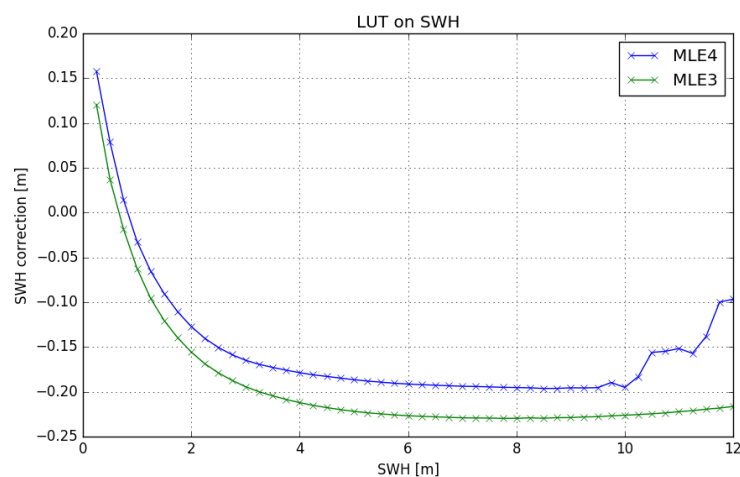
Figure 24. Look Up Tables correction for MLE-3 or MLE-4 swh estimations.

At the time the POSEIDON-1 data were archived, an additional correction was added to the sum of the instrumental corrections on the SWH: the correction due to mispointing (MegaFile variable *dep_hva_sfr*). In the current standards, the sum of the instrumental corrections does not take into account a correction due to antenna mispointing. Following today's convention, this correction has not been considered in GDR-F *net_instr_cor_range_ku* and *net_instr_cor_range_ku_mle3* (applied respectively in *range_ku* and *range_ku_mle3*).

4.4.2.8. Global biases between retracking outputs

As explained at the beginning of part 4.4.2, users are advised to use the MLE-3 altimeter parameters for typical scientific applications. Use the variables with _mle3 extension in variable name over the retracked period, and with the _mgdr extension in variable name out of this period. Users should use these data with caution on global biases between retrackings. Differences have been analyzed over the retracked period (POSEIDON-1 cycles 137 to 307) as all three SSHA and range variables are

available. The global biases between solutions are stable in time and the analysis result in the following biases (not applied in the GDR-F products) for SSHA variables (opposite sign for range differences):

$$SSHA_{MLE-4} – SSHA_{MGDR} = -1.24cm$$

$$SSHA_{MLE-3} – SSHA_{MGDR} = -0.47cm$$

$$SSHA_{MLE-3} – SSHA_{MLE-4} = +0.77cm$$

4.5. Geophysical Corrections

The atmosphere and ionosphere slow the velocity of radio pulses at a rate proportional to the total mass of the atmosphere, the mass of water vapor in the atmosphere, and the number of free electrons in the ionosphere. In addition, radio pulses do not reflect from the mean sea level but from a level that depends on wave height and wind speed. The range delays due to these processes cannot be ignored and must be accounted for in the range measured by the altimeters. Additional discussion of these effects can be found in [45].

4.5.1. Dry troposphere

The gases in the troposphere contribute to the index of refraction, where the refractive index depends on pressure and temperature. When hydrostatic equilibrium and the ideal gas law are assumed, the vertically integrated range delay is a function only of the surface pressure. The dry meteorological tropospheric range correction is principally equal to the surface pressure multiplied by -2.277 mm/mbar, with a small adjustment also necessary to reflect a small latitude dependence [46]. Two values of the dry troposphere correction are provided in the product, *model_dry_tropo_cor_zero_altitude* and *model_dry_tropo_cor_measurement_altitude*. Both are effectively computed using the following, where P_{atm} is surface atmospheric pressure in mbar, phi is latitude, and the resulting dry troposphere correction is in mm.

$$-2.277*P_{atm}*[1 + 0.0026*cos(2*phi)]$$

The variable *model_dry_tropo_cor_zero_altitude* uses surface atmospheric pressure at Mean Sea Level (MSL), while *model_dry_tropo_cor_measurement_altitude* uses surface atmospheric pressure at the altitude of a Digital Elevation Model (DEM). Inland water studies will benefit from using *model_dry_tropo_cor_measurement_altitude* instead of *model_dry_tropo_cor_zero_altitude*.

There is no straightforward way of measuring the nadir surface pressure from a satellite, so it is determined from the European Center for Medium Range Weather Forecasting (ECMWF) numerical weather prediction model. The uncertainty on the ECMWF atmospheric pressure products is somewhat dependent on location. Typical errors vary from 1 mbar in the northern Atlantic Ocean to a few mbars in the southern Pacific Ocean. A 1-mbar error in pressure translates into a 2.3 mm error in the dry tropospheric correction. In this product the ERA-Interim global atmospheric reanalysis [19] is used to compute the dry troposphere correction.

4.5.2. Wet troposphere

The amount of water vapor present along the path length contributes to the index of refraction of the Earth's atmosphere. Its contribution to the delay of the radio pulse, the wet tropospheric delay, can be estimated by measuring the atmospheric brightness near the water vapor line at 22.2356 GHz and providing suitable removal of the background. This product provides three options for the wet troposphere correction: measurements from the onboard Microwave Radiometer, the ECMWF meteorological model, and the GPD model. Values measured by the microwave radiometer are expected to have the best accuracy in the open ocean as they capture the fine spatial structures.

4.5.2.1. Radiometer

The wet troposphere correction from the onboard TOPEX Microwave Radiometer (TMR) is provided in a variable named *rad_wet_tropo_cor*. A quality flag for this correction is provided in a variable named *rad_wet_tropo_cor_qual*. The TMR measures brightness temperatures in the nadir path at 18, 21, and 37 GHz. The primary water vapor signal is sensed by the 21 GHz channel, while the 18 GHz channel removes the surface emission (wind speed influence), and the 37 GHz channel removes other atmospheric contributions (cloud cover influence). The brightness temperature measurements are combined to obtain the path delay in the satellite altimeter range measurement due to water vapor and liquid water content using algorithms described in [18]. The accuracy of these estimates is expected to be better than 1.2 cm (RMS) in the open ocean. This product also incorporates a near-land path delay algorithm first implemented in Jason-2 products [14]. This product also applies a dedicated end-of-mission recalibration of the TMR [13].

4.5.2.2. Model

This product also uses the ERA-Interim numerical weather prediction model [19] to provide an alternative value of the wet troposphere correction in a variable named *model_wet_tropo_cor_zero_altitude*. This value is the wet troposphere correction at Mean Sea Level altitude. This backup proves useful when the measurements from the radiometer are degraded by sun glint, land contamination, or anomalous sensor behavior.

4.5.2.3. Composite

This product also provides a third option for the wet troposphere correction in a variable named *composite_wet_tropo_gpd*. This value is based upon the GPD+ dataset from the University of Porto that aims to improve the wet troposphere correction for radar altimeter missions. The GPD+ Wet Tropospheric Corrections are estimated by space-time objective analysis combining all available observations in the vicinity of the point: valid measurements from the on-board microwave radiometer (MWR), from GNSS coastal and island stations, and from scanning imaging MWR on board various remote sensing missions.

See   https://www.aviso.altimetry.fr/en/data/products/auxiliary-products/gpd-wet-tropospheric-correction.html

4.5.3. Atmospheric attenuation

The atmosphere also attenuates the altimeter measurement of sigma0, and therefore also requires a correction. This product uses the radiometer to provide a measurement of the atmospheric attenuation in Ku and C band in variables named *rad_atm_cor_sig0_ku* and *rad_atm_cor_sig0_c*. Quality flags for these two variables are provided in variables named *rad_atm_cor_sig0_ku_qual* and *rad_atm_cor_sig0_c_qual*. Note that the atmospheric attenuation correction has already been applied to the sigma0 measurements from the altimeter before reporting the values in *sig0_ku*, sig0_20hz_ku, *sig0_ku_mle3*, *sig0_20hz_ku_mle3*, *sig0_c*, *sig0_20hz_c*.

4.5.4. Ionosphere

At the frequencies used by the TOPEX and POSEIDON altimeters, the propagation velocity of a radio pulse is slowed by an amount proportional to the density of free electrons of the Earth's ionosphere, also known as the total electron content (TEC). The retardation of velocity is inversely proportional to frequency squared. For instance, it causes the altimeter to slightly overestimate the range to the sea surface by typically 0.2 to 20 cm at 13.6 GHz. The amount varies from day to night (there are fewer free electrons at night), from summer to winter, and as a function of the solar cycle (there are fewer during solar minimum). Additional details can be found in [45].

Because this effect is dispersive, measuring the range at two frequencies allows it to be estimated. The TOPEX altimeter measurements of range at Ku and C bands allows retrieval of the delay from ionospheric propagation (see Section 3.2.3).

Under typical ocean conditions of 2-meter significant wave height, the Ku band ionosphere range correction determined from the dual frequency measurements from the TOPEX altimeter is expected to have an accuracy of ±0.5 cm. It is provided in variables named *iono_cor_alt_ku* and *iono_cor_alt_ku_mle3*. Note that the ionosphere correction in these two variables has been calibrated to the GIM ionosphere correction with values of -0.06945 m and -0.11088 m added to values determined from the Ku and C band ranges (corrected for sea state bias) on Side A and Side B, respectively.

The ionosphere (range) correction is expected to be negative, but positive values are allowed to accommodate instrument noise effects. To reduce noise, it is recommended to average over 100 km or more [47], which usually results in negative values. In order to provide a reversible correction, no averaging is performed on the dual frequency ionosphere correction provided on the product. Users may choose to smooth the ionosphere correction before using it to determine sea surface height.

The single frequency POSEIDON altimeter does not allow retrieval of this information and the ionosphere correction is then determined from the DORIS dual-frequency (2 GHz and 400 MHz) instrument instead. By measuring and comparing the path delay of signals transmitted at two separate frequencies, DORIS enables calculation of the electron content in the atmosphere. The frequencies are not the same as those for TOPEX or the follow-on POSEIDON altimeters, but the principle is the same (see Section 3.2.3). Products with POSEIDON data provide an ionosphere correction derived from the DORIS instrument in a variable named *iono_cor_doris*.

A backup ionosphere correction solution, derived from the Jet Propulsion Laboratory Global Ionosphere Maps (GIM) [16], is provided in a variable named *iono_cor_gim_ku*. However, it is only available from cycle 48 onward. It may be used over non ocean surfaces (ice, land, etc.) for TOPEX and is an alternative to correct POSEIDON measurements.

4.5.5. Sea state bias

Unlike the atmospheric effects, sea state effects are an intrinsic property of the large footprint of the radar altimeter measurements. The surface scattering elements do not contribute equally to the radar return. Troughs of waves tend to reflect altimeter pulses better than crests. Thus, the centroid of the mean reflecting surface is shifted away from mean sea level towards the troughs of the waves. The shift, referred to as the electromagnetic (EM) bias, causes the altimeter to overestimate the range. In addition, a skewness bias also exists from the assumption in the onboard algorithms that the probability density function of heights is symmetric, while in reality it is skewed. Finally, there is a tracker/processing bias, which is a combination of instrumental and processing choice effects. The sum of the EM bias, skewness bias, and tracking/processing bias is referred to as the sea state bias, and is frequency-dependent.

The sea state bias continues to be a topic of research. The most accurate models of sea state bias are empirical models derived from the analysis of the altimeter data themselves. The sea state bias model is typically determined as a 2-dimensional non-parametric model with SWH and wind speed as the independent variables. However, 3-dimensional non-parameter models introduce mean wave period as an additional independent variable. For a typical SWH of 2 meters, the sea state bias is ~10 cm, and the error in this correction is ~1-2 cm. The noise of the sea state bias estimates depends primarily on the noise of the SWH estimates.

The TOPEX data provide a 2-dimensional and 3-dimensional non-parametric sea state bias model, as described below. The POSEIDON data use a parametric sea state bias model.

4.5.5.1. TOPEX solution 1

The 2-dimensional non-parametric sea state bias models are provided in variables named *sea_state_bias_ku*, *sea_state_bias_ku_mle3*, and *sea_state_bias_ku_c*. The models are self-consistent with the retracked TOPEX data in that they were empirically determined from the data itself. A separate model has been computed for TOPEX Side A and Side B data, using measurements from cycles 48-100 and 280-364, respectively [20].

4.5.5.2. TOPEX solution 2

The 3-dimensional non-parametric sea state bias models are provided in variables named sea_state_bias_ku_3d and sea_state_bias_c_3d. The models are self-consistent with the retracked TOPEX data in that they were empirically determined from the data itself. A separate model has been computed for TOPEX Side A and Side B data using measurements from cycles 48-102 and 272-362, respectively [21]. The model of the mean wave period that was used to generate these sea state bias models are provided in mean_wave_period_t02 (see Section 4.7.7).

4.5.5.3. POSEIDON-1

Three sea state bias correction variables are available in POSEIDON-1 products (*sea_state_bias_ku*, *sea_state_bias_ku_mle3* and *sea_state_bias_ku_mgdr*). As previously explained, *sea_state_bias_ku* and *sea_state_bias_ku_mle3* are set to default values out of the retracked period.

The GDR-F POSEIDON-1 sea state bias is determined from an empirical model derived from analyses of altimeter data itself. Based on the results of [48] and [49], the so-called BM4 model is used to estimate the SSB of POSEIDON. This model takes the form:

$$SSB_{Ku} = SWH_{Ku} [a1 + a2 * U + a3 * U^2 + a4 * SWH_{Ku}]$$

where

SSB is the sea state bias, in meters (Ku band),

U is the wind intensity, in m/s (Ku band)

SWH is the Significant Wave Height, in meters (Ku band)

The three solutions *sea_state_bias_ku*, *sea_state_bias_ku_mle3* and *sea_state_bias_ku_mgdr* are computed using respectively (*swh_ku* and *wind_speed_alt*), (*swh_ku_mle3* and *wind_speed_alt_mle3*) and (*swh_ku_mgdr* and *wind_speed_alt_mgdr*). See part 4.8.6.1 for more details on altimeter wind speed computation and section 4.4.2.4 about SWH.

4.6. Geophysical Fields

4.6.1. Reference ellipsoid

The **Reference Ellipsoid** is the first-order definition of the non-spherical shape of the Earth as an ellipsoid of revolution. In this product the WGS84 ellipsoid is used with equatorial radius of 6378.1370 kilometers and a flattening coefficient of 1/298.257223563. These values are also reported in the product in the global attributes named *ellipsoid_axis* and *ellipsoid_flattening*.

4.6.2. Geoid

In this product, the EGM2008 geopotential is used to compute the geoid height [22] and reported in a variable named *geoid*. EGM2008 is a spherical harmonic model of the Earth's gravitational potential, developed by a least squares combination of the ITG-GRACE03S gravitational model and its associated error covariance matrix. This grid was formed by merging terrestrial, altimetry-derived, and airborne gravity data. The EGM2008 gravitational model has been used to calculate point values of geoid undulation on a 5 x 5 minute grid that spans the latitude range +90.0 deg. to -90.0 deg. The EGM2008 model is complete to spherical harmonic degree and order 2159 and contains additional coefficients up to degree 2190 and order 2159. The reported geoid height includes correction so as to refer to the WGS84 reference ellipsoid and the mean tide system (i.e., it includes the zero-frequency permanent tide). A map of the EGM2008 geoid is provided in Figure 25.
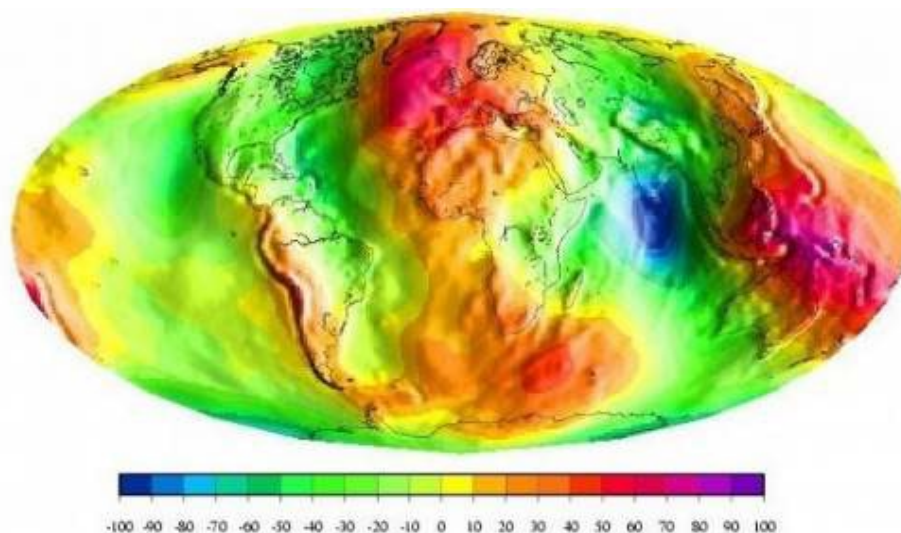
Figure 25. EGM2008 geoid (m)

4.6.3. Mean Sea Surface

Two models for the mean sea surface, MSS_CNES-CLS15 and DTU18, are provided in the product, and reported in variables named *mean_sea_surface_cnescls* and *mean_sea_surface_dtu,* along with estimates of their accuracy *(mean_sea_surface_cnescls_acc, mean_sea_surface_dtu_acc)* and respective quality flags *(mean_sea_surface_cnescls_qual and mean_sea_surface_dtu_qual)*. Both models are referenced to the mean tide system (i.e., include the zero-frequency permanent tide)

4.6.3.1. MSS_CNES_CLS15 Mean Sea Surface Model

The MSS_CNES-CLS15 model is computed from 16 years of satellite altimetry data from a variety of missions [23]. Its main characteristics are described in Table 11 below and a map of this surface is shown in Figure 26.

Name	MSS_CNES-CLS15
Reference ellipsoid	T/P
Referencing time period	1993-2013 (20 years)
Spatial coverage	Global (80°S to 84°N) - Oceanwide where altimetric data are available. Undefined on continents.
Spatial resolution	Regular grid with a 1/60° (1 minutes) spacing (i.e. ~2 km)
Grid	21600 points in longitude / 9841 points in latitude
MSS determination technique	Local least square collocation method on a 3' grid where altimetric data in a 200-km radius are selected. Estimation on a 1' grid based on SSH-Filtered MSS values (remove/restore technique to recover the full signal). The inverse method uses local anisotropic covariance functions which improve the shortest wavelengths.
Estimation error level	YES (in cm) - The Optimal Interpolation method provides a calibrated formal error
Altimetric dataset	T/P-J1-J2: 20 years mean profile (first orbit), T/P tandem & J1 tandem: 3.7 years profile GFO: 7 years mean profile ERS-2/EnviSat: 15 years mean profile, 1 year ERS-1 (geodetic phase) J1 & Cryosat-2: geodetic phase

Table 11. MSS_CNES-CLS15 model characteristics.
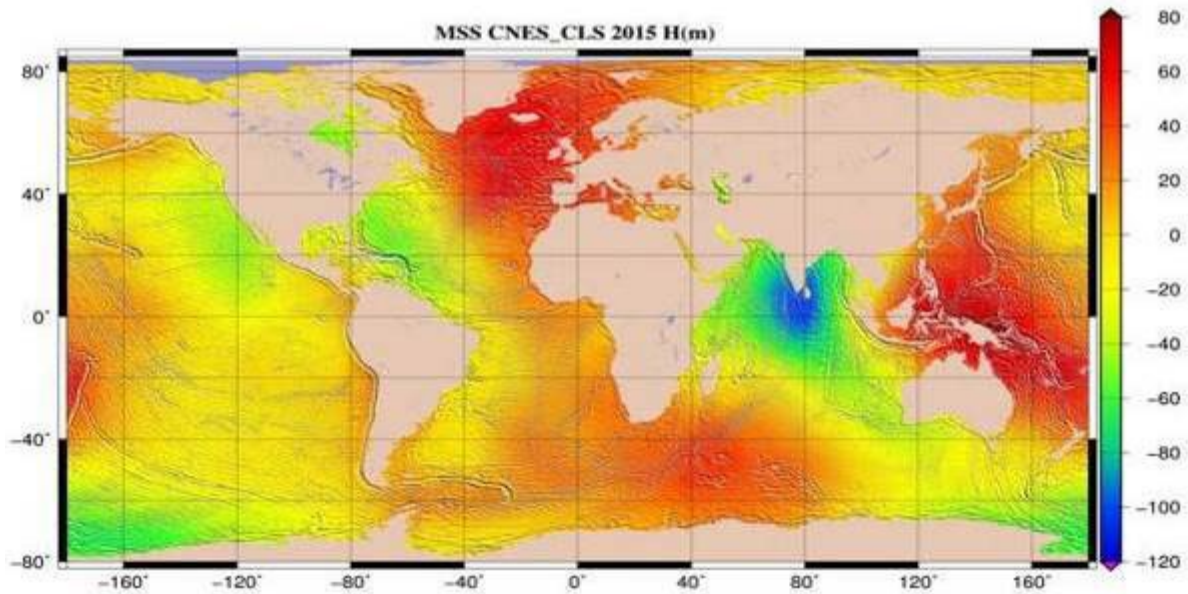
Figure 26. Mean Sea Surface MSS_CNES-CLS15 (m).

4.6.3.2. DTU18 Mean Sea Surface Model

The DTU18 mean sea surface model is described in [24].

4.6.4. Mean Dynamic Topography

The mean dynamic topography corresponds to the mean geostrophic currents and its changes and represents the mean sea surface height above the geoid. The MDT_CNES-CLS2018 model [25] of the mean dynamic topography is provided on the product in a variable named *mean_dynamic_topography*, with an estimate of accuracy and a quality flag (*mean_dynamic_topography_acc* and *mean_dynamic_topography_qual*). The MDT_CNES-CLS2018 model is computed from satellite altimetry data from a variety of missions. Its main characteristics are described Table 12 in below and a map of this surface is shown in Figure 27.

Name	MDT_CNES-CLS18
Referencing time period	1993-2012 (20 years)
Domain	Global – no Black Sea – no dedicated processing in the Arctic – the Med Sea come from the regional SOCIB MDT (Rio et al., 2014)
Spatial resolution	Regular grid with a 1/8°
Grid	2880 points in longitudes / 1440 points in latitude
MDT determination technique	Reference of the altimeter Sea Level Anomalies, computed relative to a 20 years (1993-2012) mean profile, in order to obtain absolute measurements of the ocean dynamic topography. Combined product based on GRACE and GOCE gravimetric data, altimetry and in situ data (hydrologic and drifters data)

Table 12. MDT_CNES-CLS18 model characteristics.
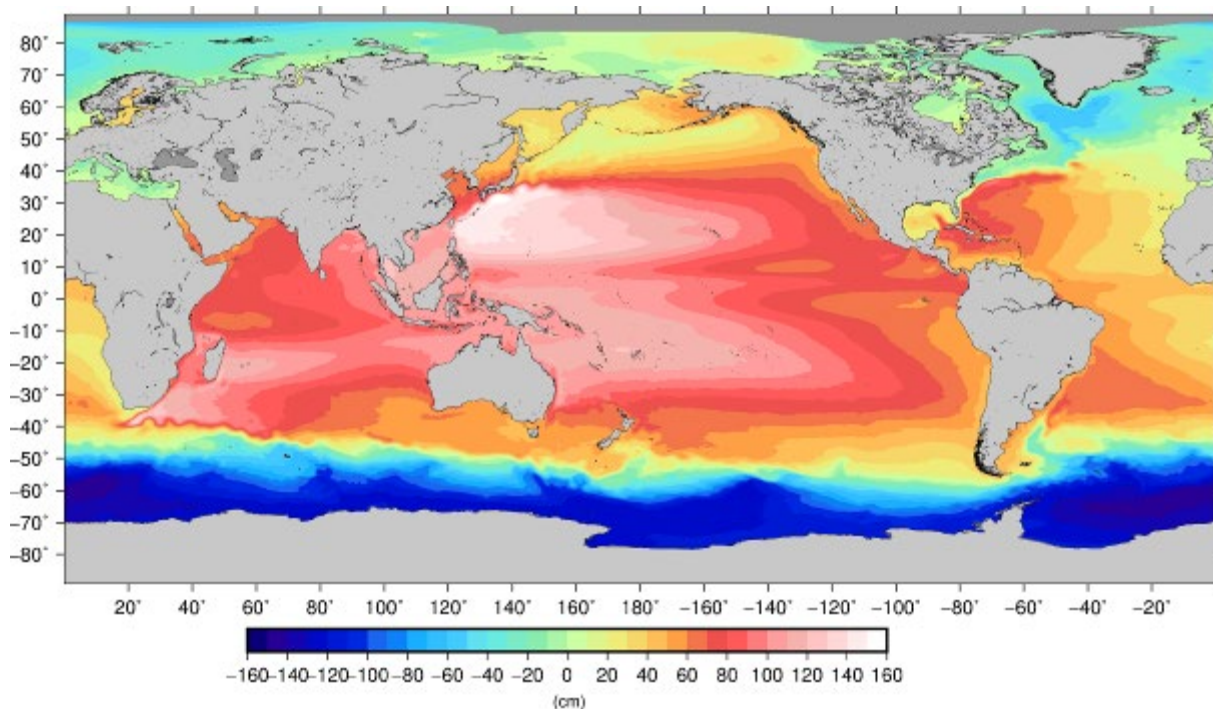
Figure 27. Mean Dynamic Topography MDT_CNES-CLS18.

4.7. Tides

Tides are a significant contributor to the observed sea surface height. While they are of interest in themselves, they have more variation than all other time-varying ocean signals. Since they are highly predictable, they are removed from the data in order to study ocean circulation. The TOPEX/POSEIDON orbit was specifically selected (inclination and repeat period) so that diurnal and semidiurnal tides would not be aliased to low frequencies.

There are several contributions to the tidal effect: the ocean tide, the load tide, the solid earth tide, the pole tide, and the internal tide. The ocean tide, load tide, solid earth tide, and internal tide are all related to luni-solar forcing of the earth, either directly as is the case of the ocean and solid earth tides, or indirectly as is the case with the load tide since it is the response of the solid Earth to the load of the ocean tide. The internal tide is forced by the ocean tide flow over sharp bottom topography. The pole tide is due to centrifugal force that results from variations in the Earth's rotation axis and is unrelated to luni-solar forcing.

The TOPEX/POSEIDON product does not explicitly provide values for the pure ocean tide, but instead provide values for a quantity referred to as the geocentric ocean tide, which is the sum of the ocean tide and the load tide. Values of the load tide that were used to compute the geocentric ocean tide are also explicitly provided, so the pure ocean tide can be determined by subtracting the load tide value from the geocentric ocean tide value. Note that the permanent tide is not included in either the geocentric ocean tide or solid earth tide corrections that are provided on the product, as the permanent tide is included in the reported values of the mean sea surface and geoid.

4.7.1. Geocentric Ocean Tide

As mentioned above, the geocentric ocean tide refers to the sum of the ocean tide and the load tide. This product provides two models of the geocentric ocean tide and the associated load tide, FES2014b [26] and GOT4.10c [27]. Each of them is computed as the sum of the ocean and load tides as predicted by a particular model for high frequencies (diurnal, semi-diurnal and non-linear tides with higher frequencies), and an equilibrium representation of the long-period ocean tides at all long-periods

except for the zero frequency (constant) term which is not included. The two geocentric ocean tide models are provided in variables named *ocean_tide_fes* and *ocean_tide_got*, respectively. The two respective load tide values are provided in variables named *load_tide_fes* and *load_tide_got*. As the ocean tide is set to zero on lakes and enclosed-seas, the parameters *ocean_tide_fes* and *ocean_tide_got* are equal to the load tide value on these surfaces. Both models are interpolated to provide the geocentric ocean and load tides at the location of the altimeter measurement, and an interpolation quality flag is provided on the product to indicate the quality of this interpolation (*ocean_tide_fes _qual* and *ocean_tide_got_qual*).

4.7.1.1. FES2014b Ocean Tide Model

The FES2014 ocean tide model [26] is a FES (Finite Element Solution) tide model developed in 2014-2016. It is an improved version of the FES2012 model, which was a fully revised version of the global hydrodynamic tide solutions initiated by the work of Christian Le Provost in the early nineties. This new FES2014 model has been developed, implemented, and validated by the LEGOS, NOVELTIS and CLS, within a CNES funded project.

FES2014 takes advantage of longer altimeter time series and better altimeter standards, improved modelling and data assimilation techniques, a more accurate ocean bathymetry and a refined mesh in most of shallow water regions. Special efforts have been dedicated to address the major non-linear tides and to the determination of accurate tidal currents.

FES2014 is based on the resolution of the tidal barotropic equations (T-UGO model) in a spectral configuration.

A new global finite element grid (~2.9 million nodes, 50% more than FES2012) is used and model physics has been improved, leading to nearly twice more accurate 'free' solution (independent of in situ and remote-sensing data) than the previous FES2012 version. The accuracy of this 'free' solution was improved by assimilating some long-term altimetry data (TOPEX/POSEIDON, Jason-1, Jason-2, TPN-J1N, and ERS-1 - ERS-2 - ENVISAT) and tidal gauges through an improved representer assimilation method.

A preliminary version, noted FES2014a, has been produced in 2015 based on GOT4v8ac loading tide. Then new tide loading effects have been computed using FES2014a oceanic tide (J.P. Boy, Univ. Strasbourg). These FES2014a tide loading effects have been used to produce the final model version noted FES2014b.

FES2014b geocentric (elastic) tide = FES2014b oceanic tide + FES2014a loading tide.

The final FES2014b solution shows strong improvement compared to FES2012 and GOT4V10, particularly in coastal and shelf regions and in some deep ocean areas and in the Arctic region.

34 tidal constituents are available for both the oceanic tide and the loading tide components: 2N2, EPS2, J1, K1, K2, L2, La2, M2, M3, M4, M6, M8, Mf, MKS2, Mm, MN4, MS4, MSf, MSqm, Mtm, Mu2, N2, N4, Nu2, O1, P1, Q1, R2, S1, S2, S4, Sa, Ssa, T2.

The FES2014b solution is provided on a 1/16° grid; moreover, the ocean tide grids have been extrapolated on ten pixels over coasts. Ocean tide values are set to zero on lakes and enclosed-seas.

See "http://www.aviso.altimetry.fr/en/data/products/auxiliary-products/global-tide-fes.html" for more information.

4.7.1.2. GOT4.10c Ocean Tide Model

The GOT4.10c ocean tide model [27], is an empirical ocean tide model generated from satellite altimeter data. This model is different from the previous version GOT4.8 as it is now based on Jason-1 and Jason-2 data, ERS-1 and ERS-2 and GFO. No TOPEX/POSEIDON data have been used in this solution.

The solution consists of independent near-global estimates of 10 tidal constituents (Q1, O1, P1, S1, K1, N2, M2, S2, K2, M4) for both the oceanic and the loading tide components. An a priori model was

used that consisted of the FES2004 hydrodynamic model and several other local hydrodynamic models.

Note that the GOT4.10c model uses accounts for geocenter motion when separating the ocean and load tide components of the geocentric ocean tide observed from satellite altimetry [50].

The GOT4.10c model is provided on a 0.5° grid; moreover, the ocean tide grids have been extrapolated on one pixel over coasts. Ocean tide values are set to zero on lakes and enclosed seas.

4.7.2. Long period Ocean Tide

The long-period ocean tides are a subject of continuing investigation. To first order, they can be approximated by an equilibrium representation. However, the true long-period ocean tide response is thought to have departures from an equilibrium response that increase with decreasing period. The two principal long-period ocean tide components, Mf and Mm, with fortnightly and monthly periods respectively, are known to have departures from an equilibrium response with magnitudes less than 1-2 cm.

This product explicitly provides a value for an equilibrium representation of the long-period ocean tide that includes all long-period tidal components, excluding the permanent tide (zero frequency) component (*ocean_tide_eq*). Note that both geocentric ocean tide values on the product (*ocean_tide_fes* and *ocean_tide_got*) already include the equilibrium long-period ocean tide, and therefore it should not be used simultaneously.

This product also provides a parameter for a non-equilibrium representation of the long-period ocean tides (*ocean_tide_non_eq*). This variable is provided as a correction to the equilibrium long-period ocean tide model so that the total non-equilibrium long period ocean tide is formed as a sum of *ocean_tide_eq* and *ocean_tide_non_eq*. The non-equilibrium long-period ocean tide provided in the products comes from FES2014b tide model, but the parameter *ocean_tide_non_eq* can be added to either of ocean_tide_fes or *ocean_tide_got*.

The FES2014b model provides a dynamic solution for 6 long-period tidal frequencies: Mf, Mm, MSqm, Mtm, Sa, Ssa.

The variables *ocean_tide_eq* and ocean_tide_non_eq are both set to zero on lakes and enclosed seas.

4.7.3. Solid Earth Tide

The solid Earth responds to external gravitational forces similarly to the oceans. The response of the Earth is fast enough that it can be considered to be in equilibrium with the tide generating forces. Then, the surface is parallel with the equipotential surface, and the tide height is proportional to the potential. The proportionality constant is the so-called Love number. It should be noted that the Love numbers are largely frequency independent. A significant exception occurs near a frequency corresponding to the K1 tide constituent due to a resonance in the liquid core [51].

This product computes the solid earth tide, or body tide, as a purely radial elastic response of the solid Earth to the tidal potential (*solid_earth_tide*.) The adopted tidal potential is the tidal potential described in [28] and [29], extrapolated to the 2000 era, and includes degree 2 and 3 coefficients of the tidal potential. The permanent tide (zero frequency) term is excluded from the tidal potential that is used to compute the solid earth tide parameter. The elastic response is modeled using frequency independent Love numbers. The effects of the resonance in the core are accounted for by scaling the tide potential amplitude of the K1 tidal coefficient and some neighboring nodal terms by an appropriate scale factor.

4.7.4. Pole Tide

The pole tide is a tide-like motion of the ocean surface that is a response of both the solid Earth and the oceans to the centrifugal potential that is generated by small perturbations to the Earth's rotation axis, polar motion. These perturbations primarily occur at periods of 433 days (called the Chandler wobble) and annual. These periods are long enough for the pole tide displacement to be considered

to be in equilibrium with the forcing centrifugal potential. This product provides a single field for the radial geocentric pole tide displacement of the ocean surface (*pole_tide*) and includes the radial pole tide displacement of the solid Earth and the oceans.

The pole tide is easily computed as described in [51] and [30]. This product uses the model described in [30], which accounts for self-gravitation, loading, conservation of mass, and geocenter motion. Over the oceans the variable *pole_tide* includes the response of the solid earth, ocean, and loading. Over land it includes only the impact on the solid earth and loading.

The pole tide is computed from polar motion variations with respect to a mean pole. The adopted model of the mean pole includes a bias and a drift [31]. As such, the computed pole tide does not include the effects of the Earth's displacement a drift in the mean pole. Modeling the pole tide requires knowledge of proportionality constants, the so-called Love numbers, and a time series of perturbations to the Earth's rotation axis, a quantity that is now measured routinely with space techniques.

4.7.5. Internal Tides

Internal tides are baroclinic tides generated by the arrival of a barotropic tide flow on an underwater sharp topography pattern (seamount or shelfbreak region). They can reach amplitudes of several tens of centimeters at the thermocline level and they have a signature of several cm at the surface with wavelengths of about 50-250 km for the first mode and shorter wavelengths for higher modes.

The global ocean tide models described in previous sections are barotropic tide models, and therefore do not include the internal tides. This product uses the model from [32] to provide a value for the internal tide surface signature in a variable named *internal_tide_hret*. This model includes the M2, S2, K1, and O1 tidal frequencies.

4.7.6. Dynamic Atmospheric Correction

The Dynamic Atmospheric Correction (DAC) uses a model to correct for the dynamic response of the ocean to atmospheric pressure and wind forcing at high frequencies. It is provided in a variable named *dac*.

The ocean response to wind and pressure is mostly dynamic and is significantly energetic at short periods so that the static inverse barometer correction is not sufficient. Several model approaches have been developed and showed that a barotropic model allows a good representation of this variability. The DAC is computed from the high frequencies of the barotropic ocean model MOG2D [33], forced by the ERA-Interim [19] numerical weather model and the low frequencies of the inverse barometer response. The cut-off frequency is 20 days and corresponds to the Nyquist frequency of the TOPEX/POSEIDON mission which has a 10-day repeat cycle. The DAC is therefore capable of removing almost all the high-frequency dynamic signal forced by the atmosphere (pressure and wind) and aliased into the altimetric measurement, except for the errors and uncertainties of the model.

Alternatively, the inverse barometer correction is provided in a variable named *inv_bar_cor*.

4.7.7. Wave model

The TOPEX/POSEIDON data product also provides significant wave height and mean wave period from a model in variables named *swh_model* and *mean_wave_period_t02*. The adopted model is from a global wave reanalysis model by the E.U. Copernicus Marine Service [36]. Note that mean_wave_period_t02 has been used to generate the 3-dimensional sea state bias model and provided correction in the variables named *sea_state_bias_ku_3d* and *sea_state_bias_c_3d*.

4.8. Flagging and Additional Information

4.8.1. Sensor status

The TOPEX/POSEIDON product provides a flag named *alt_state_flag_oper* to indicate which of the TOPEX Side A, TOPEX Side B, and POSEIDON altimeters is active for each epoch, with values of 0, 1, and 2, respectively.

For TOPEX data, flags named *alt_state_flag_ku_band_status* (0 = On, and 1 = Off), *alt_state_flag_c_band_status* (0 = On, and 1 = Off), and alt_state_flag_c_band (0 = 320 MHz, and 1 = 100 MHz) provide indicators of the state of the TOPEX instrument.

For POSEIDON-1 data, only *alt_state_flag_oper* flag is provided.

4.8.2. Rain Flag

Two rain flags are provided in the TOPEX/POSEIDON product. The variable named *rain_flag* is based upon a combination of TOPEX altimeter Ku and C band sigma0 measurements and the TMR measurements of integrated liquid water. Since POSEIDON is a single frequency Ku band altimeter, no *rain_flag* variable is available for POSEIDON data. The provided variable named rad_rain_flag is based upon TMR measurements alone.

Liquid water along the pulse's path reduces the energy returned to the altimeter, mainly at Ku band. In heavy rain, there are competing effects from attenuation and surface changes. The small-scale nature of rain cells tends to produce rapid changes in the strength of the echo as the altimeter crosses rain cells. Both effects degrade the performance of the altimeter. Data contaminated by rain are rare (most are located in the west equatorial pacific), flagged by the variable named *rain_flag* and should be ignored. The rain flag on the TOPEX/POSEIDON product is set if integrated liquid water content measured by the TMR is larger than a specified threshold, AND if the difference between the expected Ku band backscatter coefficient (estimated from the C band backscatter coefficient which is much less affected by rain) and the measured Ku band backscatter coefficient is larger than either a specified threshold or a specified multiple of the uncertainty in the expected Ku band backscatter coefficient [52]. The Ku band backscatter coefficient used for the rain flag determination is from MLE-3 retracking (*sig0_ku_mle3* and *sig0_c*). Note that biases of 2.44 dB and 1.34 dB are added to the reported values of *sig0_ku_mle3* and *sig0_c*, respectively, before applying the rain flag algorithm and associated thresholds that are based upon Jason-2 MLE-3 data. This accounts for a sigma0 bias correction to add to TOPEX to align with Jason-1 data (+2.79 dB and +1.57 dB for Ku and C band, respectively) as well as for the bias to align Jason-1 sigma0 to Jason-2 sigma0 (-0.35 dB and -0.23 dB for Ku and C band, respectively). For Ku Band TOPEX and Jason-1 have been aligned using MLE-4 sigma0 values. The rain flags algorithm and thresholds are derived from Jason-2 MLE-3 Ku band sigma0 values. The bias correction between Jason-1 and Jason-2 for Ku band has therefore been computed between Jason-2 MLE-3 Ku Sig0 and Jason-1 MLE-4 Ku sigma0. For Ku band and C band the estimation has been performed using cycle 2 for Jason-2 and cycle 240 for Jason-1 during their tandem operation.

The radiometer-derived rain flag, *rad_rain_flag*, is computed through a comparison of the radiometer measurements of 18 GHz brightness temperature and the cloud liquid water to specific thresholds. Rain is very absorptive in the microwave, and, over ocean, significantly increases the brightness temperature and liquid water content approximately proportional to the rain rate. Over the ocean, only rain will cause the 18 GHz brightness temperature to rise above ~200 K.

4.8.3. Ice Flag

4.8.3.1. Altimeter Ice Flag

The range measurement from the altimeter is likely to have larger errors when the pulse is reflected off ice surfaces. The ice surface is not at sea level, but at some unknown distance above it. The TOPEX/POSEIDON product provides a flag named *ice_flag* to indicate when the measurement is likely to be over ice. The ice flag is set if a climatological map of the latitude extent of ice predicts ice and

----

if the wind speed derived from the altimeter measurement (from *wind_speed_alt_mle3*) is less than 1 m /s, i.e., the backscatter is larger than normally expected from the ocean.

4.8.3.2. Radiometer Sea Ice Flag

The TOPEX/POSEIDON product also provides a sea ice flag that is computed from TMR brightness temperature measurements in a variable named *rad_sea_ice_flag*. This flag is set if the difference between the 37 and 18 GHz brightness temperatures is less than 20 K, and the absolute latitude is greater than 47 degrees.

4.8.4. Surface classification flag

The TOPEX/POSEIDON product provides a Surface Classification Flag named *surface_classification_flag*. The map used to determine the surface classification has been generated from three sources:

- GMT surface mask developed by Noveltis for the generation of the Jason-2 DEM (also including water body outlines from the LEGOS database)
- GLOBCOVER LC V2.0
- MODIS Mosaic of Antarctica from NSIDC

This flag has 7 possible states as follows:

- 0 = open ocean
- 1 = land
- 2 = continental water
- 3 = aquatic vegetation
- 4 = continental ice and snow
- 5 = floating ice
- 6 = salted basin

4.8.5. Bathymetry

The TOPEX/POSEIDON product provides a variable named *depth_or_elevation* that provides the depth or elevation of the measurement from a model. Ocean depths have negative values and land elevations have positive values. This variable is provided to allow users to edit data based upon ocean depth.

4.8.6. Wind Speed

Three sources of wind speed are provided on the TOPEX/POSEIDON product, from altimeter measurements, radiometer measurements, and a meteorological model.

4.8.6.1. Altimeter-derived

The altimeter-based wind speed is provided in variables named *wind_speed_alt* and *wind_speed_alt_mle3* for TOPEX, and in addition *wind_speed_alt_mgdr* for POSEIDON. These values are computed from a mathematical relationship between wind speed and the Ku band backscatter coefficient and the significant wave height. The empirical model is based upon [35] and [34]. A calibration bias is applied on altimeter Ku band backscatter coefficient before computing the wind speed. This bias is added to align the sigma0 measurements with the Jason-1 sigma0 measurements used originally by [34] to derive the windspeed table used here. The wind speed model function is evaluated for 10 meter above the sea surface, and is considered to be accurate to 2 m/s.

For TOPEX, the applied sigma0 calibration bias added to the reported values of *sig0_ku* and *sig0_ku_mle3* is + 2.69 dB. This bias includes a bias of +2.79 dB to apply to TOPEX to align with Jason-1 GDR-E Ku band sigma0 and a bias of -0.102 dB to align Jason-1 GDR-E with Jason-1 GDR-A Ku band

sigma0 values (where were used to derive the model from [34]). The wind speed model function is evaluated for 10 meter above the sea surface, and is considered to be accurate to 2 m/s.

POSEIDON-1 wind speed values are computed using respectively *swh_ku*, *swh_ku_mle3* and *swh_ku_mgdr*, applying a bias of 2.50 dB on *sig0_ku* for *wind_speed_alt* (MLE-4) and *wind_speed_alt_mle3* (MLE-3) outputs, and 2.44 dB on *sig0_ku_mgdr* for *wind_speed_alt_mgdr*.

4.8.6.2. Radiometer-derived

A radiometer-based wind speed is provided in a variable named *rad_wind_speed*. It has been computed through an empirical relationship to brightness temperatures measured by the TMR [18]. The coefficients of this relationship have been determined from the regression of island radiosonde data combined with seasonal and latitude dependent wind speed statistics.

4.8.6.3. Model

A 10-meter (above surface) wind vector, in east-west and north-south directions, is also provided in the TOPEX/POSEIDON product in variables named *wind_speed_mod_u* and *wind_speed_mod_v*, respectively. These model wind speeds have been computed from spatial and temporal interpolation of the ERA-Interim numerical weather model [19]. The accuracy for the wind vector varies from about 2 m/s in magnitude and 20 degrees in direction in the northern Atlantic Ocean, to more than 5 m/s and 40 degrees in the southern Pacific Ocean.

5. Data content & format

5.1. NetCdf format and CF convention

The netCDF data format has been chosen to store the different data sets (one file per data set). This format is extremely flexible, self-describing and has been adopted as a *de-facto* standard for many operational oceanography systems. The files follow the Climate and Forecast netCDF conventions CF-1.7 because these conventions provide a practical standard for storing data. Note that the TOPEX/POSEIDON product does not make use of the netCDF capability to use groups, unlike the Jason-3 and Sentinel-6 GDR-F products.

5.2. The NetCDF Data Model

A netCDF file contains **dimensions**, **variables**, and **attributes**, which all have both a name by which they are identified. These components can be used together to capture the meaning of data and relations among data fields in an array-oriented data set.

Note that no group has been implemented in TOPEX/POSEIDON product.

5.2.1. Dimensions

A dimension may be used to represent a real physical dimension, for example, time, latitude, longitude, or height. A dimension might also be used to index other quantities (waveforms index for example). Table 13 summarizes the dimensions are used in the TOPEX/POSEIDON product files.

Dimension Name	Value	GDR Data Set
time	Number of measurements in the file	X
meas_ind	**20** (number of elementary measurements)	X

Table 13. Dimensions used in the TOPEX/POSEIDON data products.

5.2.2. Variables

Variables are used to store the bulk of the data in a netCDF file. A variable represents an array of values of the same type. A scalar value is treated as a 0-dimensional array. A variable has a name, a data type, and a shape described by its list of specified dimensions when the variable is created. A variable may also have associated attributes, which may be added, deleted or changed after the variable is created.

A variable data type is one of a small set of netCDF types. The TOPEX/POSEIDON product uses variable types summarized in Table 14.

Variable type	Description
char	characters
byte	8-bit data signed
short	16-bit signed integer
int	32-bit signed integer
float	IEEE single precision floating point (32 bits)
double	IEEE double precision floating point (64 bits)

Table 14. netCDF variable types.

5.2.3. Coordinate variables and auxiliary coordinate variables

A variable with the same name as a dimension is called a **coordinate variable**. It typically defines a physical coordinate corresponding to that dimension. In accordance with the Climate and Forecast conventions, we must declare a coordinate variable for each dimension. What's more, missing values are not allowed in coordinate variables and they must be strictly monotonic.

An **auxiliary coordinate variable** is a netCDF variable that contains coordinates data but is not a coordinate variable as defined above. Unlike coordinate variables, there is no relationship between the name of an auxiliary coordinate variable and the name(s) of its dimension(s).

5.2.4. Attributes

NetCDF attributes are used to store information about the data (ancillary data or metadata), similar in many ways to the information stored in data dictionaries and schema in conventional database systems. Most attributes provide information about a specific variable. These are identified by the name of that variable, together with the name of the attribute.

Some attributes provide information about the data set as a whole. They are called **global attributes**.

Table 15 shows the variable attributes used in the TOPEX/POSEIDON product. There are no mandatory attributes.

Attribute	Description
_FillValue	A default value used to represent missing or undefined data
add_offset	If present, this number is to be added to the data after it is read by an application. If both *scale_factor* and *add_offset* attributes are present, the data are first scaled before the offset is added
calendar	Reference time calendar
comment	Miscellaneous information about the data or the methods used to produce it
coordinates	Identified auxiliary coordinates variables
flag_meanings	Use in conjunction with *flag_values* to provide descriptive words or phrase for each flag value
flag_values	Provide a list of the flag values. Use in conjunction with *flag_meanings*
institution	Institution which provides the data
leap_second	UTC time at which a leap second occurs
long_name	A descriptive name that indicates a variable's content. This name is not standardized
quality_flag	Name of the variable(s) (quality flag) representing the quality of the current variable
scale_factor	If present, the data are to be multiplied by this factor after the data are read by an application. See also *add_offset* attribute
source	Data source (model features, or observation)
standard_name	A standard name that references a description of a variables content in the standard name table
tai_tuc_difference	Difference between TAI and UTC reference time
units	Unit of a variable's content. The value of this attribute must be a string that can be recognized by the UNIDATA's Udunits package
valid_max	Largest theoretical valid value of a variable (this is not the maximum of actual data)
valid_min	Smallest theoretical valid value of a variable (this is not the minimum of actual data)

Table 15. Variable attributes.

5.2.5. The Common Data Language

The Common Data Language (CDL) is used to describe the content of a data set. The CDL is textual notation that describes the netCDF object and it is human readable. The netCDF utility **ncdump** converts netCDF binary objects to CDL text. The netCDF utility **ncgen** creates netCDF binary file from CDL text file.

A CDL description of a netCDF data set takes the form:

```
netCDF name {
dimension: …
variables: …
data: …
}
```

where the name is used only as a default in constructing file names by the ncgen utility. The CDL description consists of three optional parts, introduced by the keywords dimensions variables and data. NetCDF dimension declarations appear after the dimensions keyword, netCDF variables and attributes are defined after the variables keyword and variable data assignments appears after the data keyword. CDL statement are terminated by a semicolon. Spaces, tabs and newlines can be used freely for readability. Comments in CDL follow the characters '//' on any line.

Example

```
netcdf example {

  dimensions:                              //  dimensions name are declared first
    time = 2680;

   variables:
   double time(time);                      // variable <type> <name>(<dimension>)
     time:long_name = "time";              // variable attributes
     time:units = "seconds since 2000-01-01 00:00:00.0";

   int longitude(time);
     longitude:long_name = "longitude";
     longitude:standard_name = "longitude";
     longitude:units = "degrees_east";
     longitude:scale_factor = 1.0e-06;

   byte alt_echo_type(time);
     alt_echo_type:long_name = "altimeter echo type";
     alt_echo_type:_FillValue = 127b;
     alt_echo_type:flag_values = 0b, 1b ;
     alt_echo_type:flag_meanings = "ocean_like non_ocean_like";
     alt_echo_type:coordinates = "longitude latitude";

    int altitude(time);
     altitude:long_name = "1 Hz altitude of satellite";
     altitude:_FillValue = 2147483647;
     altitude:units = "m";
     altitude:add_offset = 1.30e+06;
     altitude:scale_factor = 1.00e-04;
     altitude:coordinates = "longitude latitude";
```

time is a coordinate variable

alt_echo_type is a flag fully described by the *flag_meanings* and *flag_values* attributes:

        alt_echo_type   = 0   -> ocean like echo
        alt_echo_type   = 1   -> non ocean like echo

   If alt_echo_type is not computed, it will take the value 127 (*_FillValue* attribute).

altitude is packed. The data are stored in 32-bit integers (int). The value of the altitude of the satellite can be recovered using:

        alt = (*altitude * scale_factor*) + *add_offset*

----

6. How to read the data (software & languages)

This section lists some software and languages that may be used to browse and use data from the GDR product. This list is by no means exhaustive.

6.1. Programing languages

6.1.1. Python & Python modules

Python is a high-level, interpreted, general-purpose programming language. Python supports multiple programming paradigms, including structured (particularly procedural), object-oriented, and functional programming. It has a large, comprehensive, set of modules for all purposes. The Python programming language provides a number of practical modules to read netCDF data, especially xarray or netCDF4 modules. Tutorials, including interactive Python notebooks, are available on the web.

6.1.2. Matlab (Scilab)

The Matlab package is a numerical computing and programming platform used to analyze data, develop algorithms, and create models. Scilab is an open-source alternative. Both have readers for netCDF files, and do a large variety of computation from the data.

6.2. Software provided with netCDF

The netCDF package provides a variety of programs to handle netCDF files. See https://www.unidata.ucar.edu/software for a list of software provided by Unidata, and https://www.unidata.ucar.edu/software/netcdf/software.html for a more complete list of NetCDF-reading software.

In particular, the program "ncdump" converts netCDF files to ASCII form (CDL).

See https://docs.unidata.ucar.edu/netcdf-c/current/faq.html#NetCDF-and-Other-Software

The main options are the following:

-h	Show only the header information in the output, that is the declarations of dimensions, variables, and attributes but no data values for any variables
-c	Show the values of coordinate variables (variables that are also dimensions) as well as the declarations of all dimensions, variables, and attribute values
-v *var1,...,varn*	The output will include data values for the specified variables, in addition to the declarations of all dimensions, variables, and attributes
-x *var1,...,varn*	Output XML (NcML) instead of CDL. The NcML does not include data values

6.3. Additional general software

6.3.1. netCDF Operator (NCO)

The netCDF Operators, or "NCO", are a suite of programs known as **operators**. Each operator is a standalone, command line program which is executed at the UNIX shell-level, like, e.g., ls or mkdir. The operators take netCDF files as input, then perform a set of operations (e.g., deriving new data, averaging, hyperslabbing, or metadata manipulation) and produce a netCDF file as output. The operators are primarily designed to aid manipulation and analysis of gridded scientific data. The single command style of NCO allows users to manipulate and analyze files interactively and with

----

simple scripts, avoiding the overhead (and some of the power) of a higher level programming environment.

See http://nco.sourceforge.net/

6.3.2. Panoply

Panoply is a cross-platform application that runs on Macintosh, Windows, Linux and other desktop computers. It reads and plots geo-referenced and other arrays from netCDF, HDF, GRIB, and other datasets. It is an easy tool to visualize the data and do a quick plot (it won't enable you to compute from the data).

See https://www.giss.nasa.gov/tools/panoply/

----

7. Data Distribution

7.1. PO.DAAC data distribution

The TOPEX/POSEIDON GDR-F product is accessible from the PO.DAAC under the dataset identifier: 'TOPEX_POSEIDON_GDR_F'. Data users must register a free Earthdata Login account in order to download the files. Resources for data search and access can be found on the dataset landing page:

https://podaac.jpl.nasa.gov/dataset/TOPEX_POSEIDON_GDR_F

Citation is critically important for dataset documentation and discovery. Please cite the TOPEX/POSEIDON GDR-F product as follows (including the date at which data were accessed, YYYY-MM-DD), and cite the reference papers when it is appropriate.

TOPEX/Poseidon. 2023. TOPEX/Poseidon Geophysical Data Record Version F. Ver. F. PO.DAAC, CA, USA. Dataset accessed [YYYY-MM-DD] at https://doi.org/10.5067/TPXPS-GDRF1

For any questions on TOPEX/POSEIDON data dissemination on PO.DAAC servers please contact:

podaac@podaac.jpl.nasa.gov

7.2. CNES data distribution

Users have access to public data through a dedicated AVISO ftp server with an authenticated account. This TOPEX/POSEIDON GDR-F product is available on the following server:

IP address: ftp://ftp-access.aviso.altimetry.fr

User account: authenticated

Home directory: /geophysical-data-record/topex-poseidon/

For any questions on data dissemination on AVISO servers please contact:

aviso@altimetry.fr

8. Acknowledgements

Appendix A: References

[1] L.-L. Fu, E. J. Christensen, C. A. Yamarone Jr., M. L. Lefebvre, Y. Menard, M. Dorrer and P. Escudier, "TOPEX/POSEIDON mission overview," *Journal of Geophysical Research,* vol. 99, no. C12, pp. 24369-24381, https://doi.org/10.1029/94JC01761, 1994.

[2] Y. Menard, L.-L. Fu, P. Escudier, F. Parisot, J. Perbos, P. Vincent, S. Desai, B. Haines and G. Kunstmann, "The Jason-1 Mission Special Issue: Jason-1 Calibration/Validation," *Marine Geodesy,* vol. 26, no. 3-4, pp. 131-146, https://doi.org/10.1080/714044514, 2003.

[3] J. Lambin, R. Morrow, L.-L. Fu, J. R. Willis, H. Bonekamp, J. Lillibridge, J. Perbos, G. Zaouche, P. Vaze, W. Bannoura, F. Parisot, E. Thouvenout, S. Coutin-Faye, E. Lindstrom and M. Mignogno, "The OSTM/Jason-2 Mission," *Marine Geodesy,* vol. 33, no. S1, pp. 4-25, https://doi.org/10.1080/01490419.2010.491030, 2010.

[4] C. J. Donlon et al., "The Copernicus Sentinel-6 mission: Enhanced continuity of satellite sea level measurements from space," *Remote Sensing of Environment,* vol. 258, https://doi.org/10.1016/j.rse.2021.112395, 2021.

[5] B. Tapley et al., "Precision orbit determination for TOPEX/POSEION," *Journal of Geophysical Research,* vol. 99, no. C12, pp. 24383-24404, https://doi.org/10.1029/94JC01645, 1995.

[6] F. Nouel et al., "Precise Centre National d'Etudes Spatiales orbits for TOPEX/POSEIDON: Is reaching 2 cm still a challenge," *Journal of Geophysical Research,* vol. 99, no. C12, pp. 24405-24419, https://doi.org/10.1029/94JC01039.

[7] J.-D. Desjonqueres and F. Bignalet-Cazalet, "TOPEX/POSEIDON Reprocessing," in *2022 Ocean Surface Topography Science Team Meeting*, Venice, Italy, 2022.

[8] G. S. Hayne, D. W. Hancock III, C. L. Purdy and P. S. Callahan, "The corrections for significant wave height and attitude effects in the TOPEX radar altimeter," *Journal of Geophysical Research,* vol. 99, no. C12, pp. 24941-24955, https://doi.org/10.1029/94JC01777, 1994.

[9] P. Thibaut, H. Roinard, N. Picot and T. Guinle, "Reprocessing of the Poseidon-1 French Altimeter dataset," in *2018 Ocean Surface Topography Science Team Meeting*, Ponta Delgada, Azores, 2018.

[10] C. S. Ruf, S. J. Keihm and M. A. Janssen, "TOPEX/Poseidon Microwave Radiometer (TMR): I. Instrument description and antenna calibration," *IEEE Transactions on Geoscience and Remote Sensing,* vol. 33, no. 1, pp. 125-137, https://doi.org/10.1109/36.368215, 1995.

[11] C. Ruf, S. J. Keihm, B. Subramanya and M. A. Janssen, "TOPEX/POSEIDON microwave radiometer performance and in-flight calibration," *Journal of Geophysical Research,* vol. 99, no. C12, pp. 24915-24926, https://doi.org/10.1029/94JC00717, 1994.

[12] C. Ruf, "Detection of calibration drifts in spaceborne microwave radiometer using a vicarious cold reference," *IEEE Transaction on Geoscience and Remote Sensing,* vol. 38, no. 1, pp. 44-52, https://doi.org/10.1109/36.823900, 2000.

[13] S. Brown, S. Desai, S. Keihm and W. Lu, "Microwave Radiometer Calibration on Decadal Time Scales Using On-Earth Brightness Temperature References: Application to the TOPEX Microwave Radiometer," *Journal of Atmospheric and Oceanic Technology,* vol. 26, no. 12, pp. 2579-2591, https://doi.org/10.1175/2009JTECHA1305.1.

[14] S. Brown, "A Novel Near-Land Radiometer Wet Path-Delay Retrieval Algorithm: Application to the Jason-2/OSTM Advanced Microwave Radiometer," *IEEE Transations on Geoscience and*

Remote Sensing, vol. 48, no. 4, pp. 1986-1992, https://doi.org/10.1109/TGRS.2009.2037220, 2010.

[15] W. I. Bertiger et al., "GPS precise tracking of TOPEX/POSEIDON: Results and implications," *Journal of Geophysical Research,* vol. 99, no. C12, pp. 24449-24464, https://doi.org/10.1029/94JC01171, 1994.

[16] A. Mannucci, B. Wilson, D. Yuan, C. Ho, U. Lindqwister and T. Runge, "A global mapping technique for GPS-derived ionospheric total electron content measurements," *Radio Science,* vol. 33, no. 3, pp. 565-582, https://doi.org/10.1029/97RS02707, 1998.

[17] S. D. Desai, P. S. Callahan, J. D. Desjonqueres, B. Haines, M. Talpe, J. K. Willis, G. Shirtliffe, N. Picot, T. Guinle, H. Roinard and M. Ablain, "Calibration and Validation of Reprocessed TOPEX Geophysical Data Records," in *2018 Ocean Surface Topography Science Team Meeting*, Ponta Delgada, Azores, 2018.

[18] S. J. Keihm, M. A. Janssen and C. S. Ruf, "TOPEX/POSEIDON microwave radiometer (TMR): III. Wet troposphere range correction algorithm and pre-launch error budget," *IEEE Trans. Geosci. Remote Sensing,* vol. 33, pp. 147-161, Jan. 1995.

[19] ECMWF, "ERA-Interim," European Center for Medium-Range Weather Forecasts, [Online]. Available: https://www.ecmwf.int/en/forecasts/datasets/reanalysis-datasets/era-interim.

[20] A. A. Putnam Shilleh, "Sea state bias model development and error analysis for pulse-limited altimetry.," Ph.D. Thesis, University of Colorado, Boulder, Colorado, 2021.

[21] H. Feng, D. Vandemark, N. Tran and S. Desai, "Sea state bias for retracked TOPEX altimeter data," in *2019 Ocean Surface Topography Science Team Meeting*, Chicago, IL., 2019.

[22] N. K. Pavlis, S. A. Holmes, S. C. Kenyon and J. K. Factor, "The development and evaluation of the Earth Gravitational Model 2008 (EGM2008)," *Journal of Geophysical Research: Solid Earth,* vol. 117, no. B4, pp. 1978-2012, https://doi.org/10.1029/2011JB008916, 2012.

[23] AVISO, "CNES/CLS MSS," [Online]. Available: https://www.aviso.altimetry.fr/en/data/products/auxiliary-products/mss.html.

[24] O. B. Andersen, P. Knudsen and L. Stenseng, "The DTU18 MSS mean sea surface - technical description," in *2018 Ocean Surface Topography Science Team Meeting*, Ponta Delgada, Portugal, 2018.

[25] S. Mulet, M.-H. Rio, H. Etienne, C. C. M. Artana, G. Dibarboure, H. Feng, R. Husson, N. Picot, C. Provost and P. T. Strub, "The new CNES-CLS18 Global Mean Dynamic Topography," *Ocean Science,* vol. 17, pp. 789-808, https://doi.org/10.5194/os-17-789-2021, 2021.

[26] L. Carrere, F. Lyard, M. Cancet, A. Guillot and N. Picot, "FES 2014, a new tidal model - Validation results and perspectives for improvements," in *ESA Living Planet Conference*, Prague, 2016.

[27] R. D. Ray, "Precise comparisons of bottom-pressure and altimetric ocean tides," *Journal of Geophysical Research, Oceans,* vol. 118, no. 9, pp. 4570-4584, https://doi.org/10.1002/jgrc.20336, 2013.

[28] D. E. Cartwright and R. J. Taylor, "New computations of the tide-generating potential," *Geophys. J. R. Astr. Soc.,* vol. 23, pp. 45-74, 1971.

[29] D. E. Cartwright and A. C. Edden, "Corrected tables of tidal harmonics," *Geophys. J. R. Astr. Soc.,* vol. 33, pp. 253-264, 1973.

[30] S. Desai, J. Wahr and B. Beckley, "Revisiting the pole tide for and from satellite altimetry," *J. Geod.,* vol. 89, pp. 1233-1243, 2015, https://doi.org/10.1007/s00190-015-0848-7.

[31] J. C. Ries and S. D. Desai, "Conventional model update for rotational deformation," in *Fall AGU Meeting*, New Orleans, LA, 2017, http://dx.doi.org/10.26153/tsw/2659.

[32] E. D. Zaron, "Baroclinic tidal sea level from exact-repeat mission altimetry.," *J. Phys. Oceano.*, vol. 49, pp. 193-210, 2019, https://doi.org//10.1175/JPO-D-18-0127.1.

[33] AVISO, "Dynamic Atmospheric Correction: AVISO+," [Online]. Available: https://www.aviso.altimetry.fr/en/data/products/auxiliary-products/dynamic-atmospheric-correction/description-atmospheric-corrections.html.

[34] F. Collard and S. Labroue, "New wind speed algorithms for Jason-1," in *2004 Ocean Surface Topography Science Team Meeting*, St. Petersburg, Florida, 2004.

[35] J. Gourrion, D. Vandemark, S. Bailey, B. Chapron, G. P. Gommenginger, P. G. Challenor and M. A. Srokosz, "A two-parameter wind speed algorithm for Ku-band altimeters," *Journal of Atmospheric and Oceanic Technology*, vol. 19, no. 12, pp. 2030-2048, https://doi.org/10.1175/1520-0426(2002)019<2030:ATPWSA>2.0.CO;2, 2002.

[36] S. Law, L. Aouf, B. Levier and A. Dalphinet, "Global High Resolution Production Center, GLOBAL_REANALYSIS_WAV_001_032," Copernicus Marine Environment Monitoring Service, CMEMS-GLO-QUID-001-032, 2021.

[37] G. S. Brown, "The average impulse response of a rough surface and its applications," *IEEE Transactions on Antennas and Propagation*, vol. 25, no. 1, pp. 67-74, 1977.

[38] D. W. Hancock, G. S. Hayne, R. L. Brooks, J. E. Lee and D. W. Lockwood, "TOPEX radar altimeter engineering assessment report update: From launch to turn-off of Side-A on February 10, 1999 (NASA/TM-2003-213336/Vol.12)," NASA Goddard Space Flight Center. Retried from www.sti.nasa.gov., Geenbelt, MD, 1999.

[39] D. W. Lockwood, D. W. Hancock, G. S. Hayne and R. L. Brooks, "TOPEX radar altimeter engineering assessment report final update: Side-B turn-on to end-of-mission on October 9, 2005 (NASA/TM-2006-212236/Vol. 21)," NASA Goddard Space Flight Center. Retrieved from www.sti.nasa.gov, Greenbelt, MD, 2006.

[40] L. Amarouche, P. Thibaut, O. Z. Zanife, J.-P. Dumont, P. Vincent and N. Steunou, "Improving the Jason-1 ground retracking to better account for attitude effects," *Marine Geodesy*, vol. 27, no. 1-2, pp. 171-197, https://doi.org/10.1080/01490410490465210, 2004.

[41] H. Roinard and S. Philipps, "Jason-2 reprocessing impact on ocean data (cycles 001 to 145). Comparison of Jason-2 Gdr-D with Gdr-T, as well as with Jason-1 Gdr-C and Envisat Gdr v2.1," SALP-RP-MA-EA-22140-CLS. CLS.DOS/NT/12.222, 2012.

[42] DORIS/POSEIDON, "Centre de traitement DORIS/POSEIDON. Catalogure des produits. CLS.DIE/NT/97.015. CM-IF-6-2106-CLS (1999-11-12)," CNES, Toulouse, 1999.

[43] AVISO/Altimetry, "AVISO Uder Handbook for Merged TOPEX/POSEIDON Products, Edition 3.0 AVI-NT-02-101-CN (1996-07)," CNES, Toulouse, 1996.

[44] DORIS/POSEIDON, "Specification des algorithmes de la chaine de traitement des donnees altimetriques du niveau 1.5 CLS.DT/NT/91.140. TP-ST-6135-320-CLS (1996-08-04)," CNES, Toulouse, 1995.

[45] D. B. Chelton, J. C. Ries, B. J. Haines, L.-L. Fu and P. S. Callahan, "Satellite Altimetry," in *Satellite Altimetry and Earth Sciences*, Elsevier, 2001, pp. 1-131.

[46] J. Saastamoinen, "Atmospheric correction for the toposphere and straosphere in radioranging for satellite," *Geophys. Monogr.*, vol. 15, 1972.

[47] D. Imel, "Evaluation of the TOPEX dual-frequency ionosphere correction.," *J. Geophys. Res.,* vol. 99, no. C12, pp. 24895-24905, https://doi.org/10.1029/94JC01869, 1994.

[48] P. Gaspar, F. Ogor, P. Y. Le Traon and O. Z. Zanife, "Estimating the sea state of the TOPEX and POSEIDON altimeters from crossover differences," *J. Geophys. Res.,* vol. 99, pp. 24981-24994, 1994.

[49] D. Chelton, "The sea state bias in altimeter estimates of sea level from collinear analysis of TOPEX data," *J. Geophys. Res.,* vol. 99, pp. 24995-25008, 1994.

[50] S. D. Desai and R. D. Ray, "Consideration of tidal variations in the geocenter on satellite altimeter observations of ocean tides," *Geophysical Research Letters,* vol. 41, no. 7, pp. 2454-2459, https://doi.org/10.1002/2014.GL059614, 2014.

[51] J. M. Wahr, "Deformation induced by polar motion," *J. Geophys. Res.,* vol. 90(B11), pp. 9363-9368, 1985, https://doi.org/10.1029/JB090iB11p09363.

[52] J. Tournadre and J. C. Morland, "The effects of rain on TOPEX/POSEIDON altimeter data," *IEEE Transactions in Geosciences and Remote Sensing,* vol. 35, no. 5, pp. 1117-1135, https://doi.org/10.1109/36.628780, 1997.

Appendix B: POSEIDON Active Periods

The POSEIDON altimeter was active for the periods described Table 16 in below. The TOPEX altimeter was active for the remaining periods of the mission.

Repeat Cycle	Pass Numbers	Repeat Cycle	Pass Numbers	Repeat Cycle	Pass Numbers
3	222-254	90	254	197	1-254
4	1-44	91	1-254	208	254
5	219-245	96	254	209	1-253
6	18-46, 219-245	97	1-254	215	254
8	219-254	102	254	216	1-239
9	1-46	103	1-253	223	252-254
11	219-245	113	254	224	1-254
12	21-46, 217-243	114	1-254	233	254
13	219-254	125	254	234	1-254
14	1-45	126	1-254	242	254
15	219-247	137	254	243	1-254
16	20-47	138	1-254	255	254
20	6-254	149	254	256	1-254
30	254	150	1-254	265	254
31	1-254	161	254	266	1-254
40	254	162	1-254	277	254
41	1-254	173	254	278	1-254
54	254	174	1-254	288	254
55	1-254	179	254	289	1-254
64	254	180	1-254	298	254
65	1-254	185	254	299	1-254
78	254	186	1-254	307	4-252
79	1-254	196	254	361	1-252

Table 16. Periods when POSEIDON altimeter was active.

Appendix C: Equator Crossing Longitudes

Table 17 and Table 18 below provides the equator crossing longitudes for the nominal TOPEX/POSEIDON ground track.

Pass	Longitude	Pass	Longitude	Pass	Longitude	Pass	Longitude	Pass	Longitude	Pass	Longitude
1	99.9249	44	30.4744	87	321.0274	130	251.5783	173	182.1282	216	112.6813
2	265.7517	45	196.3012	88	126.8541	131	57.4042	174	347.9550	217	278.5075
3	71.5776	46	2.1280	89	292.6810	132	223.2310	175	153.7829	218	84.3343
4	237.4044	47	167.9557	90	98.5078	133	29.0576	176	319.6096	219	250.1600
5	43.2305	48	333.7825	91	264.3336	134	194.8843	177	125.4369	220	55.9867
6	209.0573	49	139.6102	92	70.1603	135	0.7117	178	291.2636	221	221.8129
7	14.8844	50	305.4370	93	235.9862	136	166.5385	179	97.0902	222	27.6397
8	180.7112	51	111.2637	94	41.8130	137	332.3659	180	262.9170	223	193.4666
9	346.5387	52	277.0905	95	207.6395	138	138.1927	181	68.7430	224	359.2934
10	152.3655	53	82.9167	96	13.4663	139	304.0198	182	234.5697	225	165.1212
11	318.1928	54	248.7435	97	179.2937	140	109.8466	183	40.3959	226	330.9479
12	124.0196	55	54.5694	98	345.1205	141	275.6727	184	206.2227	227	136.7755
13	289.8463	56	220.3962	99	150.9484	142	81.4995	185	12.0499	228	302.6023
14	95.6731	57	26.2229	100	316.7751	143	247.3252	186	177.8767	229	108.4290
15	261.4989	58	192.0497	101	122.6022	144	53.1520	187	343.7042	230	274.2558
16	67.3256	59	357.8771	102	288.4290	145	218.9782	188	149.5309	231	80.0819
17	233.1515	60	163.7039	103	94.2556	146	24.8050	189	315.3582	232	245.9087
18	38.9783	61	329.5313	104	260.0823	147	190.6320	190	121.1850	233	51.7347
19	204.8049	62	135.3580	105	65.9083	148	356.4588	191	287.0117	234	217.5614
20	10.6317	63	301.1851	106	231.7351	149	162.2866	192	92.8384	235	23.3883
21	176.4592	64	107.0119	107	37.5614	150	328.1133	193	258.6642	236	189.2150
22	342.2860	65	272.8379	108	203.3881	151	133.9409	194	64.4909	237	355.0425
23	148.1139	66	78.6647	109	9.2154	152	299.7676	195	230.3169	238	160.8693
24	313.9406	67	244.4904	110	175.0422	153	105.5943	196	36.1437	239	326.6966
25	119.7676	68	50.3172	111	340.8697	154	271.4211	197	201.9704	240	132.5234
26	285.5944	69	216.1435	112	146.6964	155	77.2471	198	7.7971	241	298.3504
27	91.4209	70	21.9702	113	312.5237	156	243.0739	199	173.6248	242	104.1772
28	257.2477	71	187.7974	114	118.3505	157	48.8999	200	339.4515	243	270.0031
29	63.0736	72	353.6242	115	284.1770	158	214.7267	201	145.2793	244	75.8299
30	228.9004	73	159.4520	116	90.0038	159	20.5536	202	311.1061	245	241.6556
31	34.7268	74	325.2788	117	255.8295	160	186.3804	203	116.9330	246	47.4824
32	200.5535	75	131.1062	118	61.6562	161	352.2079	204	282.7598	247	213.3088
33	6.3809	76	296.9330	119	227.4823	162	158.0346	205	88.5862	248	19.1355
34	172.2076	77	102.7596	120	33.3090	163	323.8620	206	254.4130	249	184.9628
35	338.0351	78	268.5864	121	199.1358	164	129.6887	207	60.2389	250	350.7896
36	143.8619	79	74.4124	122	4.9626	165	295.5157	208	226.0657	251	156.6174
37	309.6891	80	240.2392	123	170.7903	166	101.3425	209	31.8922	252	322.4442
38	115.5159	81	46.0652	124	336.6170	167	267.1683	210	197.7189	253	128.2715
39	281.3423	82	211.8920	125	142.4448	168	72.9951	211	3.5463	254	294.0983
40	87.1690	83	17.7190	126	308.2716	169	238.8209	212	169.3731		
41	252.9947	84	183.5458	127	114.0984	170	44.6477	213	335.2005		
42	58.8215	85	349.3733	128	279.9252	171	210.4741	214	141.0273		
43	224.6476	86	155.2000	129	85.7515	172	16.3009	215	306.8545		

Table 17. Equator crossings by pass number order.

Pass	Longitude	Pass	Longitude	Pass	Longitude	Pass	Longitude	Pass	Longitude	Pass	Longitude
135	0.7117	118	61.6562	101	122.6022	84	183.5458	67	244.4904	50	305.4370
46	2.1280	29	63.0736	12	124.0196	249	184.9628	232	245.9087	215	306.8545
211	3.5463	194	64.4909	177	125.4369	160	186.3804	143	247.3252	126	308.2716
122	4.9626	105	65.9083	88	126.8541	71	187.7974	54	248.7435	37	309.6891
33	6.3809	16	67.3256	253	128.2715	236	189.2150	219	250.1600	202	311.1061
198	7.7971	181	68.7430	164	129.6887	147	190.6320	130	251.5783	113	312.5237
109	9.2154	92	70.1603	75	131.1062	58	192.0497	41	252.9947	24	313.9406
20	10.6317	3	71.5776	240	132.5234	223	193.4666	206	254.4130	189	315.3582
185	12.0499	168	72.9951	151	133.9409	134	194.8843	117	255.8295	100	316.7751
96	13.4663	79	74.4124	62	135.3580	45	196.3012	28	257.2477	11	318.1928
7	14.8844	244	75.8299	227	136.7755	210	197.7189	193	258.6642	176	319.6096
172	16.3009	155	77.2471	138	138.1927	121	199.1358	104	260.0823	87	321.0274
83	17.7190	66	78.6647	49	139.6102	32	200.5535	15	261.4989	252	322.4442
248	19.1355	231	80.0819	214	141.0273	197	201.9704	180	262.9170	163	323.8620
159	20.5536	142	81.4995	125	142.4448	108	203.3881	91	264.3336	74	325.2788
70	21.9702	53	82.9167	36	143.8619	19	204.8049	2	265.7517	239	326.6966
235	23.3883	218	84.3343	201	145.2793	184	206.2227	167	267.1683	150	328.1133
146	24.8050	129	85.7515	112	146.6964	95	207.6395	78	268.5864	61	329.5313
57	26.2229	40	87.1690	23	148.1139	6	209.0573	243	270.0031	226	330.9479
222	27.6397	205	88.5862	188	149.5309	171	210.4741	154	271.4211	137	332.3659
133	29.0576	116	90.0038	99	150.9484	82	211.8920	65	272.8379	48	333.7825
44	30.4744	27	91.4209	10	152.3655	247	213.3088	230	274.2558	213	335.2005
209	31.8922	192	92.8384	175	153.7829	158	214.7267	141	275.6727	124	336.6170
120	33.3090	103	94.2556	86	155.2000	69	216.1435	52	277.0905	35	338.0351
31	34.7268	14	95.6731	251	156.6174	234	217.5614	217	278.5075	200	339.4515
196	36.1437	179	97.0902	162	158.0346	145	218.9782	128	279.9252	111	340.8697
107	37.5614	90	98.5078	73	159.4520	56	220.3962	39	281.3423	22	342.2860
18	38.9783	1	99.9249	238	160.8693	221	221.8129	204	282.7598	187	343.7042
183	40.3959	166	101.3425	149	162.2866	132	223.2310	115	284.1770	98	345.1205
94	41.8130	77	102.7596	60	163.7039	43	224.6476	26	285.5944	9	346.5387
5	43.2305	242	104.1772	225	165.1212	208	226.0657	191	287.0117	174	347.9550
170	44.6477	153	105.5943	136	166.5385	119	227.4823	102	288.4290	85	349.3733
81	46.0652	64	107.0119	47	167.9557	30	228.9004	13	289.8463	250	350.7896
246	47.4824	229	108.4290	212	169.3731	195	230.3196	178	291.2636	161	352.2079
157	48.9999	140	109.8466	123	170.7903	106	231.7351	89	292.6810	72	353.6242
68	50.3172	51	111.2637	34	172.2076	17	233.1515	254	294.0983	237	355.0425
233	51.7347	216	112.6813	199	173.6248	182	234.5697	165	295.5157	148	356.4588
144	53.1520	127	114.0984	110	175.0422	93	235.9862	76	296.9330	59	357.8771
55	54.5694	38	115.5159	21	176.4592	4	237.4044	241	298.3504	224	359.2934
220	55.9867	203	116.9330	186	177.8767	169	238.8209	152	299.7676		
131	57.4042	114	118.3505	97	179.2937	80	240.2392	63	301.1851		
42	58.8215	25	119.7676	8	180.7112	245	241.6556	228	302.6023		
207	60.2389	190	121.1850	173	182.1282	156	243.0739	139	304.0198		

Table 18. Equator crossings in longitude order.

Appendix D: Leap seconds

Year	30/06	31/12	
1992	**1**	0	Beginning of TOPEX cycle 003 on 1992-10-13
1993	**1**	0	cycle 029 / pass 083 > leap_second=1993-07-01 00:00:00 TP_GPN_2PfP029_083_19930630_234630_19930701_004239.nc
1994	**1**	0	cycle 066 / pass 035 > leap_second=1994-07-01 00:00:00 TP_GPN_2PfP066_035_19940630_235333_19940701_004940.nc
1995	0	**1**	cycle 121 / pass 003 > leap_second=1996-01-01 00:00:00 TP_GPN_2PfP121_128_19951231_234021_19960101_003631.nc
1996	0	0	
1997	**1**	0	cycle 176 / pass 170 > leap_second=1997-07-01 00:00:00 TP_GPN_2PfP176_170_19970630_234018_19970701_003630.nc
1998	0	**1**	cycle 232 / pass 009 > leap_second=1999-01-01 00:00:00 TP_GPN_2PfP232_009_19981231_232708_19990101_002319.nc
1999	0	0	
2000	0	0	
2001	0	0	
2002	0	0	
2003	0	0	
2004	0	0	
2005	0	**1**	end of TOPEX cycle 480 on 2005-10-04
Year	30/06	31/12	

Table 19. Leap seconds during TOPEX/POSEIDON mission.

Appendix E: Acronyms

AGC	Automatic Gain Control
CLS	Collecte Localisation Satellites
CM	satellite Center of Mass
CNES	Centre National d'Etudes Spatiales
CTDP	Centre de Traitement DORIS/POSEIDON
DAC	Dynamic Atmosphere Correction
DEM	Digital Elevation Model
DORIS	Doppler Orbitography and Radiopositioning Integrated by Satellite
ECMWF	European Centre for Medium-Range Weather Forecasts
ERA	European Centre for Medium-Range Weather Forecasts Reanalysis
ERS	European Remote Sensing
FES	Finite Element Solution
FHC	Fine Height Command
GDR	Geophysical Data Record
GFO	Geosat Follow-On
GIM	Global Ionosphere Maps
GMT	Generic Mapping Tools
GNSS	Global Navigation Satellite System
GOT	Goddard Ocean Tide
GPD	GNSS-derived Path Delay
GPS	Global Positioning System
GPSDR	Global Positioning System Demonstration Receiver
GSFC	Goddard Space Flight Center
ITRF	International Terrestrial Reference Frame
JPL	Jet Propulsion Laboratory
LRA	Laser Retroreflector Array
LSE	Least Squares Estimate
LUTs	Look Up Tables
MDT	Mean Dynamic Topography
MGDR	(also M-GDR or GDR-M) Merged GDR, combining TOPEX and POSEIDON data
MLE	Maximum Likelihood Estimation
MODIS	Moderate Resolution Imaging Spectroradiometer
MQE	Mean Quadratic Error
MSS	Mean Sea Surface

MWR	Microwave Radiometer
OSTM	Ocean Surface Topography Mission
NASA	National Aeronautics and Space Administration
NRA	NASA Radar Altimeter
NSIDC	National Snow and Ice Data Center
POE	Precise Orbit Ephemeris
PTR	Point Target Response
SDR	Sensor Data Record
SLR	Satellite Laser Ranging
SSALT	Solid State ALTimeter
SSB	Sea State Bias
SSH(A)	Sea Surface Height (Anomaly)
SWH	Significant Wave Height
TAI	Temps Atomique International (International Atomic Time)
TEC	Total Electron Content
TOPEX	TOpography EXperiment
TMR	TOPEX Microwave Radiometer
UTC	Universal Time Coordinated

Appendix F: Contacts

NASA/JPL

PO.DAAC User Services:

Web: https://podaac.jpl.nasa.gov

e-mail: podaac@podaac.jpl.nasa.gov

CNES

AVISO Altimetry

User Helpdesk:

11 rue Hermès
F-31520 Ramonville StAgne, France

Web   : https://www.aviso.altimetry.fr
e-mail : aviso@altimetry.fr